Study the impact of Smile and Tail dependence on the prices of European Style Bivariate Equity and Interest Rate derivatives using Copulas and UVDD Model

Master's Thesis

Pankaj Chauhan

University of Twente
Faculty of Electrical Engineering,
Mathematics and Computer Science
Enschede

and

ING Bank
CMRM / TRM Department
Amsterdam

Project Supervisor
Prof. Arun Bagchi
Drs. Jan de Kort
Dr. Drona Kandhai
Dr. Jeroslav Krystul

December 2009

Keywords: Bivariate Copulas, Comovement, UVDD Model, Swap rates, Pricing Equity/CMS Spread options using copulas, Monte Carlo Simulation, Constrained Calibration

Abstract

After the introduction of Black's formula in 1973 numerous attempts have been made to price options more realistically, efficiently and consistently with market observations. Although smile effects can be incorporated into pricing European style bivariate options by following well-known methodologies, tail dependence is often neglected. This could be due to little need or interest to introduce tail dependence in pricing models and the great complexity introduced by adding this extra feature. But after the recent Credit Crisis, which started in 2007, various researchers and institutions are turning back-to-basics by understanding and revising the assumptions made within a model and trying to develop alternative ways to price more realistically the products which are more sensitive to joint behavior of underlying assets. The integration of new features into the existing models is also very demanding as it challenges the current market practices.

This thesis seeks to develop a better understanding of tail dependence and also volatility smile by studying its impact on the prices of some selected Equity and Interest rate derivates, and comparing the results with the existing models. It also explores the ways to successfully integrate these features into the existing models and practices.

The basic building block used in this thesis is the Black Scholes model (no smile and zero tail dependence) which will be extended to add smile by assuming Uncertain Volatility and Displaced Diffusion (UVDD) model for each underlying and assuming various Copula functions to add the different types of tail dependence among them. With the use of copula functions we will replace the Gaussian copula while leaving the marginal distributions intact. The options analysed in this thesis are – Spread options, Spread Digital options, Double-Digital options, Worst-of and Best-of options.

The results show that the tail dependence cannot be neglected in many cases and the impact on option price can be higher than the due to addition of smile. The impact of tail dependence is comparably more on short maturity options and the impact of smile if comparably more on long maturity options. Another result shows that the impact of tail dependence decreases with increase in option maturity. This result is quite general since it applied to both Equity and Interest rate derivates.

Acknowledgment

It is a pleasure to thank the many people who made this thesis possible.

First of all I would like to thank my first internal supervisor Prof. Arun Bagchi for providing me the opportunity to conduct this research at the ING Bank in Amsterdam. It was a tremendous experience for me and an honour to work under your guidance.

My thanks also to Dr. Drona Kandhai for his tremendous attention, guidance, insight, and support provided during this research and the preparation of this thesis.

In addition I would like to gratefully acknowledge the supervision of my second external advisor, Mr. Jan de Kort, who has been abundantly helpful and has assisted me in numerous ways. I specially thank him for his infinite patience and support during my research. The discussions I had with him were invaluable and highly motivating. This work would not have been possible without your support.

My gratitude also goes to my second internal supervisor Prof. Jaroslav Krystul for his assistance, especially for sharing the very helpful programming techniques.

Special thanks to Dr. Veronica Malafai from ING Brussels for her comments, suggestions and the valuable literature materials she provided during my project. It helped me to take my project in the right direction. My special thanks also to Dr. Norbet Hari and Dr Dmytro Fedorets from ING Amsterdam for helping me fixing numerous unexpected bugs during the execution of my computer programs, you always had time to help no matter how busy you were. I am also grateful to Dr. Gero Kleineidam from ING Brussels for his unconditional support, advice and suggestions.

I want to thank my family for all the unconditional love and support I received from them all my life. I also want to thank all my friends, most importantly Avijit and Vivien for their continued help, support and constructive comments.

At last I would like to thank the whole ING family and the University of Twente Faculty for supporting me especially during these last months and also throughout my whole study period.

Pankaj Chauhan, December 2009

Table of contents

Chapter 1
Introduction and Overview

1.1 Introduction

Pricing of bivariate products to account for both smile and tail dependence has always been an area of research in financial industry. Neglecting any of the two can result in imperfect hedges and hence leading to significant losses.

Suppose we want to price a bi-digital call option which gives a unit payoff only if both underlyings are above certain individual strikes. In this case the value of the option will increase if the probability of underlyings to move up together increases. This clearly shows that the probability of simultaneous extreme movements – better known as "tail dependence"- is of great importance. In this thesis we will try to solve the question: how smile and tail dependence can affect pricing of some common bivariate products?

We will analyse various scenarios and use different dependent structures to see the impact of some important variables on option pricing. The thesis is restricted to European style options on equities and interest rates.

Instead of deriving joint distribution functions analytically we will replace them by using copula functions which will enable us to isolate the dependence between the random variables (equity prices or interest rates) from their marginal distributions. The most common is the Gaussian copula but the use of this copula does not solve the problem of tail dependence, as in this case tail dependence is observed as "increasing correlation" as the underlying quantities simultaneously move towards extreme, and we will show later that Gaussian copula has zero tail dependence. Hence a change of copula is required to price efficiently and consistently.

For the univariate case similar problems have been dealt with earlier: the classic Black-Scholes model assumed a normal distribution for daily increments of underlyings underestimating the probability of extreme (univariate) price changes. This is usually solved by using a parameterization of equivalent normal volatilities, i.e. the volatilities that lead to the correct market prices when used in the Black-Scholes model instead of one constant number. Due to the typical shape of such parameterisations the problem of underestimation of univariate tails is usually referred to as 'volatility smile'. Tail dependence similarly leads to a 'correlation skew' in the implied correlation surface.

We divide the thesis in eight chapters: in Chapter 2 and 3 we talk about copula theory and dependence. Chapter 4 will deal with some important copula families together with copula parameter estimation and simulation of random samples from such families.

In Chapter 5 we introduce the UVDD model which will be used to incorporate the effect of volatility smile into the marginal distributions. We will also calibrate the UVDD model parameters for both equity and interest rate cases.

Chapter 6 will involve the estimation of the copula shape parameters using likelihood methods for both equity and interest rates. After deriving all the parameters we will use it to price some common bivariate options in Chapter 7 - equity case and Chapter 8 - interest rate case. The pricing is done using Monte-Carlo simulations. We will analyse the results for various parameters of the pricing model and study of effect of change of copula functions.

1.2 Evidence of Smile

Using the Black Scholes option pricing model [1], we can compute the volatility of the underlying by plugging in the market prices for the options. Under Black Scholes framework options with the same expiration date will have same implied volatility regardless of which strike price we use. However, in reality, the IV we get is different across the various strikes. This disparity is known as the volatility skew.

Figures 1.1-1.4 plots the volatility smiles obtained from the market for the swaps and equities. Here AY-BY swap refers to swap rate with maturity of A years and tenor of B years, later in the thesis we will represent this swap as S_{AB}. In equity case Bank of America Corp (BAC) and Wells Fargo & Company (WFC) are used between the period 11-Sep'00 and 04-Sept'09. We will later judge our choice for the underlying. The base currency is US Dollars in Equity case and Euro in interest rate case.

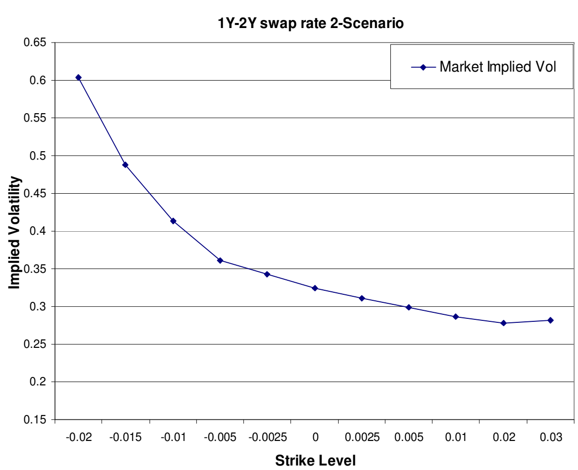

Figure 1.1 Volatility smile for 1Y-2Y Swap

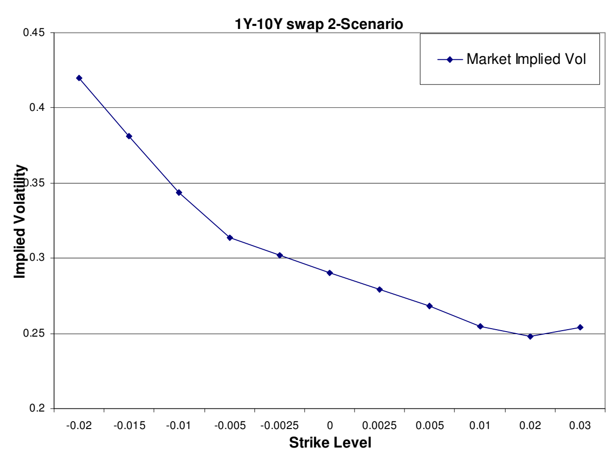

Figure 1.2 Volatility smile for 1Y-10Y Swap

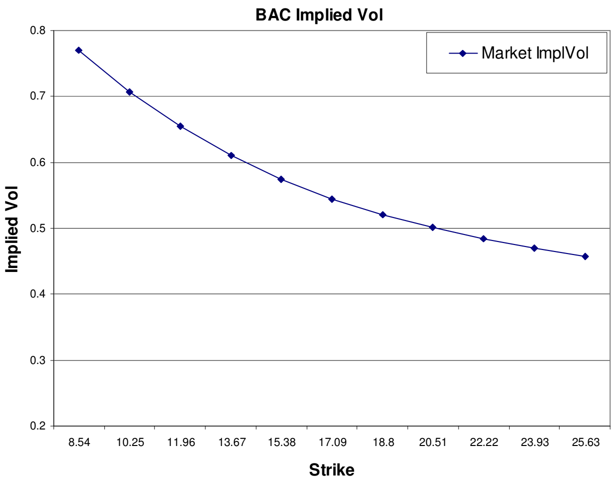

Figure 1.3 Volatility smile for BAC Equity

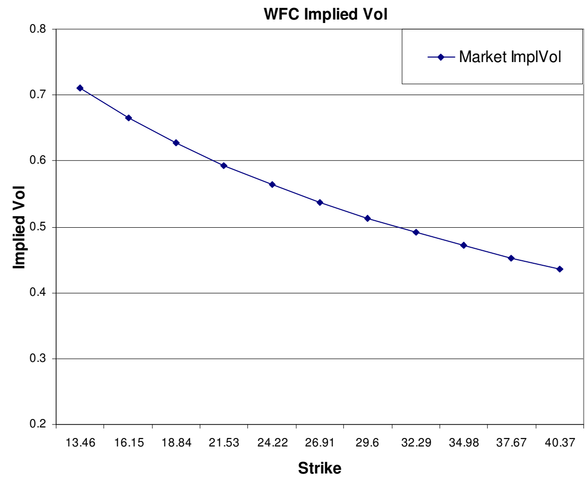

Figure 1.4 Volatility smile for WFC Equity

1.3 Evidence of tail dependence

Tail dependence expresses the probability of a random variable taking extreme values conditional on another random variable taking extremes. For two random variables X, Y with respective distribution F, G the coefficient of tail dependence is given by:

$$\text{Lower tail dependence coefficient} = \lim_{u \downarrow 0} \frac{P[F(X) < u, G(Y) < u]}{P[G(Y) < u]} \tag{1.1}$$

$$\text{Upper tail dependence coefficient} = \lim_{u \uparrow 1} \frac{P[F(X) > u, G(Y) > u]}{P[G(Y) > u]} \tag{1.2}$$

Given a set of historical observations from (X, Y) consisting of the pairs (x_i, y_i), $1 \le i \le n$, how can one calculate the limits using equation 1.1 and 1.2. This can be done by approximating the limit for equation 1.1 by using their empirical counterparts:

$$\hat{P}[F(X) < u, G(Y) < u] = \frac{1}{n} \sum_{i=1}^{n} \mathbf{1}(F^{emp}(x_i) < u, G^{emp}(y_i) < u),$$

$$\mathrm{P}[G(Y) < u] = \frac{1}{n} \sum_{i=1}^{n} \mathbf{1}(G^{emp}(y_i) < u),$$

where

$$F^{emp}(x) = \frac{1}{n} \sum_{i=1}^{n} 1(x_i) < x), \text{ and } G^{emp}(y) = \frac{1}{n} \sum_{i=1}^{n} 1(x_i) < y).$$

We can approximate equation (1.2) by applying a similar approach.

In Table 1.1 we present some pairs of equity and swap rates which we considered for our analysis. In the table we present intuitively what type of tail dependence is present among these selected pairs and if it is profound or very weak? The tail dependence coefficient between them is calculated using the empirical formula presented above over their historical log returns.

Asset Pair	Linear Correlation	Tail Dependence	
		Lower	Upper
JPMorgan-BAC	0.75	+ +	+ +
JPMorgan-WFC	0.76	+ +	+ +
BAC-WFC	0.82	+ +	+ +
JPMorgan-Toyota	0.36	+	–
Microsfot-Apple	0.40	– –	+ +
Toyota-Honda	0.73	+ +	+ +
Toyota-Daimler	0.55	+ +	+
Toyota-Ford	0.37	+ +	+
Toyota-Microsoft	0.34	–	– –
Ford-Daimler	0.48	+	–
Ford-Honda	0.34	+	–
1Y-2Y & 1Y-10Y	0.86	+ +	++
1Y-2Y & 1Y-30Y	0.76	–	++
5Y-2Y & 5Y-10Y	0.73	–	+
5Y-2Y & 5Y-30Y	0.61	– –	– –

Table 1.1 Evidence of tail dependence in pairs of financial assets (++ = clear evidence of empirical tail dependence, + = possible tail dependent, – = unclear, – – = no tail dependence)

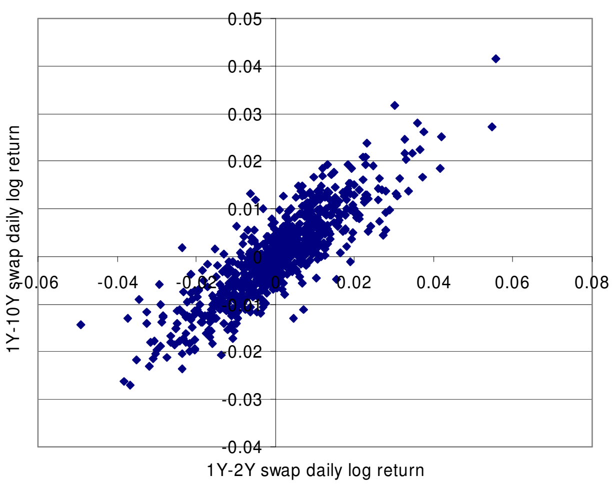

Figure 1.5 Scatter plot for 1Y-2Y and 1Y-10Y Swap daily log returns(3-Jan'05 till 31-Dec'07)

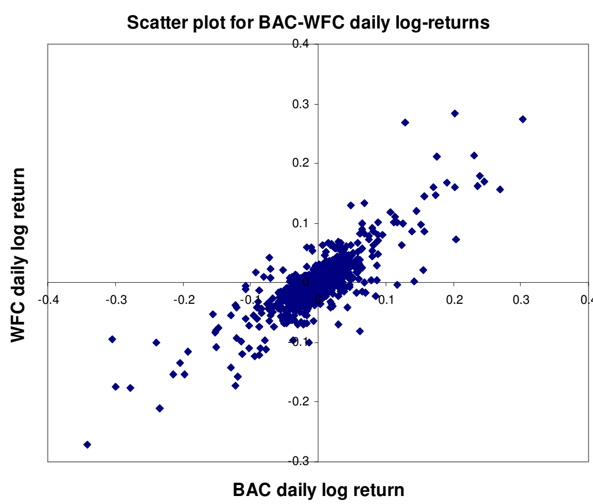

Figure 1.6 Scatter plot for BAC and WFC equity daily log returns (07-Sept'09 till 11-Sept'00)

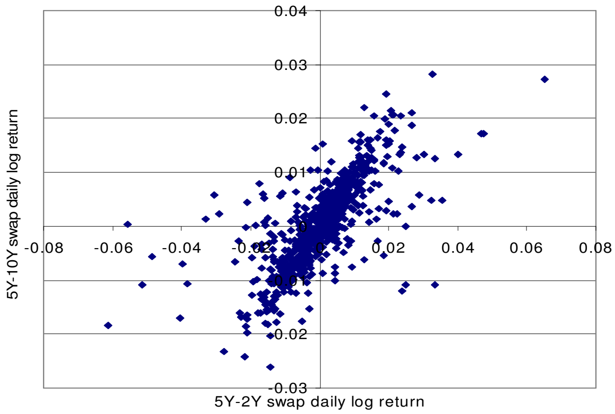

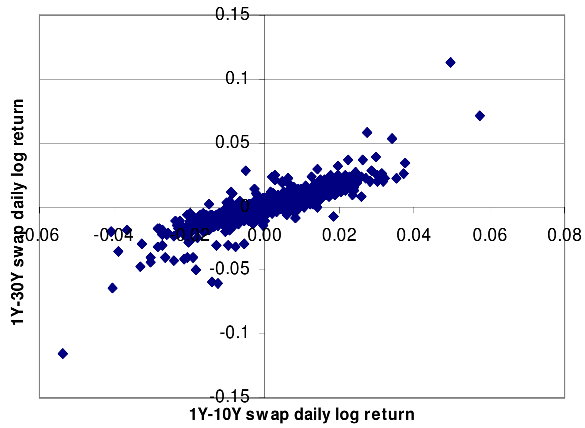

Figure 1.7 Scatter plot for 5Y-2Y and 5Y-10Y Swap daily log returns (3-Jan'05 till 31-Dec'07)

Figure 1.8 Scatter plot for 1Y-10Y and 1Y-30Y Swap daily log returns (3-Jan'05 till 31-Dec'07)

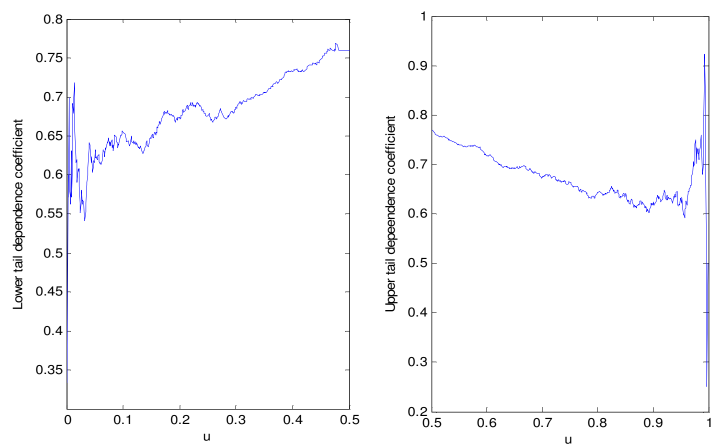

Figure 1.9 Estimated lower (left) and upper (right) tail dependence coefficient for BAC and WFC equity pair

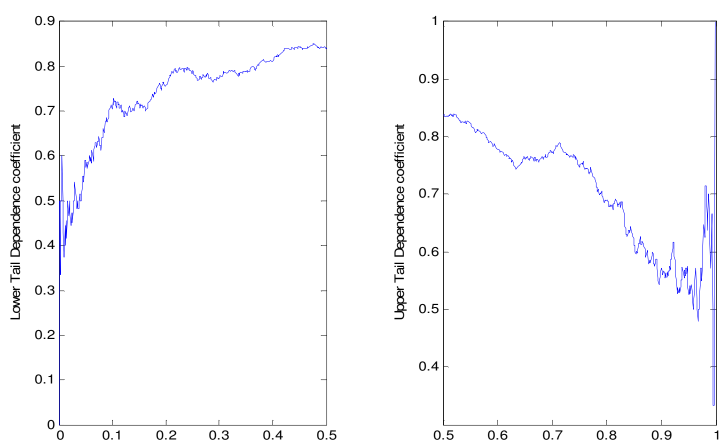

Figure 1.10 Estimated lower (left) and upper (right) tail dependence coefficient for 1Y-2Y and 1Y-10Y swap pair

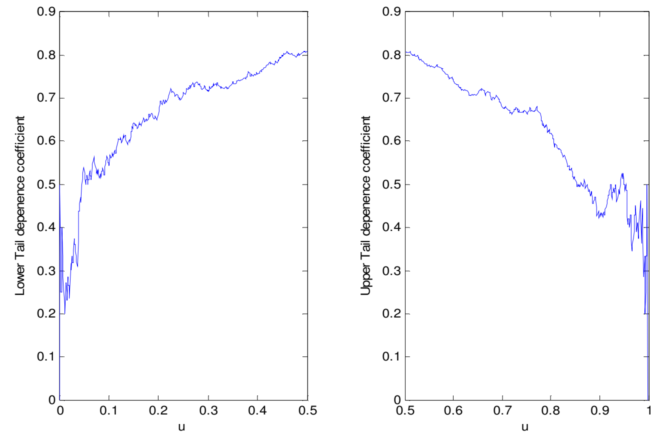

Figure 1.11 Estimated lower (left) and upper (right) tail dependence coefficient for 1Y-2Y and 1Y-30Y swap pair

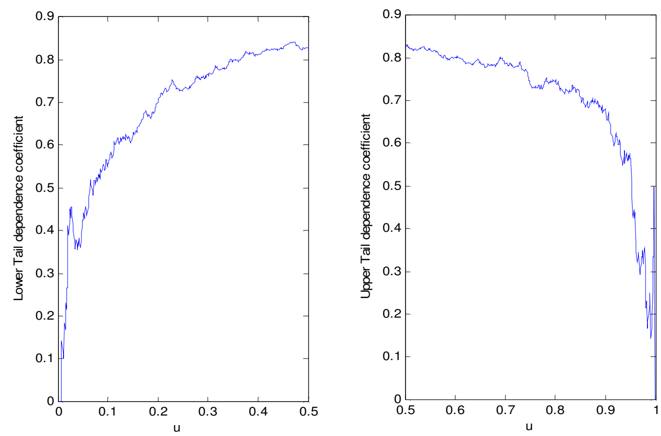

Figure 1.12 Estimated lower (left) and upper (right) tail dependence coefficient for 5Y-2Y and 5Y-10Y swap pair

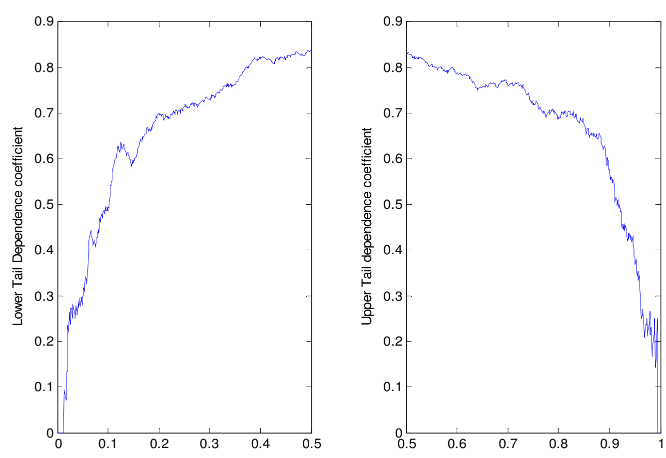

Figure 1.13 Estimated lower (left) and upper (right) tail dependence coefficient for 5Y-2Y and 5Y-30Y swap pair

1.4 Scope of the project

In this thesis we will study and analyse the impact of smile coming from section 1.1 and tail dependence coming from section 1.2 on prices of some common bivariate contracts, especially spread options.

The choice of underlyings is inspired by our observation in Section 1.3:

1) Equity case:
   - BAC and WFC pair

We notice from Table 1.1 that within the selected equity pairs the pair BAC (Bank of America) and WFC (Wells Fargo Corp) gives the maximum value of linear correlation, and also from Figure 1.9 we observe that the empirical tail dependence between them is quite high, the period used in calculation is between 07-Sept'09 and 11-Sept'00 from the *yahoo-finance* website, this is approximately equal to *2260* trading days.

Since equity case are almost similar with different underlyings we restrict ourselves to a single pair.

Whereas for the interest rate case maturity of the swap can play a crucial part in the price of the options hence we considered four pairs.

2) Interest Rate case:

In the interest rate case we considered four pairs:

- Swap Rate 1Y-2Y and 1Y-10Y pair
- Swap Rate 1Y-2Y and 1Y-30Y pair
- Swap Rate 5Y-2Y and 1Y-10Y pair
- Swap Rate 5Y-2Y and 1Y-30Y pair

Figure 1.10 suggests that there is a clear presence of both upper and lower tail dependence between the swap rates 1Y-2Y and 1Y-10Y. This pair also shows the highest correlation between all the other swap pairs considered in my thesis.

Figure 1.11 suggests that upper tail dependence is present between the swap rates 1Y-2Y and 1Y-30Y but the lower tail dependence is still unclear. This pair has a correlation less than the first pair but is higher for swap pairs with higher maturity.

Figure 1.12 suggests presence of upper tail dependence between the swap rates 5Y-2Y and 5Y-10Y but the lower tail dependence is unclear.

From Figure 1.13 we can interpret that both upper and lower tail dependence are missing for the swap pair 5Y-2Y and 5Y-30Y.

The products considered are European style with a single maturity, that is contracts whose payoff depends on two simultaneous observations (one from each underlyings) and the payment is made without delay in case of Equity, for the interest rate products there is a delay between the observation and payment time. The choice of contracts is based on concerns in industry about possible sensitivity to tail dependence:

Spread Call option = $max\ (S_1(T) - S_2(T) - K\ , 0)$, (1.3)

Spread Put option = $max\ \{K - (S_1(T) - S_2(T))\ , 0.0\}$ (1.4)

$$\textbf{Spread Digital Call option} = \begin{cases} c & if \quad S_{a,b1}(T_\alpha) - S_{a,b2}(T_\alpha) \geq K, \\ 0.0 & Otherwise. \end{cases} \tag{1.5}$$

$$\textbf{Digital Call options} = \begin{cases} 1.0 & if \quad S_1(T) \geq K_1 \ \& \ S_2(T) \geq K_2, \\ 0.0 & Otherwise. \end{cases} \tag{1.6}$$

Worst-of Call option = $max\ (min\ (S_1(T)/S_1(0), S_2(T)/S_2(0)) - K, 0.0)$ (1.7)

Best-of Call option = $max\ (max\ (S_1(T)/S_1(0), S_2(T)/S_2(0)) - K, 0.0)$ (1.8)

Chapter 2

Introduction and properties of Copulas

2.1 Copulas – Intuitive Approach

During the last decades, capital markets have transformed rapidly. Derivative securities - or more simply derivatives - like swaps, futures, and options supplemented the trading of stocks and bonds. Theory and practice of option valuation were revolutionized in 1973, when Fischer Black and Myron Scholes published their celebrated Black Scholes formula in the landmark paper "*The pricing of options and corporate liabilities*" [1]. Advancing option valuation theory to options with multiple underlyings [2], which is the claims written on "baskets" of several underlying assets, lead to the problem that the dependence structure of the underlying securities needs to be considered together with the right distributional assumptions of the asset returns. Though linear correlation is a widely used dependence measure, it may be inappropriate for multivariate return data.

For example, in risk-neutral valuation, we price European style financial assets by calculating expected value, under the risk-neutral probability measure, of the future payoff of the asset discounted at the risk-free rate. To apply this technique we need the joint terminal distribution function to calculate the expected value. But due to complex dependent structure between the multiple underlyings it becomes extremely difficult to couple their margins. Furthermore it is sometimes difficult to add variables having different marginal distributions and hence adding more complexity to the models.

Consider a call option written on the minimum or maximum among some market indices. In these cases, assuming perfect dependence (correlation) among the markets may lead to substantial mispricing of the products, as well as to inaccurate hedging policies, and hence, unreliable risk evaluations.

While the multi-asset pricing problem may be already complex in a standard Gaussian world, the evaluation task is compounded by the well known evidence of departures from normality [3]. Following the stock market crash in October 1987, departures from normality [4] have shown up in the well known effects of smile [5]-[6] and term structure of volatility [7]. A possible strategy to address the problem of dependency under non-normality is to separate the two issues, i.e. working with non-Gaussian marginal probability distributions and using some technique to combine these distributions in a multivariate setting. This can be achieved by the use of copula functions. The main advantage of the copula approach to pricing is to write the multivariate pricing kernel as a function of univariate pricing functions. This enables us to carry out sensitivity analysis with respect to the dependence structure of the underlying assets, separately from that on univariate prices. Also calibration of the model can be done in two ways, treating the marginal univariate distribution and the copula parameter separately: more details on calibration in chapter 5.

An important field where copulas have been applied is to price credit derivatives. The famous paper by David X. Li, "*On Default Correlation: A Copula Function Approach*", 2000, proposes Gaussian copulas to be used to valuate CDS and first-to-default contracts [8]. In particular, the copula approach is used to derive the joint distribution function of survival times after deriving marginal distributions from the market information.

Hence copula functions proved to be of great help in addressing to the following two major problems encountered in the derivatives pricing:

- To Model departure from normality for multivariate joint distributions,
- And pricing credit derivatives.

Let us consider a very simple example to get an intuitive understanding of the copula concept in regard to finance.

Take a bivariate European digital put option which pays one unit of related currency if the two stocks S_1 and S_2 are below the strike price levels of K_1 and K_2 respectively, at the maturity. According to risk-neutral pricing principles, the price of the digital put option at time t in a complete market setting is

$$\mathrm{D_P(t)} = exp\,[-\,\mathrm{r}\,(\mathrm{T}-\mathrm{t})]\; Q\,(K_1, K_2)$$

where $Q(K_1, K_2)$ is the joint risk-neutral probability that both stocks are below the corresponding strike prices at maturity T. We assumed the risk free rate r to be constant during the life of the option.

To recover a price consistent to market quotes we do the following:

We recover Q_1 and Q_2, the risk-neutral probability density for the individual stock, for e.g. from the market price of the plain vanilla put options on S_1 and S_2 respectively. In financial terms, we are asking the forward prices of univariate digital options with strikes K_1 and K_2 respectively; in statistical terms, we are indirectly estimating the implied marginal risk-neutral distributions for the stocks S_1 and S_2 from their vanilla put options.

In order to compare the price of our bivariate product with that of the univariate ones, it would be great if we could write the prices as a function of the univariate option prices

$$\mathrm{D_P(t)} = exp\,[-\,\mathrm{r}\,(\mathrm{T}-\mathrm{t})]\; Q\,(K_1, K_2) = exp\,[-\,\mathrm{r}\,(\mathrm{T}-\mathrm{t})]\; C\,(Q_1, Q_2)$$

where $C\,(x, y)$ is some *bivariate function*.

We can discover, from the above expression, the general requirements the bivariate function C must satisfy in order to be able to represent a joint probability distribution,

- The range of the function C must be a subset of the unit interval, including 0 and 1, as it must represent a probability.
- If any one of the two events ($S_1 < K_1$ and $S_2 < K_2$) has probability zero, then the joint probability that both the events occur must also be zero, hence $C(x, 0) = C(0, y) = 0$.
- If any one event will occur for sure, the joint probability that both the events will take place is equal to the probability that the second event will be observed, hence $C(x, 1) = x$ and $C(1, y) = y$.
- We also notice, intuitively, that if the probabilities of both events increase, the joint probability should also increase, and for sure it cannot be expected to decrease, hence $C(x, y)$ is increasing in two arguments (2-increasing in mathematical framework).

We will show in section 2.2 that such a bivariate function C is called a copula, and are extensively used to price a large variety of payoffs. These functions will enable us to express a joint probability distribution as a function of the marginal ones. So that we can price consistently the bivariate product as a function of the univariate options prices.

In regard to our previous discussion we give an abstract definition for a function satisfying the above properties but in a more mathematical setting. We will also provide some of its basic and important properties. We will also present Sklar's Theorem which will help us in understanding the above example in a greater depth. Here we stick to the bivariate case: nonetheless, all the results carry over to the general multivariate setting [9].

2.2 Definition of a Copula

We first start with a more abstract definition of copulas and then switch to a more "operational" one.

Definition 2.1 A two-dimensional copula is a function C: $[0, 1] \times [0, 1] \Rightarrow [0, 1]$ with the following properties:

For every $u, v \in [0, 1]$:

1. $C(u, 0) = C(0, v) = 0$.
2. $C(u, 1) = u$, and $C(1, v) = v$.

For every $u_1, u_2, v_1, v_2 \in [0, 1]$ with $u_1 \leq u_2$, $v_1 \leq v_2$:

3. $C(u_2, v_2) - C(u_2, v_1) - C(u_1, v_2) + C(u_1, v_1) \geq 0$.

The property 1 is called the ***groundedness*** property of a function. The property 3 is the two-dimensional analogue of a nondecreasing one-dimensional function and a bivariate function satisfying this property is called a ***2-increasing*** function.

As a consequence of the 2-increasing and groundedness properties in copulas, we also have the following properties for a copula function C [10, pp. 10-14]:

1. C is *nondecreasing* in each variable.
2. C satisfies the following Lipschitz condition for every u_1, u_2, v_1, v_2 in [0, 1],

$$|C(u_2, v_2) - C(u_1, v_1)| \leq |u_2 - u_1| + |v_2 - v_1| \tag{2.1}$$

thus, every copula C is uniformly continuous on its domain.

3. For every u $\in$ [0, 1], the partial derivate $\frac{\partial C(u,v)}{\partial v}$ exists for almost every[1] v in [0, 1].

   For such u and v one has

$$0 \leq \frac{\partial C(u,v)}{\partial v} \leq 1$$

the analogous statement is true for the partial derivative $\frac{\partial C(u,v)}{\partial u}$.

4. The functions $u \to \frac{\partial C(u,v)}{\partial v}$ and $v \to \frac{\partial C(u,v)}{\partial u}$ are defined and nondecreasing almost everywhere on [0, 1].

Alternatively we present an "operational" definition of a copula [11, pp. 52], which describes it as a multivariate distribution functions whose one-dimensional margins are uniform on the interval [0, 1].

$$C(u, v) = \Pi (U_1 \leq u, U_2 \leq v) \tag{2.2}$$

The extended real line R U{-∞, +∞} is denoted by R^*.

A univariate distribution function of a random variable X is a function F which assigns to all x in R^* a probability $u = F(x) = \mathrm{P}[X \leq x]$.

The joint distribution function of two random variables X and Y is given by

$$S(x, y) = P(X \leq x, Y \leq y).$$

---

[1]The expression "almost every" is used in the sense of the Lebesgue measure.

We know from elementary probability theory that the probability-integral transforms of the r.v.s (random variables) X and Y, if $X \sim F(x)$ and $Y \sim G(y)$ then $F(X)$ and $G(Y)$, are distributed as standard uniform U_i, i = 1, 2:

$$P(F(X) \le c) = P(X \le F^{-1}(c)) = F(F^{-1}(c)) = c \ ,$$

Analogously, the transforms according to F^{-1} of standard uniforms are distributed according to F:

$$F^{-1}(U_i) \sim F$$

Since copulas are joint distribution functions of standard uniforms, a copula computed at $F(x)$, $G(y)$ gives a joint distribution function at (x, y):

$$\begin{aligned} C(F(x), G(y)) &= P(U_1 \le F(x), U_2 \le G(y)) \\ &= P(F^{-1}(U_1) \le x, G^{-1}(U_2) \le y) \\ &= P(X \le x, Y \le y) \\ &= S(x, y). \end{aligned}$$

The above relation between the copulas and the distribution functions will be the content for the next theorem. Sklar used the word copula to describe “a function that links a multidimensional distribution to its one-dimensional margins” [12].

2.3 Sklar’s Theorem

Theorem 2.2 (Sklar’s (1959): Let S be a joint distribution function with given marginal distribution functions $F(x)$ and $G(y)$. Then there exists a copula C such that for all $(x, y) \in R^{*2}$

$$S(x, y) = C(F(x), G(y)). \tag{2.3}$$

If F and G are *continuous* (hence *Range F* = *Range G* = [0, 1]) then C is *unique*.

Conversely, if F and G are continuous univariate distribution functions and C is a copula, then S defined by (2.3) is a joint distribution function with marginals F and G. [12]

While writing equation 2.3 we split the joint probability into the marginals and a copula, so that the latter only represent the “association” between random variables X and Y. For this reason copulas are also called **dependence functions**. We will touch upon this part in more details in the later sections.

2.4 Fréchet-Hoeffding bounds

In this section we will present bounds for the copulas, which show that the every copula is bounded by a maximal and minimal copula. These bounds are called Fréchet-Hoeffding bounds; also the upper bound corresponds to perfect positive dependence and the lower bound to perfect negative dependence. [11, pp. 70-72]

Theorem 2.3 Let C be a copula. Then for every (u, v) in [0, 1],

$$W(u, v) := \max(u + v - 1, 0) \le C(u, v) \le \min(u, v) := M(u, v). \tag{2.4}$$

The functions W and M are called the Fréchet-Hoeffding lower and upper bounds respectively. In the next section we present the relationship between the bounds and the random variables in a bivariate setting.

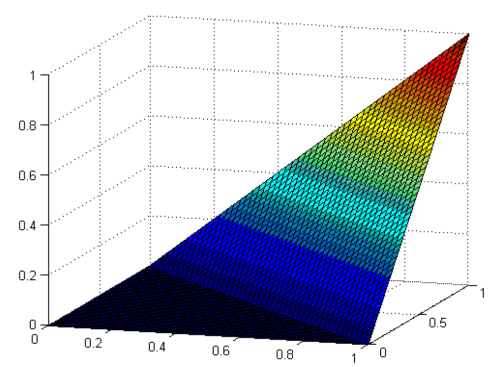

Figure 2.1 Fréchet-Hoeffding lower bound

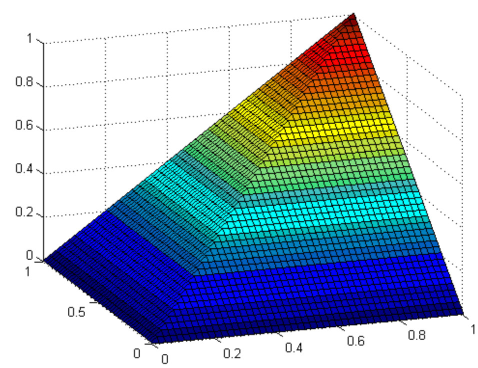

Figure 2.2 Fréchet-Hoeffding upper bound

2.5 Copulas as Dependence functions

The property of the copulas to be described as dependence functions will permit us to characterize independence and in the similar way characterize perfect dependence in a straightforward way. We will also present a very useful property of copulas called the invariant property with the help of a theorem. We will try to establish a relationship between the sections 2.2 and 2.3 by using copula as dependence functions.

2.5.1 Independence

We know that if X and Y are two independent random variables, with their individual univariate distribution functions given by $F(x)$ and $G(y)$ respectively, then their joint distribution function S is given by

$$S(x, y) = F(x)\, G(y)$$

for all x, y in $\boldsymbol{P}^*$.

From Sklar's Theorem we can write a copula function to describe this independence property between the two random variables as:

$$C\,(F\,(x), G\,(y)) = S(x, y) = F\,(x) \times G\,(y) \tag{2.5}$$

We write this new copula as $C^{\perp}$, given by

$$C^{\perp}(u, v) = uv$$

if the two random variables are independent.

The converse also holds and the proof can be found in [10, pp. 25].

2.5.2 Upper bound and perfectly positively dependence

Throughout this section we assume that X and Y are continuous random variables.

Definition 2.4 (Comonotone) A set $A \subset R^{*2}$ is said to be comonotonic if and only if, for every (x_1, y_1), (x_2, y_2) in A it holds that either,

$$x_1 \geq x_2 \text{ and } y_1 \geq y_2, \text{ or,}$$

$$x_2 \geq x_1 \text{ and } y_2 \geq y_1.$$

Definition 2.5 (Perfectly positively dependent) A random vector (X, Y) is comonotonic or perfectly positively dependent if and only if there exits a comonotonic set $A \subset R^{*2}$ such that

$$P((X, Y) \in A) = 1.$$

Theorem 2.6 Let X and Y have a joint distribution function S. Then S is identically equal to its Fréchet-Hoeffding upper bound M if and only if the random vector (X, Y) are comonotonic. [11, pp. 70]

A symmetric definition for countermonotonic (opposite to comonotonic) or perfectly negatively dependent random variates can be given.

2.5.3 Lower bound and perfectly negative dependence

Theorem 2.7 Let X and Y have a joint distribution function S. Then S is identically equal to its Fréchet-Hoeffding lower bound W if and only if the random vector (X, Y) are countermonotonic. [11, pp. 71]

2.5.4 Monotone transforms and copula invariance

Copula C is invariant under increasing transformations of X and Y. It means that the copula of increasing or decreasing transforms of X and Y can easily be written in terms of the copula before the transformation.

Theorem 2.8 Let $X \sim F$ and $Y \sim G$ be random variables with copula C. If α, β are increasing functions on *Range* X and *Range* Y, then $\alpha \circ X \sim F \circ \alpha^{-1} := F_\alpha$ and $\beta \circ Y \sim G \circ \beta^{-1} := G_\beta$ have copula $C_{\alpha\beta} = C$.

Proof:

$$\begin{aligned} C_{\alpha\beta}(F_\alpha(x), G_\beta(y)) &= P[\alpha \circ X \leq x, \beta \circ Y \leq y] = P[X < \alpha^{-1}(x), Y < \beta^{-1}(y)] \\ &= C(F \circ \alpha^{-1}(x), G \circ \beta^{-1}(y)) = C(P[X < \alpha^{-1}(x)], P[Y < \beta^{-1}(y)]) \\ &= C(P[\alpha \circ X < x], P[[\beta \circ Y \leq y]) = C(F_\alpha(x), G_\beta(y)) \end{aligned}$$

The properties mentioned above are of immense importance and are widely exploited in financial modelling. It is due to these properties that copulas are superior to linear correlation. We will touch upon this part in more details in the next chapter.

2.6 Survival Copula

For a pair (X, Y) of random variables with joint distribution function S, the joint survival function is given by

$$\overline{S}(x, y) = P[X > x, Y > y].$$

The margins of the function $\overline{S}$ are the functions $\overline{S}(x, -\infty)$ and $\overline{S}(-\infty, y)$, which are the univariate survival functions $\overline{F}(x) = P[X > x] = 1 - F(x)$ and $\overline{G}(y) = P[Y > y] = 1 - G(y)$, respectively. The relationship between the univariate and joint survival functions is given by:

$$\begin{aligned} \overline{S}(x, y) &= 1 - F(x) - G(y) + S(x, y), \\ &= \overline{F}(x) + \overline{G}(y) - 1 + C(F(x), G(y)), \\ &= \overline{F}(x) + \overline{G}(y) - 1 + C(1 - \overline{F}(x), 1 - \overline{G}(y)). \end{aligned}$$

so that we define a *survival copula* $\hat{C}$ from $[0, 1]^2$ to $[0, 1]$ by using Sklar's theorem,

$$\hat{C}(u, v) = u + v - 1 + C(1 - u, 1 - v), \tag{2.6}$$

We write the relation between the joint survival distribution function and survival copula from the above definitions to be:

$$\overline{S}(x, y) = \hat{C}(\overline{F}(x), \overline{G}(y)).$$

Note that the *joint survival function* $\hat{C}$ for two uniform (0, 1) random variables whose joint distribution copula is C is given by

$$\overline{C}(u, v) = 1 - u - v + C(u, v) = \hat{C}(1 - u, 1 - v).$$

Chapter 3

Comovement

Our concern of this chapter is to study how random variables relate to each other. We study this relation with the help of the concept "**measure of association**" which briefly describes how two random variables are associated when they are not independent.

Scarsini [14] describes measures of association as follows:

"*Dependence is a matter of association between X and Y along any measurable function, i.e. the more X and Y tend to cluster around the graph of a function, either y = f(x) or x = g(y), the more they are dependent.*"

The choice of such functions is exactly the point where the most important measures of association will differ.

Linear correlation is most frequently used in practice as a measure of association. Though the terms association and correlation are used interchangeably, we will show that correlation is an imperfect measure of association. We will show that linear correlation is not a copula-based measure of association; hence it can often be quite misleading and should not be taken as the canonical dependence measure [15]. Below we recall the basic properties of linear correlation and its shortcomings, and then continue with copula based measures of dependence.

3.1 Correlation

Linear correlation measures how well two random variables cluster around a linear function.

Definition 3.1 If X and Y are two random variables, then the linear correlation coefficient between them is given by

$$\rho(X,Y) = \frac{Cov(X,Y)}{\sqrt{Var(X)}\sqrt{Var(Y)}}, \ -1 \le \rho(X,Y) \le 1. \tag{3.1}$$

Where $Var(X)$ and $Var(Y)$ are the variances of X and Y respectively and $Cov(X, Y)$ is their covariance. If X and Y are perfectly linearly dependent, i.e., $Y = aX + b$ for $a \in R \setminus \{0\}$, $b \in R$, then $\rho = \pm 1$. If X and Y are independent then $\rho = 0$.

Correlation concept is suitable mostly for elliptical distributions such as normal and student-t distributions. These distributions are attractive and easy to use because their multivariate distributions can be determined from their variances and correlations alone. But one drawback of using correlation is that a correlation coefficient of zero implies independence only if they are normally distributed but not when they have student-t distribution.

We list some of the major shortcomings of linear correlation coefficient [16]:

1. Correlation is defined only when the variances are finite. It fails when applied to heavy-tail distribution where variances appear infinite, e.g. student-t distributions variance is given by $\nu/\nu\text{-}2$ hence we get infinite variance when degree of freedom $\nu = 2$.
2. Correlation is *not invariant* under (non-linear) increasing transformations of the variables. For example, log(X) and log(Y) generally do not have the same correlation as X and Y. It is invariant only under increasing *linear* transformations. [11, pp.104]
3. A correlation of zero does not always imply independence of variables, e.g. student-t distribution. [11, pp.107]
4. It cannot model asymmetries which are very common in finance: there is evidence of stronger dependence between big losses than between big gains.
5. Perfectly positively dependent (Comonotone) variables can have correlation less than 1; similarly negatively dependent (Countermonotone) variables do not have necessarily a correlation of -1. [11, pp.105]

As a consequence of the shortcomings faced while using linear correlation, copulas as dependence functions are becoming more popular and are more accurate in the financial settings.

The major advantage of using copula based measures over correlation is as follows:

1. Unlike correlation, copulas are invariant under strictly increasing transformations of random variables. For example the change of units of measurements from X to *exponential*(X) does not affect our copula; a direct consequence of Theorem 2.8 from Chapter 2.
2. Copula based measures allows for parameterization of dependence structure, e.g. Archimedean copulas: measure of association tau (= τ) is related to Clayton family shape parameter α by $\alpha/(\alpha + 2)$.
3. We have a wide range of copula families from which we can always construct a suitable measure, depending on the random variables of the multivariate data we are trying to model.

Apart from the above applications, Copula functions can be used for:

4. If the marginal distributions are known, a copula can be used to suggest a suitable form for the joint distribution. We can create multivariate distribution functions by

joining the marginal distributions and can extract copulas from well-known multivariate distribution functions.

5. Finally, Copula represents a way of trying to extract the dependence structure from the joint distribution function and to separate dependence and the marginal behaviour.

We now put the above properties in the form of formal definitions. The most common measures of association are the *measure of concordance* and the *measure of dependence*. First we study measure of concordance and later we compare it to measure of dependence in section 3.3. We will also give two important measures associated with concordance namely Kendall's tau and Spearman's rho.

3.2 Measure of Concordance

Let X and Y be two random variables, then they are said to be concordant if large(small) values of X tend to be associated with large (small) values of Y.

Definition 3.2 Let (x_1, y_1) and (x_2, y_2) be two observations from a vector (X, Y) of continuous random variables. We say they are *concordant* if $x_1 < x_2$ and $y_1 < y_2$ or $x_1 > x_2$ and $y_1 > y_2$ that is $(x_1 - x_2)(y_1 - y_2) > 0$. Similarly, they are *discordan*t if $x_1 < x_2$ and $y_1 > y_2$ or $x_1 > x_2$ and $y_1 < y_2$ that is $(x_1 - x_2)(y_1 - y_2) < 0$.

Definition 3.3 A measure of association $\kappa_{X,Y} = \kappa_C$ is called measure of concordance if it satisfies the following properties [14]:

1. κ is defined for every pair X, Y of continuous random variables.
2. $-1 \leq \kappa_{X,Y} \leq 1$, $\kappa_{X,X} = 1$ and $\kappa_{X,-X} = -1$.
3. $\kappa_{X,Y} = \kappa_{Y,X}$.
4. If X and Y are independent, then $\kappa_{X,Y} = \kappa_{C^\perp} = 0$.
5. $\kappa_{-X,Y} = \kappa_{X,-Y} = -\kappa_{X,Y}$.
6. If C_1 and C_2 are copulas such that $C_1 << C_2$, then $\kappa_{C1} \leq \kappa_{C2}$.(concordance order is preserved)
7. If $\{(X_n, Y_n)\}$ is a sequence of continuous random variables with copulas C_n, and if $\{C_n\}$ converges pointwise to C, then $lim_{n\to\infty} \kappa_{Cn} = \kappa_C$.

The direct connection between the measure of concordance and copula can be studied by noticing the following points [11, pp. 96]:

1. They both are invariant under strictly monotone transformations of random variables, which follow from property 6 and theorem 2.8.

2. A measure of concordance assumes its maximal (minimal) value if the random variables are comonotonic (countermonotonic) that is they have only concordant (discordant) pairs.

Linear correlation coefficient satisfies only axioms 1 to 6 of the concordance measure definition 3.3, therefore is not a true measure of concordance. [11, pp. 103]

3.2.1 Kendall's tau

We define Kendall's coefficient first introduced by Fechner around 1900 and rediscovered by Kendall (1938). [10, pp. 158-164]

Theorem 3.4 Let (X_1, Y_1) and (X_2, Y_2) be independent vectors of continuous random variables with joint distribution functions S_1 and S_2, respectively, with common margins F (of X_1 and X_2) and G (of Y_1 and Y_2). Let C_1 and C_2 denote the copulas of (X_1, Y_1) and (X_2, Y_2), respectively, so that $S_1(x, y) = C_1(F(x), G(y))$ and $S_2(x, y) = C_2(F(x), G(y))$. Let P_c denote the difference between the probability of concordance and discordance of $((X_1, Y_1)$ and (X_2, Y_2), i.e. let

$$P_c = P\{(X_1 - X_2)(Y_1 - Y_2) > 0\} - P\{(X_1 - X_2)(Y_1 - Y_2) < 0\}.$$

Then

$$P_c \equiv P_c(C_1, C_2) = 4\iint_{I^2} C_1(v,z)dC_2(v,z) - 1. \tag{3.2}$$

Add proof in appendix.

Definitions 3.5 In case (X_1, Y_1) and (X_2, Y_2) are independent and identically distributed random vectors, with the identical copula C, that is $S_1(x, y) = S_2(x, y) = C$, then the quantity P_c is called ***Kendall's tau*** τ_C.

Kendall's tau satisfies axioms 1 to 7 of definition 3.3 for a concordance measure [14].We can also interpret τ_C as a normalized expected value since the double integral in the theorem 3.4 calculates the expected value of the function $C(U_1, U_2)$, where both U_1 and U_2 are standard uniform and have joint distribution C:

$$\tau_C = 4\,\mathrm{E}\,[C(U_1, U_2)] - 1.$$

Theorem 3.6 Kendall's τ_C can also be computed as:

$$\tau_C = 1 - 4\iint_{\mathrm{I}^2} \frac{\partial C(u,v)}{\partial u}\frac{\partial C(u,v)}{\partial v}\,\mathrm{d}u\mathrm{d}v\,, \tag{3.3}$$

Since, for continuous X and Y we have

$$\mathrm{d}C = \frac{\partial^2 C(u,v)}{\partial u \partial v}\mathrm{d}u\mathrm{d}v\ .$$

Theorem 3.7 The Kendall's taus of a copula and of its associated survival copula coincide [11, pp.99]:

$$\tau_C = \tau_{\bar{C}}$$

3.2.1.1 Estimating τ from random sample

Given a sample of n observation pairs (x_i, y_i), i = 1, 2, …, n ,from a random vector (X, Y), an unbiased estimator of Kendall's coefficient [11, pp. 99] can be estimated to be τ_s, given by:

$$\tau_s = \frac{2}{n(n-1)}\sum_{i=1}^{n}\sum_{j>i} A_{ij}\ ,$$

where A_{ij} is given by,

$$A_{ij} \equiv sgn\ (X_i - X_j)(Y_i - Y_j\ ),$$

Where the signum function *sgn* for a real number x is defined as follows:

$$sign\,x = \begin{cases} -1 & if\ \ x<0, \\ 0 & if\ \ x<0, \\ 1 & if\ \ x<0, \end{cases}$$

3.2.2 Spearman's rho

As the case for Kendall's tau, the population version of the measure of association known as Spearman's rho is also based on discordance and concordance. [10, pp.167]

Theorem 3.8 Given (X_1, Y_1), (X_2, Y_2) and (X_3, Y_3) be i.i.d random vectors with identical copula C and margins F an G, then

$$\rho_C(X, Y) = 3(P\{(X_1 - X_2)(Y_1 - Y_3) > 0\} - P\{(X_1 - X_2)(Y_1 - Y_3) < 0\}).$$

The random variables X_2 and Y_3 are independent and thus the copula of (X_2, Y_3) is a product copula $C^{\perp}$ that is, joint distribution function of (X_2, Y_3) is $F(x)G(y)$.

By using theorem 3.4 together with the theorem 3.8 we can similarly get an integral representation for Spearman's rho.

Theorem 3.9 Let (X, Y) be a vector of continuous random variables with copula C. Then Spearman's rho for (X, Y) is given by

$$\rho_C(X,Y) = 12\iint_{I^2} C(v,z)dvdz - 3 = 12\iint_{I^2} vzdC(v,z) - 3 \tag{3.4}$$

Hence, if $X \sim F$ and $Y \sim G$, then the integral transforms $U_1 = F(X)$ and $U_2 = G(Y)$ are standard uniform with the joint distribution function C, then we have,

$$\rho_C(X,Y) = 12\iint_{I^2} vzdC(v,z) - 3 = 12\,\mathrm{E}(U_1U_2) - 3$$

$$= \frac{\mathrm{E}(U_1U_2) - 1/4}{1/12} = \frac{Cov(U_1,U_2)}{\sqrt{Var(U_1)}\sqrt{Var(U_2)}}$$

$$= \rho(F(X), G(Y)).$$

which shows that Spearman's rho is equivalent to the linear correlation between $F(X)$ and $G(Y)$.

Spearman's rho also satisfies the properties in Definition 3.3 for a measure of concordance. [14]

From the above theorem we see that Spearman's rho is the rank correlation, in the sense of correlation of the integral transforms, of X and Y. We can exploit this relation in the estimation of ρ_C.

3.2.1.1 Estimating ρ_C from random sample

Given a sample of n observation pairs (x_i, y_i), $i = 1, 2,\ldots, n$,from a random vector (X, Y), an unbiased estimator of Spearman's rho [11, pp.101-102] is given by :

$$\rho_s = \frac{\sum_{i=1}^n (R_i - \overline{R})(S_i - \overline{S})}{\sqrt{\sum_{i=1}^n (R_i - \overline{R})^2 \sum_{i=1}^n (S_i - \overline{S})^2}},$$

where $R_i \equiv \mathrm{rank}(X_i)$ and $S_i \equiv \mathrm{rank}(Y_i)$,with the ranking done in ascending order. Taking into consideration the fact that the ranks of n data are the first n integer numbers, the above expression simplifies into

$$1 - 6\frac{\sum_{i=1}^n (R_i - S_i)^2}{n(n^2-1)}.$$

If tied ranks exist the coefficient between ranks has to be used instead of this formula:

$$\rho = \frac{n\left(\sum x_i y_i\right) - \left(\sum x_i\right)\left(\sum y_i\right)}{\sqrt{n\left(\sum x_i^2\right) - \left(\sum x_i\right)^2}\sqrt{n\left(\sum y_i^2\right) - \left(\sum y_i\right)^2}}$$

One has to assign the same rank to each of the equal values. It is an average of their positions in the ascending order of the values:

Although the properties listed under Definition 3.3 are useful, there are some additional properties that would make a measure of concordance even more useful. Recall that for a random vector (X, Y) with copula C,

$C = M \Rightarrow \tau_C = \rho_S = 1$,

$C = W \Rightarrow \tau_C = \rho_S = -1$.

Where M and W refers to Fréchet-Hoeffding upper and lower bound respectively.

The next theorem states that the converse is also true [17].

Theorem 3.10 Let X and Y be continuous random variables with copula C, and let κ denote Kendall's tau or Spearman's rho. Then the following are true and the copula C is said to be *Comprehensive*:

1. $\kappa(X, Y) = 1 \Rightarrow C = M$.
2. $\kappa(X, Y) = -1 \Rightarrow C = W$.

3.3 Measure of Dependence

Definition 3.11 A measure of association $\delta_C = \delta_{X,Y}$ is called measure of dependence if it satisfies the following properties,

1. $\delta_{X,Y}$ is defined for every pair X, Y of continuous random variables.
2. $0 \leq \delta_{X,Y} \leq 1$,
3. $\delta_{X,Y} = \delta_{Y,X}$,
4. $\delta_{X,Y} = 0$ *iff* X and Y are independent,
5. $\delta_{X,Y} = 1$ *iff* $Y = f(X)$ is a monotone function of X,
6. If α and β are strictly monotone functions on *Range of* X and *Range of* Y respectively, then $\delta_{X,Y} = \delta_{\alpha(X),\beta(Y)}$,
7. If $\{(X_n, Y_n)\}$ is a sequence of continuous random variables with copulas C_n, and if $\{C_n\}$ converges pointwise to C, then $\lim_{n\to\infty} \delta_{X_n,Y_n} = \delta_C$.

The points where concordance and dependence measures differ are as follows:

(i). Dependence measure takes its maximum value when X and Y are perfectly dependent (comonotonic/countermonotonic), whereas concordance measure takes it's maximum *only* when X and Y are perfectly positively dependent (comonotonic).

(ii). Dependence measure takes its minimum when X and Y are independent, whereas concordance measure takes its minimum only when X and Y are perfectly negatively dependent (countermonotonic).

(iii). Concordant measure being zero doesn't not always imply X and Y to be independent whereas dependent measure equal to zero imply independence.

3.4 Tail Dependence

The concept of tail dependence relates to the amount of dependence in the upper-right quadrant tail or lower-left-quadrant tail of a bivariate distribution. It is a concept that is relevant for the study of dependence between extreme values. We can say that it is the probability of having a high (low) extreme value of Y given that a high (low) extreme value of X has occurred. It turns out that tail dependence between two continuous random variables X and Y is a copula property and hence the amount of tail dependence is invariant under strictly increasing transformations of X and Y.

Definition 3.12 Let (X, Y) be a vector of continuous random variables with marginal distribution functions F and G. The coefficient of upper tail dependence λ_U of (X, Y) is given by:

$$\begin{aligned}\lambda_U &= \lim_{u\to 1^-} P\{G(Y) > u \mid F(X) > u\},\\ &= \lim_{u\to 1^-} P\{Y > G^{-1}(u) \mid X > F^{-1}(u)\},\\ &= \lim_{u\to 1^-} \frac{1-2u+C(u,u)}{1-u}.\end{aligned}$$

And the lower tail dependence is given by

$$\begin{aligned}\lambda_L &= \lim_{u\to 0^+} P\{G(Y) < u \mid F(X) < u\},\\ &= \lim_{u\to 0^+} P\{Y < G^{-1}(u) \mid X < F^{-1}(u)\},\\ &= \lim_{u\to 0^+} \frac{C(u,u)}{u},\end{aligned}$$

provided the limits λ_U, $\lambda_L \in [0, 1]$ exists.

The variables X and Y are said to exhibit upper (lower) dependence if $\lambda_U \neq 0$ $(\lambda_L \neq 0)$, it means that their copula C also has upper (lower) tail dependence.

Lemma 3.13 Denote the lower (upper) coefficient of tail dependence of the survival copula $\overline{C}$ by $\overline{\lambda_L}$, $\overline{\lambda_U}$, then

$$\lambda_L = \overline{\lambda_U},$$

$$\lambda_U = \overline{\lambda_L}.$$

Example 3.14: Consider the bivariate Clayton copula given by

$$C_\alpha(u, v) = max[(u^{-\alpha} + v^{-\alpha} - 1)^{-1/\alpha}, 0], \text{ for } \alpha \in [-1, 0) \cup (0, +\infty).$$

Then, for α >0,

$$\lambda_U = \frac{d}{du}\left[2u - 1 + C(1-u, 1-u)\right]_{u=0} = 2 - \left[\frac{d}{dv} v(2 - v^{-\alpha})^{-1/\alpha}\right]_{v=1}$$

$$= 2 - \left[v^{\alpha}(2 - v^{\alpha})^{-1-1/\alpha} + (2 - v^{\alpha})^{-1/\alpha}\right]_{v=1}$$

$$= 2 - \left[\frac{2}{(2 - v^{\alpha})^{1/\alpha + 1}}\right]_{v=1} = 0.$$

Now,

$$\lambda_L = \lim_{u \to 0^+} \frac{C(u,u)}{u} = \lim_{u \to 0^+} \frac{(2u^{-\alpha} - 1)^{-1/\alpha}}{u} = \lim_{u \to 0^+} \frac{1}{(2 - u^{\alpha})^{1/\alpha}}$$

$$= 2^{-1/\alpha}.$$

This implies that for $\alpha > 0$, Clayton copula C_α has lower tail dependence only.

Chapter 4
Bivariate Copula Families

This chapter is divided in three sections: Definition and important properties of some widely used copulas, Copula shape parameter estimation and Simulation from desired copulas.

We start with an overview of two classes of copulas, namely Elliptical and Archimedean copulas. Since most of our work will be related to only bivariate family we will exclude the multivariate from our discussion. These bivariate one-parameter families of copulas are absolutely continuous and have domain of $[0, 1]^2$.

For each family, we give the copula definition and write down the respective densities. We will also discuss the concordance order and comprehensiveness properties of the family. And whenever possible the relationship between the copula parameter and the measure of association or tail dependence will be presented.

4.1 Elliptical Copulas

Elliptical copulas are the copulas of elliptical distributions; examples are Student-t and Gaussian (normal) distribution. They are the widely used copula family in empirical finance. But the drawback of using Elliptical copulas is that they do not have closed form expressions and are restricted to have radial asymmetry, hence they have equal lower and upper tail dependence. As in many insurance and financial applications, there is evidence that there is a stronger dependence between big losses than between big gains. Such asymmetries cannot be modeled with elliptical copulas.

4.1.1 Gaussian Copula

The copula family most commonly used for modeling in finance is the Gaussian copula, which is constructed from the bivariate normal distribution via Sklar's theorem.

Definition 4.1 With Φ_ρ being the standard bivariate normal cumulative distribution function with correlation ρ, the Gaussian copula function is

$$C_\rho^{Ga}(u,v) = \Phi_\rho(\Phi^{-1}(u), \Phi^{-1}(v)). \tag{4.1}$$

where u and $v \in [0,1]$ and Φ_ρ given by

$$\Phi_\rho(x,y) = \int_{-\infty}^{x} \int_{-\infty}^{y} \frac{1}{2\pi\sqrt{1-\rho^2}} \exp\left(-\frac{1}{2(1-\rho^2)}[s^2 + t^2 - 2\rho\, st]\right) ds dt \tag{4.2}$$

and Φ denotes the standard normal univariate cumulative distribution function.

Differentiating C_ρ^{Ga} yields the copula probability density function (pdf), (Figure 4.1):

$$c_\rho(u,v) = \frac{\phi_{X,Y,\rho}(\Phi^{-1}(u), \Phi^{-1}(v))}{\phi(\Phi^{-1}(u))\phi(\Phi^{-1}(v))}, \tag{4.3}$$

where $\phi_{X,Y,\rho}$ is the density function for the standard bivariate Gaussian with linear correlation coefficient ρ and ϕ is the standard normal density.

Proposition 4.2 The Gaussian copula generates the joint standard normal distribution iff. $u = \Phi(x)$ and $v = \Phi(y)$, that is iff. – via Sklar's Theorem- the margins are standard normal.

As a consequence of the fact that it is parameterized by the linear correlation coefficient, which respects concordance order (Definition 3.3: axiom 6, Chapter 3), the Gaussian copula is **positively ordered** with respect to its parameter:

$$C^{Ga}_{\rho=-1} << C^{Ga}_{\rho<0} << C^{Ga}_{\rho=0} << C^{Ga}_{\rho>0} << C^{Ga}_{\rho=1}$$

Also, it is **comprehensive** (Theorem 3.10, Chapter 3):

$$C^{Ga}_{\rho=-1} = W \text{ and } C^{Ga}_{\rho=1} = M.$$

and in addition .

$$C^{Ga}_{\rho=0} = C^{\perp}.$$

The measure of association and correlation coefficient for Gaussian copula are related by:

$$\tau = \frac{2}{\pi}\arcsin\rho \quad \text{and} \quad \rho_s = \frac{6}{\pi}\arcsin\frac{\rho}{2}.$$

It is also shown that Gaussian copulas have neither upper nor lower tail dependence [19], unless $\rho = 1$:

$$\lambda_U = \lambda_L = \begin{cases} 0 & iff\ \rho < 1 \\ 1 & iff\ \rho = 1 \end{cases}$$

4.1.2 Student-t Copula

Definition 4.3 The bivariate Student-t copula $T_{\rho,v}(u, v)$ with v degrees of freedom is defined as:

$$C^s_{\rho,v}(u,v) = t_{\rho,v}(t_v^{-1}(u), t_v^{-1}(v)) \tag{4.4}$$

where the univariate (central) Student-t distribution function t_v is given by:

$$t_v(x) = \int_{-\infty}^{x} \frac{\Gamma((v+1)/2))}{\sqrt{\pi v}\,\Gamma(v/2)}\left(1+\frac{s^2}{v}\right)^{-\frac{v+1}{2}} ds \tag{4.5}$$

and the corresponding bivariate function $t_{\rho,v}(x,y)$ is given by:

$$t_{\rho,v}(x,y) = \int_{-\infty}^{x}\int_{-\infty}^{y} \frac{1}{2\pi\sqrt{1-\rho^2}}\left(1+\frac{s^2+t^2-2\rho st}{v(1-\rho^2)}\right)^{-\frac{v+2}{2}} dsdt, \tag{4.6}$$

and Γ is the Euler function [18].

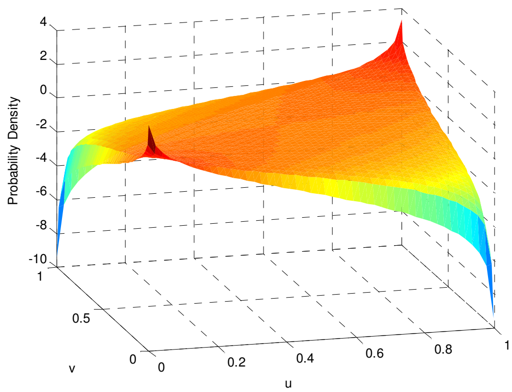

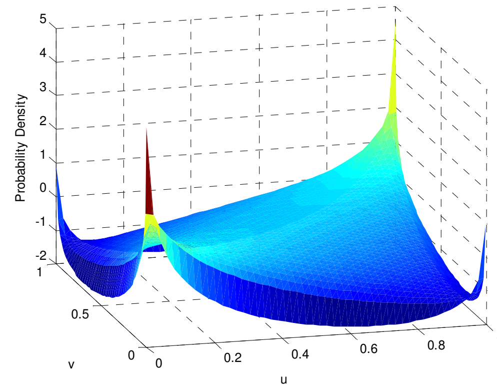

Fig 4.1.Gaussian Copula pdf ρ = 0.5. **Fig 4.2.Student-t Copula pdf ρ = 0.5.**

When the number of degrees of freedom diverges, the copula converges to the Gaussian one. The copula $C^s_{\rho,\nu}$ is also positively ordered with respect to ρ, for given degrees of freedom. It also reaches the upper (lower) bound for $\rho = +1$ (-1) respectively.

But $C^s_{0,\nu} \neq C^{\perp}$ as the variances become infinite for $\nu = 2$ for Student-t distributions.

As for the tail dependency, for finite $\nu > 2$

$$\lambda_U = \lambda_L = \begin{cases} > 0 & \text{iff } \rho > -1 \\ 0 & \text{iff } \rho = 1 \end{cases}$$

4.2 Archimedean Copulas

Archimedean copulas are an important family of copulas, which have a simple form with properties such as associativity and have a variety of dependence structures. Unlike Elliptical copulas most of the Archimedean copulas have closed-form expressions and are not derived from the multivariate distribution functions using Sklar's Theorem.

These copulas can take a great variety of forms. Furthermore, they can have distinct upper and lower tail dependence coefficients. This makes them suitable candidates for modelling asset prices, due to profound upper or lower tail dependence in their market data.

Instead they are constructed by using a function φ: $[0, 1] \rightarrow R^{*+}$, which is continuous, decreasing, convex and such that $\varphi(1) = 0$. Such a function φ is called *generator*. It is called a strict generator whenever $\varphi(0) = +\infty$ also holds.

We will need the inverse of this generator function in the construction of Archimedean copulas. The *pseudo-inverse* of φ is defined as follows:

$$\varphi^{[-1]}(v) = \begin{cases} \varphi^{-1}(v) & 0 \le v \le \varphi(0) \\ 0 & \varphi(0) \le v \le +\infty \end{cases}$$

Definition 4.4 Given a generator and its pseudo-inverse, an Archimedean copula C^A is generated as follows:

$$C^A(u, v) = \varphi^{[-1]}(\varphi(u) + \varphi(v)). \quad (4.7)$$

Theorem 4.5 Let C^A be an Archimedean copula with generator φ .Then

1. C^A is symmetric; $C^A(u, v) = C^A(v, u)$ for all u, v in [0, 1].
2. C^A is associative; $C^A(C^A(u, v), z) = C^A(u, C^A(v, z))$ for u, v, z in [0, 1].

The density of an Archimedean copula, provided $\varphi' \neq 0$ and is finite, is given by [11, pp. 122]

$$c^A(u,v) = -\frac{\varphi''(C(u,v)\varphi'(u)\varphi'(v)}{(\varphi'(C(u,v)))^3} \tag{4.8}$$

4.2.1 One-parameter Archimedean copulas

We will consider in particular the one-parameter copulas, which are constructed using a generator $\varphi_\alpha(t)$, where parameter α is any real number. Table 4.1 describes some well-known families and their generators.

Name	$C_\alpha(u, v)$	$\varphi_\alpha(t)$	α Range	τ	λ_L	λ_U
Clayton	$(\max\{0, u^{-\alpha} + v^{-\alpha} - 1\})^{-1/\alpha}$	$\frac{1}{\alpha}(t^{-\alpha} - 1)$	$[-1,\infty)\backslash\{0\}$	$\frac{\alpha}{\alpha+2}$	$2^{-1/\alpha}$	0
Frank	$-\frac{1}{\alpha}\log\left(1+\frac{(e^{-\alpha u}-1)(e^{-\alpha}v-1)}{e^{-\alpha}-1}\right)$	$-\log\frac{(e^{-\alpha t}-1)}{e^{-\alpha}-1}$	$(-\infty, \infty)\backslash\{0\}$	--	0	0
Gumbel-Hougaard	$\exp\left(-[(-\log u)^\alpha + (-\log v)^\alpha]^{\frac{1}{\alpha}}\right)$	$(-\log t)^\alpha$	$[1, \infty)$	$\frac{\alpha-1}{\alpha}$	0	$2\text{-}2^{1/\alpha}$

Table 4.1 One-parameter Archimedean copulas

As seen in Table 4.1 the computation of the copula parameter from the association one, for most of the families, is elementary and the relationship between the two is one-to-one. The following figures present the probability density function for Clayton and Frank copula for parameter value 5.

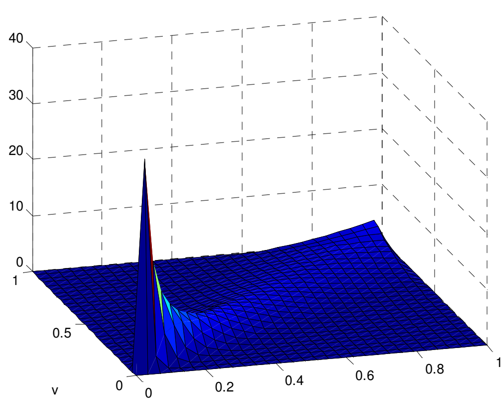

Fig 4.3.Clayton Copula pdf α = 5

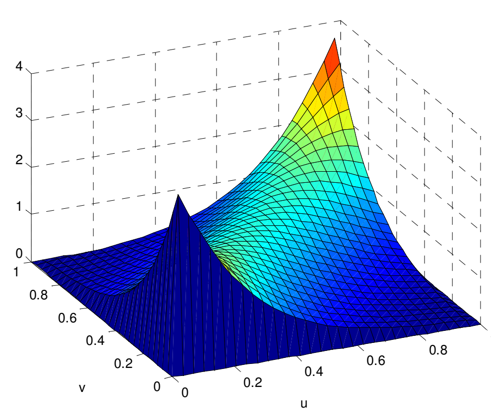

Fig 4.4.Frank Copula pdf α = 5

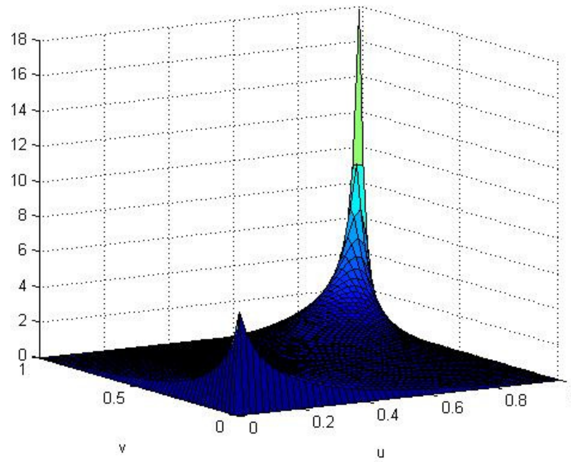

Figure 4.5 Gumbel Copula pdf α = 5

4.2.2 Archimedean copula and dependency

Kendall's τ can also be written as [20]

$$\tau = 4\int_I \frac{\varphi(v)}{\varphi'(v)}\,dv + 1 \tag{4.9}$$

Where φ' exists almost everywhere since the generator is convex.

This makes Archimedean copulas easily amenable for estimation, as we will see in next chapter.

4.3 Copula Parameter Estimation

There are several ways to estimate parameter of a copula-function. Most popular methods deal with maximization of log-likelihood function of the copula density with respect to the parameters. Joe [21], Durrleman [22] suggest three different ways: the full maximum likelihood (FML) method, the inference for margins (IFM) method and the canonical maximum likelihood (CML) method. All three methods are briefly introduced further.

For a random vector $X = (x_{1t}, \ldots, x_{dt})_{t=1}^{T}$ with parametric univariate marginal distributions $F_j = (x_j, \delta_j)$, $j = 1, \ldots, d$ the conditional distribution of X_t can be written as:

$$F(\alpha; x_1, \ldots, x_T) = C(F_1(x_1, \delta_1), \ldots, F_d(x_d, \delta_d); \theta)\ , \tag{4.10}$$

where C is from parametric copula family with dependence parameter θ.

Assuming that c is density of C we get the conditional density of X_t

$$f(\alpha; x_1, \ldots, x_T) = c\{F_1(x_1, \delta_1), \ldots, F_d(x_d, \delta_d); \theta_t\} \prod_{i=1}^{d} f_i(x_i; \delta_i). \tag{4.12}$$

Then the log-likelihood function is given by

$$\ell\,(\alpha; x_1,\ldots, x_T) = \sum_{t=1}^{T} \log c\,\{F_1\,(x_{1,t}, \delta_1), \ldots, F_d\,(x_{d,t}, \delta_d);\theta_t\} + \sum_{t=1}^{T}\sum_{j=1}^{d} \log\, f_j\,(x_{j,t}\,;\,\delta_j). \quad (4.13)$$

where $c\{u_1, \ldots, u_d\} = \dfrac{\partial^d C(u_1,\ldots,u_d)}{\partial u_1 \ldots \partial u_d}$ is a copula density, and $\alpha = (\theta, \delta_1, \ldots, \delta_d)'$ are the parameters to be estimated.

4.3.1 Fully parametric standard maximum-likelihood

This method requires distributional assumptions for the margins. If the margins are specified correctly, this estimator possesses the usual optimality properties of the ML-estimator.

The maximum likelihood method implies choosing C and $F_{1,\ldots\ldots}F_n$ such that the probability of observing the data set is maximal. The data set is assumed to consist of independent observations.

The possible choices for the copula and the margins are unlimited; therefore we usually restrict ourselves to certain classes of functions, parameterized by some vector $\alpha \in \Theta \subset R^n$.

It estimates the parameters exactly from equation 4.13, by maximizing the likelihood function with respect to the unknown parameter $\alpha \in \Theta$ which is called the maximum likelihood estimator (MLE):

$$\alpha_{\text{MLE}} := \arg\max_{\alpha \in \Theta} \ell(\alpha)$$

But the maximization of such log-likelihood function is complicated as it involves estimation of all the parameters simultaneously, and the increase of scale problem makes the algorithm too cumbersome. Also these solutions can also be local maxima, minima or infection points. On the other hand, maxima can occur at the boundary of Θ (or if $\|\alpha\| \to \infty$), in discontinuity points and in points where the likelihood is not differentiable.

For joint distributions satisfying some regularity conditions, it can be shown Shao [23] that if the sample size increases, the subsequent MLEs converges to a limit. This property is called *consistency*.

4.3.2 Inference for Margins (IFM) Method

The above estimation problem can also be approached in a different and relatively easy way as proposed by Joe and Xu [24]. They propose to estimate the parameter α in two steps:

1. Estimate the margins' parameters δ by performing the estimation of the univariate marginal distributions:

$$\hat{\delta} = \arg\max_{\delta} \sum_{t=1}^{T} \sum_{j=1}^{d} \ln f_j(x_{j,t}; \delta)$$

2. Estimate the copula parameter θ given the margins' parameter $\hat{\delta}$:

$$\hat{\theta} = \arg\max_{\theta} \sum_{t=1}^{T} \log c\ \{F_1(x_{1,t}, \delta_1), \ldots, F_d(x_{d,t}, \delta_d); \theta, \ \hat{\delta}\ \}$$

The IFM estimator is defined as the vector

$$\hat{\alpha}_{IFM} = (\hat{\delta}, \hat{\theta})'$$

Let ℓ be the entire log-likelihood function, ℓ_j the log-likelihood of the jth marginal, and ℓ_c the log-likelihood for the copula itself. Then the IFM estimator is the solution of:

$$\left(\frac{\partial \ell_1}{\partial \delta_1}, \frac{\partial \ell_2}{\partial \delta_2}, \ldots\ldots, \frac{\partial \ell_n}{\partial \delta_n}, \frac{\partial \ell_c}{\partial \theta} \right) = 0'$$

While the MLE comes from solving

$$\left(\frac{\partial \ell}{\partial \delta_1}, \frac{\partial \ell}{\partial \delta_2}, \ldots\ldots, \frac{\partial \ell}{\partial \delta_n}, \frac{\partial \ell}{\partial \theta} \right) = 0'$$

The equivalence of the two estimators does not hold but it is simple to see that the IFM estimator provides a good starting point for obtaining an exact MLE. By doing so, the computational cost of finding the optimal set of parameters reduces significantly.

4.3.3 Canonical Maximum Likelihood (CML) Method

In the canonical maximum likelihood (CML) method proposed by Mashal and Zeevi [25] no assumptions on the distributions of the marginals are needed. Instead, empirical marginal distributions are estimated and the approximation of the unknown marginal distribution $F_j(\cdot)$ is given by

$$\hat{F}_j(x) = \frac{1}{T+1} \sum_{t=1}^{T} \mathrm{I}\{X_{j,t} \le x\},$$

where $\mathrm{I}\{X_{j,t} \le x\}$ is an indicator function. Thus, pseudo-samples of uniform variates are obtained. Then we can maximize the pseudo log-likelihood function given by

$$\ell(\alpha) = \sum_{t=1}^{T} \log c\left\{\hat{F}_1(X_{1t}), \ldots\ldots., \hat{F}_n(X_{nt}); \alpha\right\}$$

and obtain the desired estimate

$$\hat{\alpha}_{CML} = \arg\max_{\alpha}\ \ell(\alpha)$$

This method is computationally more advantageous than the two other described above as it is numerically more stable.

4.4 Simulation

In the following sections some useful techniques to draw random samples from the Gaussian and one-parameter Archimedean copulas are presented. These random samples are the key ingredients for the Monte Carlo simulations.

The simulations for Gaussian copula are obtained easily, but for Archimedean copulas we will discuss conditional sampling method and much simpler Marshall and Olkin's method. And once a copula has been decided bivariate/multivariate random samples can be drawn easily.

4.4.1 Simulation Method for Gaussian Copula

As we already stated that Gaussian Copula is one of the most widely known and applied copula to Empirical finance. Since this copula has no closed form and hence not very easy to write, but the random draws from n-copula C_R, where R is the correlation matrix, follow very simple algorithm given by [11, pp. 181]:

- Find the Cholesky decomposition A of R.
- Simulate n independent (n=2 for bi-variate copulas) random samples $z = (z_1, z_2, \ldots\ldots, z_n)'$ from $\Phi(0, 1)$ (Standard Normal Distribution)
- Set $\mathbf{x} = A\mathbf{z}$;
- Set $u_i = \Phi(x_i)$, i=1,2,….,n.
- $(u_1, u_2, \ldots\ldots, u_n)' = (F_1(t_1), F_2(t_2), \ldots. F_n(t_n))'$ where F_i denotes the i^{th} margin.

4.5 Conditional Sampling

This is a very handy technique in the case of Archimedean copulas [11, pp. 182-188] but is not applicable for few families like the Gumbel Copula, and also sometimes it involves solving quite a number of equations numerically (like for n-Frank copula one needs to solve n – 1 dimensional polynomial equation).

The components of the realization of the copula are generated one by one. The first component is drawn from a uniform distribution, the second in based on the copula conditional on the first draw and so on.

- Define $C_k(u_1, u_2, \ldots\ldots, u_k) = C(u_1, u_2, \ldots\ldots, u_k, 1, 1, \ldots., 1)$, $1 \le k \le n$,
- Simulate a vector $(v_1, v_2, \ldots\ldots, v_n)$ of standard uniform random variates,
- Put $\left\{ \begin{array}{c} v_1 = u_1 \\ v_2 = P[U_2 \le u_2 \mid U_1 = u_1 \\ . \\ . \\ v_k = P[U_n \le u_n \mid U_1 = u_1, \ldots.., U_{n-1} = u_{n-1}] \end{array} \right\}$
- The solution $(u_1, u_2, \ldots\ldots, u_n)$ of this system is a realization of the copula.

Where the conditional distribution of the k-th component given the preceding ones is

$$P[U_k \le u_k \mid U_1 = u_1, \ldots\ldots, U_{k-1} = u_{k-1}] = \frac{P[U_k \le u_k, U_1 = u_1, \ldots\ldots, U_{k-1} = u_{k-1}]}{P[U_1 = u_1, \ldots\ldots, U_{k-1} = u_{k-1}]} \qquad (4.14)$$

Cherubini et al [11] show that for Archimedean copulas

$$P[U_k \le u_k \mid U_1 = u_1, \ldots\ldots, U_{k-1} = u_{k-1}] = \frac{\varphi^{-1(k-1)}(\varphi(u_1) + \varphi(u_2) + \ldots + \varphi(u_k))}{\varphi^{-1(k-1)}(\varphi(u_1) + \varphi(u_2) + \ldots + \varphi(u_{k-1}))}$$

We demonstrate below how to use conditional sampling to draw random samples from bivariate Clayton and Frank copulas.

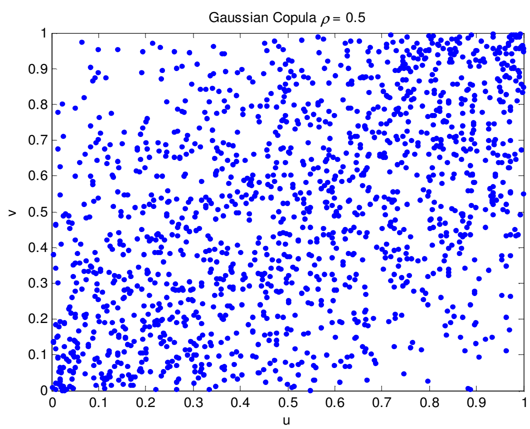

Figure. 4.5 Gaussian random sample ρ = 0.5.

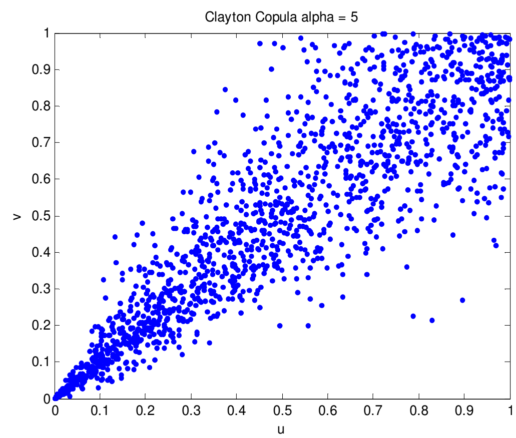

Figure 4.6 Clayton random sample, α = 5

4.5.1 Clayton bivariate simulation

The generator of the Clayton Copula is $\varphi(u) = u^{-\alpha} - 1$ with pseudo inverse given by $\varphi^{-1}(u) = (t + 1)^{-1/\alpha}$ and $\partial_t \varphi^{-1} = \frac{1}{\alpha}(t+1)^{-\frac{1+\alpha}{\alpha}}$ Draw v_1 and v_2 from a standard uniform distribution and put

$$\left\{ \begin{aligned} & v_1 = u_1, \\ & v_2 = \frac{\partial_t \varphi^{-1}(\varphi(u_1) + \varphi(u_2))}{\partial_t \varphi^{-1}(\varphi(u_1))} = \left(\frac{u_1^{-\alpha} + u_1^{-\alpha} - 1}{u_1^{-\alpha}} \right)^{-\frac{1+\alpha}{\alpha}} \end{aligned} \right\}$$

using the algorithm from section 4.5.

Solving for u_2 gives

$$u_2 = (u_1^{-\alpha}(v_2^{-\frac{\alpha}{1+\alpha}} - 1) + 1)^{-\frac{1}{\alpha}}$$

Figure 4.6 shows 1500 random samples from a Clayton Copula with parameter alpha = 5 using above algorithm.

4.5.2 Frank bivariate simulation

The generator of the Frank Copula is $\varphi(u) = \frac{\log(e^{-\alpha u} - 1)}{e^{-\alpha} - 1}$ with pseudo inverse given by $\varphi^{-1}(u) = -\frac{1}{\alpha}\log\left(1 + e^{t}(e^{-\alpha} - 1)\right)$ and $\partial_t \varphi^{-1} = \frac{1}{\alpha}(t+1)^{-\frac{1+\alpha}{\alpha}}$ Draw v_1 and v_2 from a standard uniform distribution and put

$$\begin{Bmatrix} v1 = u1, \\ v2 = \frac{\partial_t \varphi^{-1}(\varphi(u_1) + \varphi(u_2))}{\partial_t \varphi^{-1}(\varphi(u_1))} = \frac{e^{-\alpha u_2} - 1}{e^{-\alpha} - 1 + (e^{-\alpha u_1} - 1)(e^{-\alpha u_2} - 1)} \end{Bmatrix}$$

Solving for u_2 gives

$$u_2 = -\frac{1}{\alpha}\log\left(1 + \frac{v_2(1 - e^{-\alpha})}{v_2(e^{-\alpha u_1} - 1) - e^{-\alpha u_2}}\right)$$

Figure 4.7 shows 1500 random samples from a Frank Copula with parameter 5 using above algorithm.

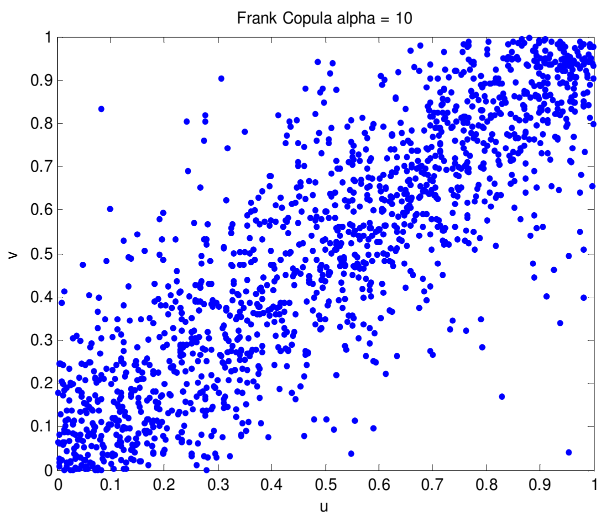

Figure 4.7 Frank Random numbers, α = 10

4.6 Marshall and Olkin's Method

This method involves the Laplace transform and its inverse function [26].

The Laplace transform of a positive random variable γ is defined by:

$$\tau(s) = E_\gamma(e^{-s\gamma}) = \int_0^\infty e^{-st} dF_\gamma(t) \tag{4.15}$$

where F_γ is the distribution function of γ. As we know Laplace transforms have well defined inverse. The inverse τ^{-1} serves as the generator for an Archimedean copula.

Let *F, G* be two univariate distributions, then

$$H(x) := \int G(x)^\gamma dF(\gamma) \tag{4.16}$$

is also a distribution- it is the mixture of distributions G_γ with weights determined by *F*.

We can also write using the Laplace transform as

$$H(x) = \tau(-\log G(x))$$

i.e, given H and F, there always exist a distribution function G such that equation (4.16) holds.

4.6.1 Gumbel bivariate simulation

We will apply Marshal and Olkin's method to generate random sample from Gumbel copula with parameter α [11].

- Generate a r.v. γ Stable(1, 0, 0) with parameter 1/α (hence, γ has Laplace transform $\tau(s) = \exp\{-s^{\frac{1}{\alpha}}\}$);
- Independently of the previous step, generate $U_1, U_2, \ldots\ldots, U_n$ independent Uniform (0, 1) r.v.s
- For k = 1, 2, …., n calculate $X_K = F_k^{-1}(U_k^*)$ where

$$U_k^* = \tau\left(-\frac{1}{\gamma}\ln U_k\right)$$

Figure 4.8 shows 1500 random samples from a Gumbel Copula with shape parameter 2 using above algorithm.

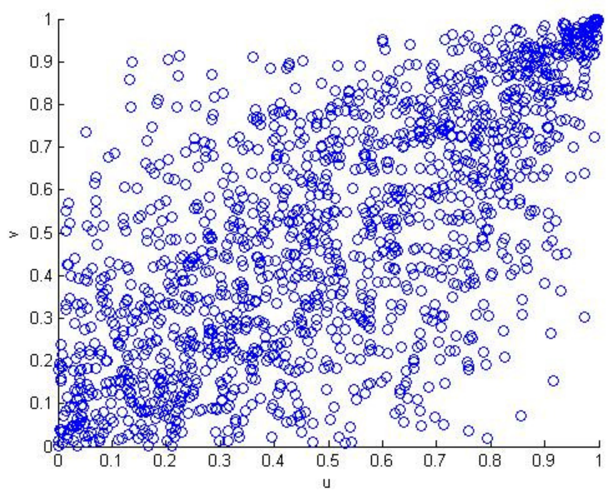

Figure 4.8 Gumbel random sample, α = 2

Chapter 5
UVDD Model and Calibration

In this chapter we will briefly discuss the theory and application of *Uncertain Volatility model with Displaced Diffusion* (UVDD) and later apply it to fit to the market smile of swaps and equities. Calibration of the model parameters will be done using swaption prices in case of swaps and vanilla call options prices in case of equities. These calibrated models will be used later in the pricing of various bivariate products.

5.1 Uncertain Volatility model with Displaced Diffusion

These models are proposed as an easy-to-implement alternatives to stochastic volatility models (SVMs), based on the assumption that the asset's volatility is stochastic in the simplest possible way, that is modeled by a *random variable* rather than a *diffusion process*.

The risk-neutral dynamics of an underlying asset *S*(t) under the UVDD assumption is given by

$$dS(t) = r[S(t) + \alpha_I]dt + \sigma_I[S(t) + \alpha_I]dZ(t) \tag{5.1}$$

where,

- I is a discrete random variable, independent of the Brownian motion Z, and taking values in the set $\{1,2,\ldots,m\}$ with probabilities $\lambda_i := Q(I=i)>0$ with $\sum_{i=1}^{m} \lambda_i = 1$;
- σ_i (*volatility*) and α_i(*displacement*) are positive constants for all i's;, which occur as a random vector pair with probability λ_i, the random value (σ_i, α_i) is drawn immediately after time zero.
- And r is the interest rate which is assumed to be constant.

The intuition behind the model is as follows. The underlying asset *S*(t) dynamics are given by displaced geometric Brownian motion where the model parameters are not known at the initial time, and one assumes different scenarios for them. The volatilities and displacements are random variables whose values will be known immediately after time zero.

The volatility of such a swap process, therefore, is not constant and one assumes several possible scenarios {*1, 2,…, m*) for its value. The implied volatilities are smile shaped with a minimum at the at-the-money level. And to account for skews in implied volatilities, UVDD models are usually extended by introducing (uncertain) shift parameters α_i.

UVDD model have a number of advantages that strongly support their use in practice. They preserve analytical tractability, are relatively easy to implement and are flexible enough to accommodate general implied volatility surfaces in the markets.

A drawback of the UVDD model is that future implied volatilities lose the initial smile shape almost immediately, i.e. as soon as the random value of the model parameters is drawn, since from that moment on the underlying asset dynamics evolves according to displaced geometric Brownian motions under their respective measure (when the shift parameters are zero the implied volatilities become flat in the future).

5.1.1 Probability distribution of *S*

Using (*eq*. 5.2) and the independence of the scenarios (*I* and *Z*), the probability distribution *p* of $S_{a,b}$ can be easily derived as the mixture of lognormal distributions given by:

$$p(S) = \sum_{i=1}^{m} \lambda_i LN(S + \alpha_i ; m_i, v_i) \tag{5.2}$$

where $LN(x;\, m_i,\, v_i)$ is the probability density for the i^{th} lognormal distribution with mean m_i given by

$$m_i = \ln(S(0) + \alpha_i) + (r - \sigma_i^{\,2}/2)T$$

and standard deviation v_i given by

$$v_i = \sigma_i \sqrt{T} \; .$$

5.2 UVDD Model - Swap Rates

The dynamics of a swap rate $S_{a,b}$(t) (Appendix A – Section A.1) under the UVDD assumption is given by:

$$dS_{a,b}(t) = \sigma^{I}_{a,b} \left[S_{a,b}(t) + \alpha^{I}_{a,b} \right] dZ^{a,b}(t) \tag{5.3}$$

where the variables have their usual meaning. Here the displacement term is absent, hence r = 0. The UVDD model can accommodate a smile consistent with the market data (section 5.3) allowing at the same time for a simple extension of the Black-like formulas. Another drawback of the model is that the swap rate $S_{a,b}$ is not guaranteed to be positive, as we are assuming log-normality only for ($S_{a,b}+\alpha_{a,b}$). More precisely, with displaced diffusion the swap rate $S_{a,b}$ can take values in $[-\alpha_{a,b}, \infty)$ and consequently, there is some probability mass associated with negative values.

5.3 Fitting the UVDD parameters – Swap rates

The swap rate dynamics (Equation 5.3) depends on the volatility and displacement parameters ($\sigma_i^{a,b}$ and $\alpha_i^{a,b}$), as well as on the number of scenarios *m* and the probability $\lambda_i^{a,b}$ assigned to each scenario. Our approach consisted in assuming ***2 scenarios*** (i.e. *m=2*) and then fitting the free parameters to market data. Namely,

1. For each point of the swaption volatility cube, the BS swaption price was calculated using (*eq*. 7.7) (with $m=1$, $\lambda_1^{a,b}=1$ and $\alpha_1^{a,b}=0$);
2. $\sigma_i^{a,b}$, $\alpha_i^{a,b}$ and $\lambda_i^{a,b}$ were then determined by minimizing the differences between the prices calculated in 1 and the prices given by (*eq*. 5.4);
3. To analyze the results, we calculated the *implied volatility* corresponding to each fitted price calculated in 2.

We remark that:

- The swaption volatility cube has the volatilities for different pairs (*swaption expiry, maturity of the underlying swap*) for strikes ranging from -200bp to 300bp in most of the cases. As these strikes refer to the *ATM* level, we had to exclude from the fit all the strike levels for which the *strike* = (*ATM swap rate* + *strike level*) < 0 for at least one swap rate (e.g., for a pair of 1Y-2Y swap the *ATM swap rate* is 2.65%, the -300bp strike was replaced with -200bp in almost all of the cases for the fit for all points of the surface);
- The minimization is done across all selected *strikes* for a given pair, i.e.,

$$\sum_{k=1}^{n_{strikes}} \left[Swaption^{BS}(0;a,b;K_k) - Swaption^{UVDD}(0;a,b;K_k) \right]^2 \tag{5.4}$$

- We imposed the following constraints on the parameters:
  a) $0.01 \le \sigma_i^{a,b} \le 0.7$, to ensure non-negative and not very high volatilities.
  b) $0.001 \le \alpha_i^{a,b} \le 0.1$, to get left skew in swap rates we want positive displacements and an upper bound of 0.1 to reduce frequency of negative rates during Monte Carlo Simulations.
  c) $0.2 \le \lambda_1^{a,b} \le 0.8$, to ensure that each scenario has significant positive weights.

We started by choosing a calibration method which can estimate the parameters in their respective bounds and minimize our objective function given by Equation (5.4). The valuation date used for swaption prices in all the calibration is 16-Mar-09.

5.3.1 UVDD Model for 1Y-2Y Swap Rate

Table 5.1 shows the market and model prices with implied volatilities obtained after calibration of *2-scenario* UVDD model for 1Y-2Y swap rate with *ATM swap rate* of 2.6575% and *strikes* between -200bp and +300bp.

Strike Level	Strike	Market Price	Model Price	Market Implied Vol	Model Implied Vol	% diff in Vol
-0.02	0.006575	380.0540	380.1720	0.6040	0.6206	2.75%
-0.015	0.011575	287.5370	287.3120	0.4880	0.4804	-1.56%
-0.01	0.016575	200.0650	199.1730	0.4140	0.4028	-2.70%
-0.005	0.021575	123.3380	122.4380	0.3610	0.3550	-1.65%
-0.0025	0.024075	91.7394	90.9408	0.3425	0.3381	-1.29%
0	**0.026575**	**64.9019**	**64.9977**	**0.3240**	**0.3245**	**0.15%**
0.0025	0.029075	44.3128	44.7271	0.3115	0.3136	0.67%
0.005	0.031575	28.6243	29.7111	0.2990	0.3049	1.97%
0.01	0.036575	11.1559	12.0281	0.2860	0.2929	2.40%
0.02	0.046575	1.4717	1.6407	0.2775	0.2823	1.72%
0.03	0.056575	0.2332	0.1941	0.2820	0.2768	-1.85%

Table 5.1 Market and UVDD Model Price/Volatilities with strikes for 1Y-2Y swap rate

The estimated parameters for the UVDD model for 1Y-2Y swap is given by table 5.2

$\sigma_1^{a,b}$ =	0.0578141
$\sigma_2^{a,b}$ =	0.0871436
$\alpha_1^{a,b}$ =	0.1
$\alpha_2^{a,b}$ =	0.1
$\lambda_1^{a,b}$ =	0.658039
$\lambda_2^{a,b}$ = $(1-\lambda_1^{a,b})$	0.341961

Table 5.2 Estimated UVDD parameters for 1Y-2Y swap rate

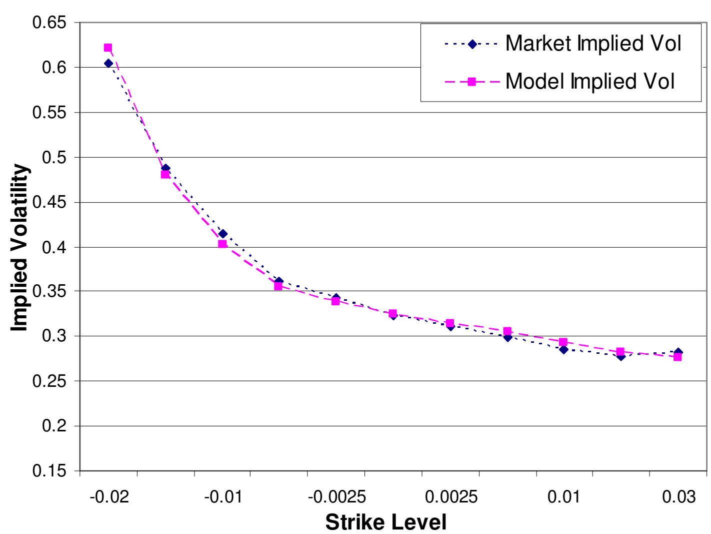

Figure 5.1 Market and UVDD Model implied Volatilities vs Strikes plot for 1Y-2Y swap rate

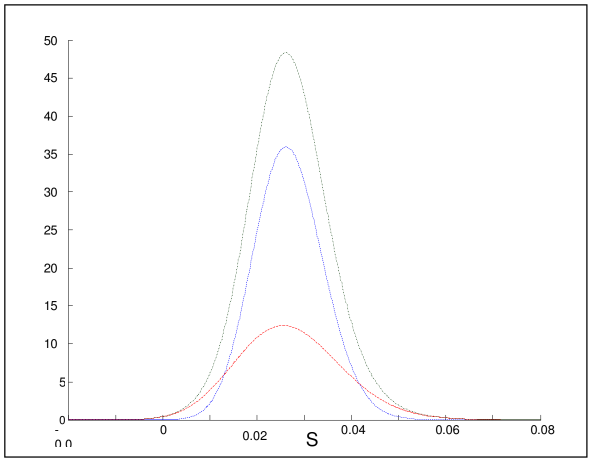

Figure 5.2 Implied Distributions for individual scenarios (Red, Blue) and combined (Green) for 1Y-2Y Swap rate under UVDD framework

From Figure 5.2 we notice that the distribution for the 1Y-2Y swap rate (top most line) has a small probability mass attached to negative rates (left most part), because the estimated displacement parameters are greater than ATM swap rate (see Table 5.1 and 5.2).

5.3.2 UVDD Model for 1Y-10Y Swap Rate

Table 5.3 shows the market and model implied volatilities obtained after calibration of *2-scenario* UVDD model for 1Y-10Y swap rate with *ATM swap rate* of 3.79411% and *Strike level* between -200bp and +300bp.

Strike Level	Strike	Market Price	Model Price	Market Implied Vol	Model Implied Vol	% diff in Vol
-0.02	0.0179411	1651.670	1649.910	0.4200	0.4092	-2.576%
-0.015	0.0229411	1268.530	1261.210	0.3810	0.3617	-5.071%
-0.01	0.0279411	912.176	901.675	0.3437	0.3286	-4.407%
-0.005	0.0329411	602.241	593.698	0.3135	0.3052	-2.649%
-0.0025	0.0354411	471.985	465.569	0.3017	0.2962	-1.841%
0	**0.0379411**	**358.362**	**356.661**	**0.2900**	**0.2886**	**-0.478%**
0.0025	0.0404411	263.024	267.044	0.2790	0.2823	1.166%
0.005	0.0429411	185.105	195.670	0.2680	0.2770	3.344%
0.01	0.0479411	85.868	99.338	0.2546	0.2691	5.707%
0.02	0.0579411	17.019	22.374	0.2480	0.2620	5.639%
0.03	0.0679411	3.914	4.826	0.2540	0.2611	2.814%

Table 5.3 Market and UVDD Model Price/Volatilities with strikes for 1Y-10Y swap rate

The estimated parameters for the UVDD model for 1Y-10Y swap is given by Table 5.4

$\sigma_1^{a,b}$ =	0.0689751
$\sigma_2^{a,b}$ =	0.1055930
$\alpha_1^{a,b}$ =	0.1
$\alpha_2^{a,b}$ =	0.1
$\lambda_1^{a,b}$ =	0.722606
$\lambda_2^{a,b}$ = $(1-\lambda_1^{a,b})$	0.277394

Table 5.4 Estimated UVDD parameters for 1Y-10Y swap rate

Figure 5.3 plots the implied volatilities from Table 5.3 for qualitative analysis.

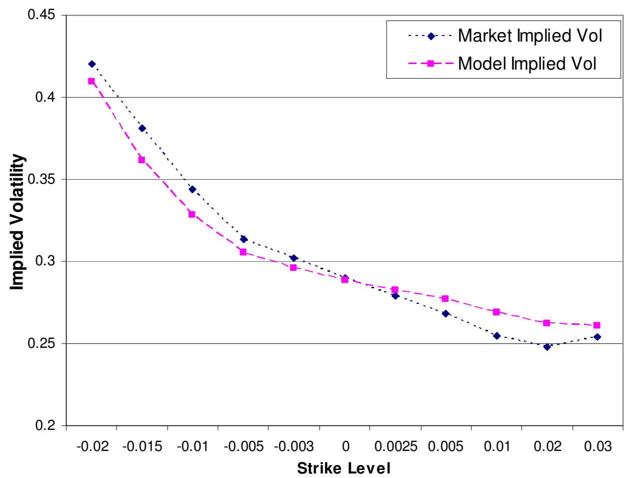

Figure 5.3 Market and UVDD Model implied Volatilities vs Strikes plot for 1Y-10Y swap rate

Figure 5.4 in next page also suggest that the distribution for the 1Y-10Y swap rate (top most line) has a small probability mass attached to negative rates (left most part), because the estimated displacement parameters are greater than *ATM swap rate* (see Table 5.3 and 5.4).

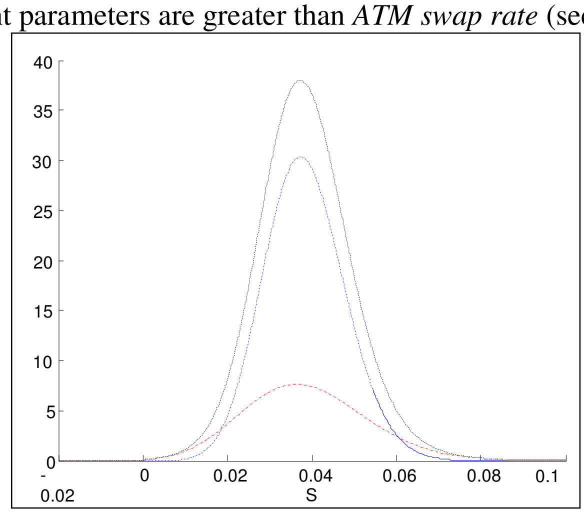

Figure 5.4 Implied Distributions for individual scenarios (Red, Blue) and combined (Green) for 1Y-10Y Swap rate under UVDD framework

5.3.3 UVDD Model for some selected swap rates

The two swap rates discussed in previous sections are of most importance and hence we presented the complete results with data to get a deeper understanding of the model. In this section we will select few more swap rates which we will use in the pricing chapter. But we restrict ourselves by providing only the estimated UVDD model (*2-scenario*) parameters for each rate and skipping the plots and data tables. We will provide the plots of the market and model implied volatilities and also plot the relative percentage difference (Rel %Diff) between them to get an idea of error in our fits. The strike level used for all the rates is between -200bp and +300bp.

We start with 1Y-30Y swap rate and give the estimated UVDD model parameters in Table 5.5 and the respective implied volatility plot in Figure 5.5. The *ATM swap rate* is equal to 3.7812% and *ATM volatility* is equal to 35.6%.

$\sigma_1^{a,b}$ =	0.051901
$\sigma_2^{a,b}$ =	0.107019
$\alpha_1^{a,b}$ =	0.1
$\alpha_2^{a,b}$ =	0.1
$\lambda_1^{a,b}$ =	0.183141
$\lambda_2^{a,b}$ = $(1-\lambda_1^{a,b})$	0.816859

Table 5.5 Estimated UVDD parameters for 1Y-30Y swap rate

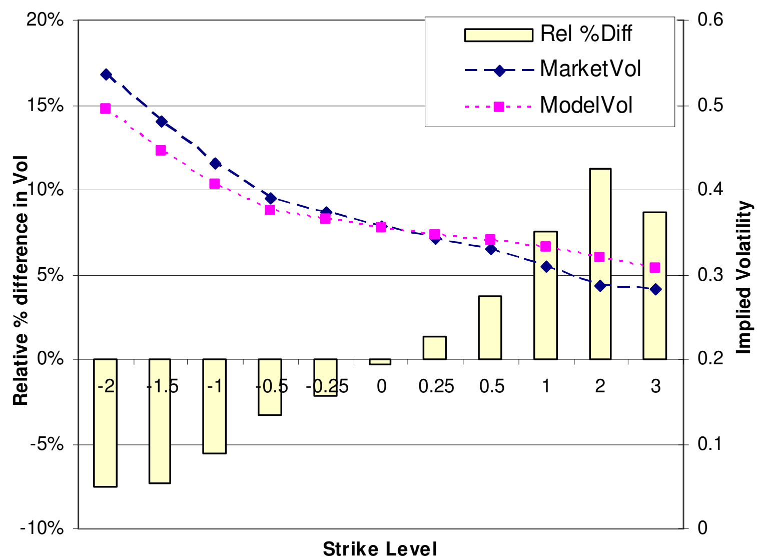

Figure 5.5 Implied Volatility and Relative % Difference for 1Y-30Y swap rate

The next rate in consideration is the 5Y-2Y swap rate. The estimated UVDD model parameters are given in Table 5.6 and the respective implied volatility plot in Figure 5.6. The *ATM swap rate* is equal to 4.12% and *ATM volatility* is equal to 16.7%.

$\sigma_1^{a,b}$ =	0.024279
$\sigma_2^{a,b}$ =	0.080325
$\alpha_1^{a,b}$ =	0.1
$\alpha_2^{a,b}$ =	0.1
$\lambda_1^{a,b}$ =	0.568418
$\lambda_2^{a,b}$ = $(1-\lambda_1^{a,b})$	0.431582

Table 5.6 Estimated UVDD parameters for 5Y-2Y swap rate

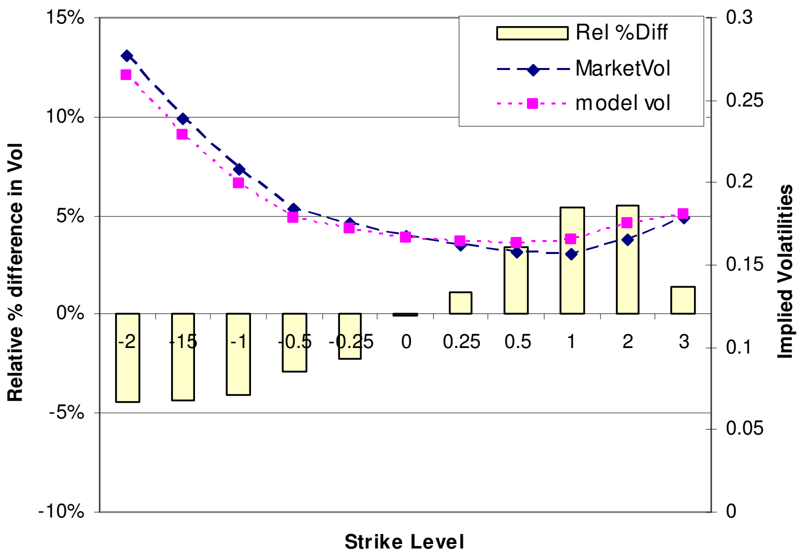

Figure 5.6 Implied Volatility and Relative % Difference for 5Y-2Y swap rate

Table 5.7 gives the estimated UVDD model parameters for the 5Y-10Y swap rate, the *ATM swap rate* is equal to 4.4683% and ATM volatility is given by 18.4%. The implied volatility plot is given in Figure 5.7.

$\sigma_1^{a,b}$ =	0.022448
$\sigma_2^{a,b}$ =	0.088631
$\alpha_1^{a,b}$ =	0.1
$\alpha_2^{a,b}$ =	0.1
$\lambda_1^{a,b}$ =	0.486882
$\lambda_2^{a,b}$ = $(1-\lambda_1^{a,b})$	0.513118

Table 5.7 Estimated UVDD parameters for 5Y-10Y swap rate

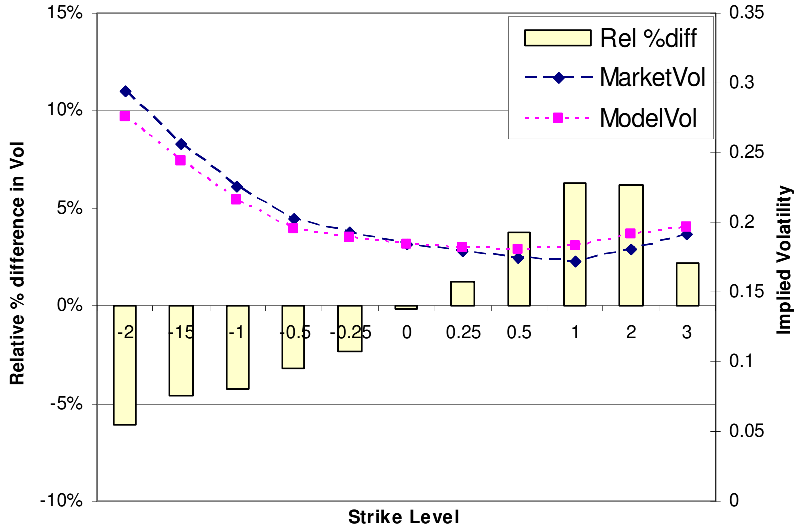

Figure 5.6 Implied Volatility and Relative % Difference for 5Y-10Y swap rate

The last rate in consideration is the 5Y-30Y swap rate whose *ATM swap rate* is equal to 3.8229% and *ATM volatility* is equal to 24.6%. The estimated parameters for the UVDD model is given in Table 5.8 and the implied volatility plot in Figure 5.8.

$\sigma_1^{a,b}$ =	0.024817
$\sigma_2^{a,b}$ =	0.092298
$\alpha_1^{a,b}$ =	0.1
$\alpha_2^{a,b}$ =	0.1
$\lambda_1^{a,b}$ =	0.372596
$\lambda_2^{a,b}$ = $(1-\lambda_1^{a,b})$	0.627404

Table 5.8 Estimated UVDD parameters for 5Y-30Y swap rate

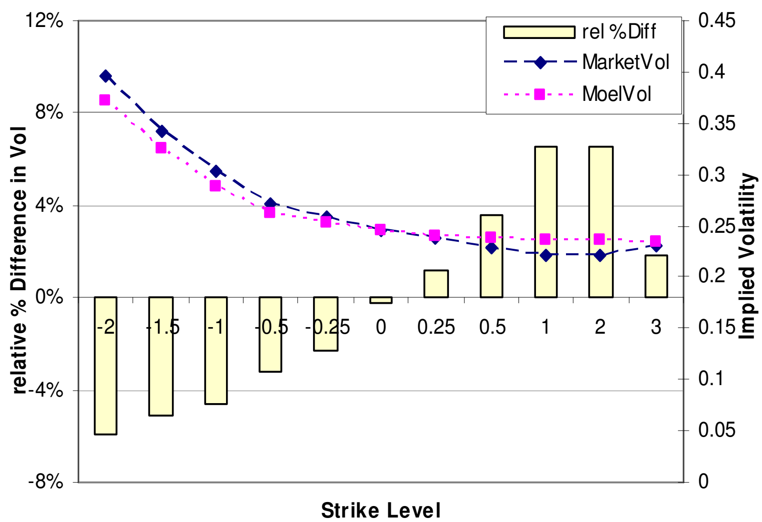

Figure 5.8 Figure 5.6 Implied Volatility and Relative % Difference for 5Y-30Y swap rate

5.4 UVDD Model Calibration – Equity

This section will deal with the calibration of the UVDD model for the equity case. As shown in chapter one the presence of lower and upper tail dependence in these financial stocks make it very important for the pricing models to incorporate such dependence.

We will represent the marginal dynamics under the UVDD assumption and estimate the model parameters from the historical log returns. The data used in the calibration are the call prices on different strikes on the respected stocks. The expiry for the call option used in calibration is 16-Jan-10 and the strikes vary accordingly to the data available. The interest rate used for discounting between the period 07-Sept-09 and 16-Jan-10 is equal to 0. 3346%.

5.4.1 Bank of America Corp Equity

The UVDD Model for the *Bank of America Corp* (*BAC- NYSE*) is given in Table 5.9. The option maturity used is 16-Jan-10 and the spot at 07-Sept-09 is *17.09 USD.*

Strike	Market Price	Model Price	Market Implied Vol	Model Implied Vol	% Diff Vol
8.54	8.71765	8.71903	0.7696	0.771123	0.20%
10.25	7.15661	7.13508	0.7076	0.692918	-2.07%
11.96	5.6878	5.65411	0.6549	0.639499	-2.35%
13.67	4.34949	4.31929	0.6105	0.600315	-1.67%
15.38	3.1841	3.16862	0.5741	0.569842	-0.74%
17.09	**2.22354**	**2.22568**	**0.5446**	**0.545130**	**0.10%**
18.80	1.47908	1.49396	0.5208	0.524480	0.71%
20.51	0.936121	0.95737	0.5011	0.506855	1.15%
22.22	0.563826	0.585623	0.4845	0.491557	1.46%
23.93	0.322836	0.342119	0.4700	0.478100	1.72%
25.63	0.17575	0.191741	0.4568	0.466197	2.06%

Table 5.9 Market and UVDD Model Price/Volatilities with strikes for BAC equity

The estimated parameters for the UVDD model for *BAC* stock are given by table 5.10. The fit was done by using new bounds:

- $0.01 \leq \sigma_i^{a,b} \leq 0.7,$
- $0.001 \leq \alpha_i^{a,b} \leq 50$ and
- $0.05 \leq \lambda_1^{a,b} \leq 0.8.$

$\sigma_1^{a,b}$	=	0.110728
$\sigma_2^{a,b}$	=	0.137750
$\alpha_1^{a,b}$	=	50
$\alpha_2^{a,b}$	=	50
$\lambda_1^{a,b}$	=	0.05
$\lambda_2^{a,b}$	= $(1-\lambda_1^{a,b})$	0.95

Table 5.10 Estimated UVDD parameters for BAC equity

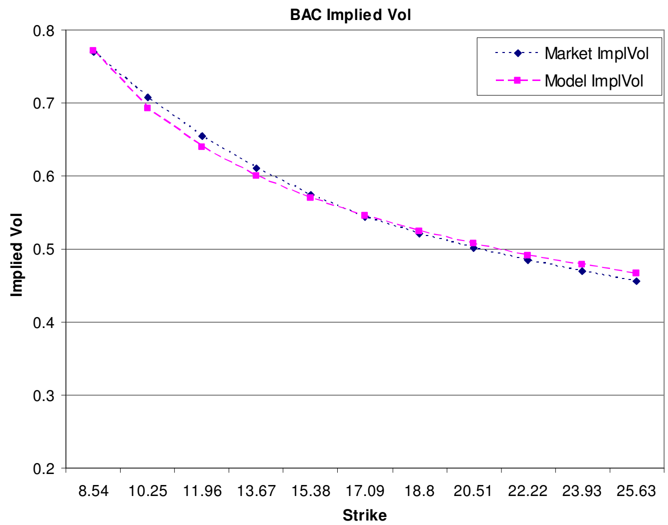

Figure 5.9 Market and UVDD Model implied Volatilities vs Strikes plot for BAC equity

Figure 5.10 plots the implied probability distribution for the BAC equity and as we can notice that there is a very small probability mass attached to negative stock prices. This is one drawback of the UVDD model as already discussed in the interest rate framework.

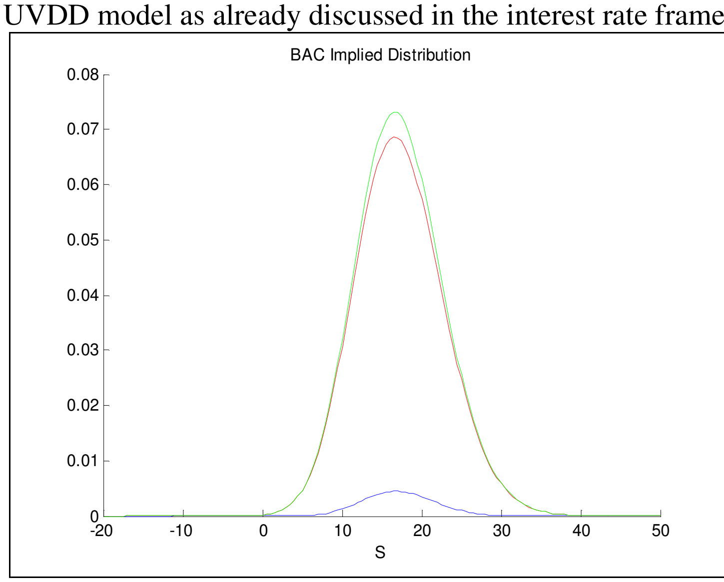

Figure 5.10 Implied Distributions for individual scenarios (Red, Blue) and combined (Green) for BAC under UVDD framework

5.4.2 Wells Fargo & Company Equity

The UVDD Model for the *Wells Fargo & Company* (*WFC- NYSE*) is given in Table 5.11. The Maturity used is 16-Jan-10 and the spot at 07-Sept-09 is *26.91 USD.*

Strike	Market Price	Model Price	Market Implied Vol	Model Implied Vol	% Diff Vol
13.46	13.6394	13.6391	0.7114	0.711126	-0.04%
16.15	11.166	11.13	0.6657	0.648552	-2.58%
18.84	8.85471	8.78773	0.627	0.60676	-3.23%
21.53	6.76605	6.68588	0.5935	0.576122	-2.93%
24.22	4.9539	4.88653	0.5639	0.552113	-2.09%
26.91	**3.45553**	**3.42417**	**0.5374**	**0.532458**	**-0.92%**
29.6	2.28336	2.29853	0.5135	0.515885	0.46%
32.29	1.4208	1.47822	0.4917	0.501623	2.02%
34.98	0.827191	0.911577	0.4716	0.48916	3.72%
37.67	0.447874	0.539811	0.453	0.478137	5.55%
40.37	0.223617	0.306854	0.4357	0.468259	7.47%

Table 5.11 Market and UVDD Model Price/Volatilities with strikes for WFC equity

The estimated parameters for the UVDD model for *WFC* stock is given by Table 5.12. Figure 5.11 plots the implied volatilities from Table 5.11 for qualitative analysis. The fit was done by using the bounds:

- $0.01 \leq \sigma_i^{a,b} \leq 0.7,$
- $0.001 \leq \alpha_i^{a,b} \leq 45$ and
- $0.05 \leq \lambda_1^{a,b} \leq 0.8.$

$\sigma_1^{a,b}$ =	0.196945
$\sigma_2^{a,b}$ =	0.196947
$\alpha_1^{a,b}$ =	45
$\alpha_2^{a,b}$ =	45
$\lambda_1^{a,b}$ =	0.317478
$\lambda_2^{a,b}$ = $(1-\lambda_1^{a,b})$	0.682522

Table 5.12 Estimated UVDD parameters for WFC equity

From Table 5.12 we notice that the UVDD Model for the WFC equity is equivalent to a single displaced lognormal distribution.

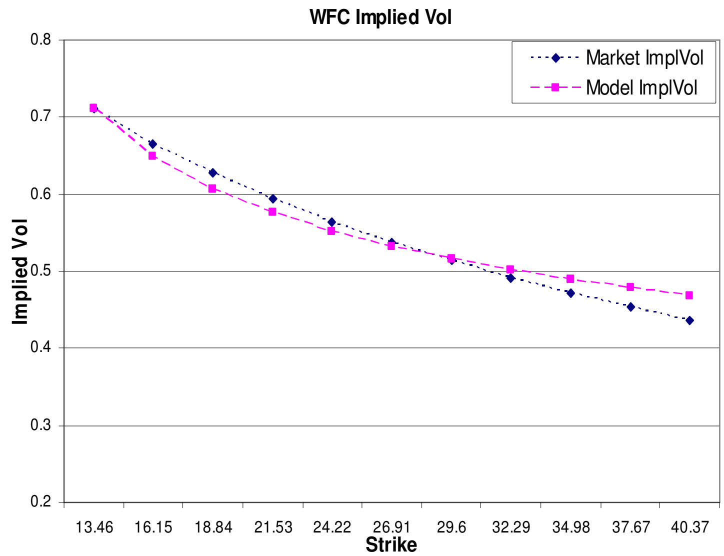

Figure 5.11 Market and UVDD Model implied Volatilities vs Strikes plot for WFC equity

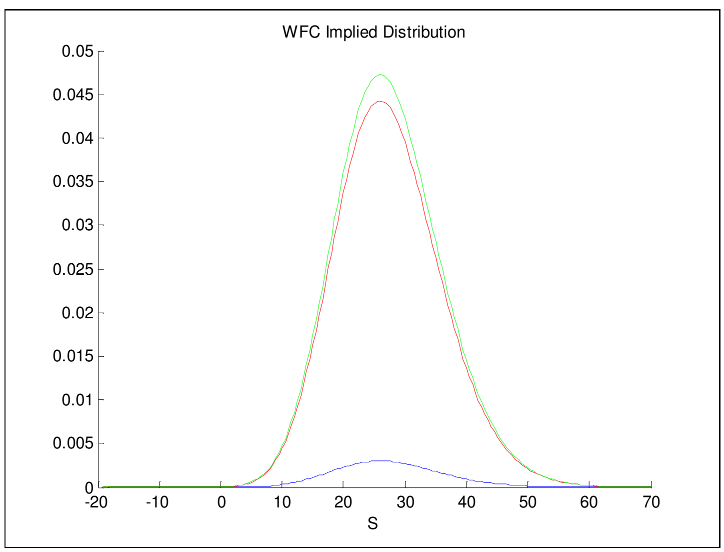

Figure 5.12 Implied Distributions for individual scenarios (Red, Blue) and combined (Green) for WFC under UVDD framework

Chapter 6
Calibration - Copula

In this chapter we will derive the copula parameters for the equity and interest rates (IR) framework. We have used two methods for calibration: Measure of Concordance Method and CML Method. We will stick to the latter method for calibrating our models for reasons discussed later in this chapter.

6.1 Calibration using Measure of Concordance

The calibration of the copula parameter will require historical time-series, where the daily log returns on the equity and interest rates will be used. The reason for using daily log returns for calibrating the copula parameters will be explained in details in Chapter 7 – section 7.1.

The calibration under this method is done in the following steps:

- Calculate Kendall's tau or Spearman's rho from the historical log returns time-series by using empirical methods given in section 3.2.1 and 3.2.2.
- Calculate linear correlation coefficient from the calculated Kendall's tau/Spearman's rho using the formulas given in Table 4.1, which ever is easy to invert analytically as for some copulas a closed solution for these measures does not exist. Kendall's tau τ for the Gaussian copula with shape parameter ρ is given by:

  $$\tau = \frac{2}{\pi}\arcsin\rho ,$$

  and Kendall's tau τ for the Clayton copula with shape parameter α is given by:

  $$\tau = \frac{\alpha}{\alpha + 2} .$$

- We assume that the Kendall's tau (or Spearman's rho) are invariant while shifting between copulas, hence we can equate the above relationships and get

  $$\tau = \frac{2}{\pi}\arcsin\rho = \frac{\alpha}{\alpha + 2}$$

  and get a one to one relation between the linear correlation coefficient ρ of the Gaussian copula and the shape parameter α of the Clayton copula. Similarly we can derive relationships between shape parameters of different copulas.

6.2 Calibration using CML Method

The theory behind this method has been discussed in details in section 4.3.3. We will first apply this method to a test case to study the convergence of the CML method and then move to the equity case to calibrate the copula parameter and at last the Interest Rate case with swaps.

Figure 6.1 demonstrates the copula parameter for Clayton copula with respect to shape parameter rho for Gaussian copula.

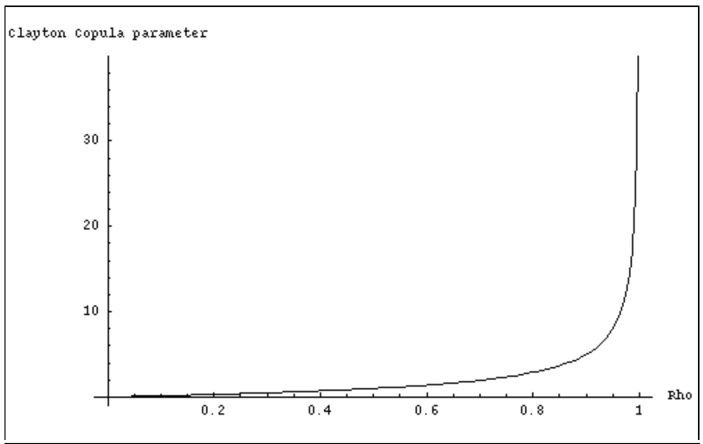

Figure 6.1: Clayton Copula parameter α vs. linear correlation coefficient ρ

This method is chosen over the method described in section section 6.1 because in the first method all information on the returns of the underlying is summed up into a single number (measure of concordance). Instead running the calibration each time over the historical log returns for each copula separately and then comparing the outcome of the likelihood function used makes sure that each copula uses the complete available information.

6.2.1 CML convergence

We started by carrying out a test to see how many number of data points are needed approximately to calibrate back the copula parameters within acceptable limits. This information is useful when we apply calibration to real life problems. Figure 6.2 shows the calibrated parameter for Clayton and Gumbel copulas versus number of observations. We started by first choosing the Kendall's tau equal to 0.5 and this choice gives us the true parameter value of 2.0 for both the copulas. Then we simulated some fixed number of random samples from each copula and used CML method on the simulated samples to calibrate back the true parameter.

We observed that the calibration parameter approaches the true parameter with the increase in the observation points. Though, we observed that we get *acceptable* result after roughly 2400 observations. Also the Gumbel parameter converges much faster then the Clayton parameter to the true value. We ran the same test for higher values of Kendall's tau and observed same pattern in the convergence of Gumbel and Clayton parameters hence we excluded it from the report and concentrated on one result.

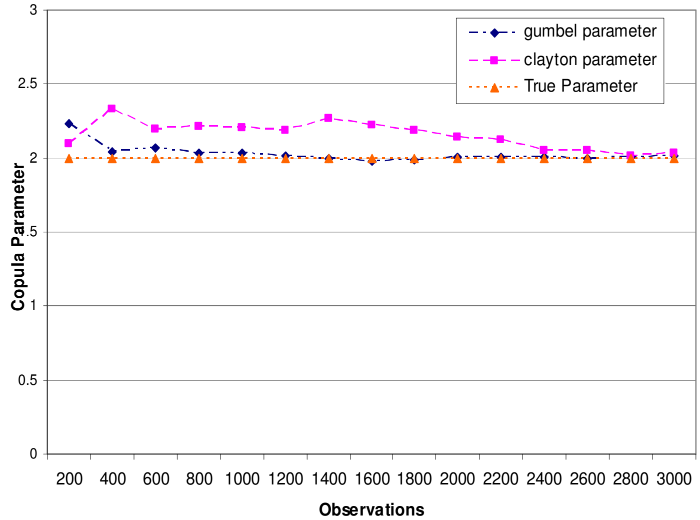

Figure 6.2 CML method convergence for different copulas

6.3 Copula Calibration - Equity Case

The equity pair BAC-WFC has been chosen due to presence of high empirical lower and upper dependence in their data sets. The data used is the historical daily log returns on each stock.

Table 6.1 shows the calibration results for the BAC-WFC pair using the CML method. The data used is from date 07-Sept'09 till 11-Sept'00 from the *yahoo-finance* website, this is approximately equal to *2260* trading days. Using the results from section 6.2.1 we conclude that we have enough data points to carry out the calibration.

Copula	**Estimated Parameter**	**Theoretical Lower Tail (λ_L)**	**Theoretical Upper Tail (λ_U)**
Normal	**0.74685**	0.000	0.000
Clayton	**1.88459**	0.692	0.000
Gumbel	**2.26684**	0.000	0.642

Table 6.1 Estimated parameters for various copulas for BAC and WFC equity pair

Figure 6.3 plots the historical stock price levels for BAC and WFC equities.

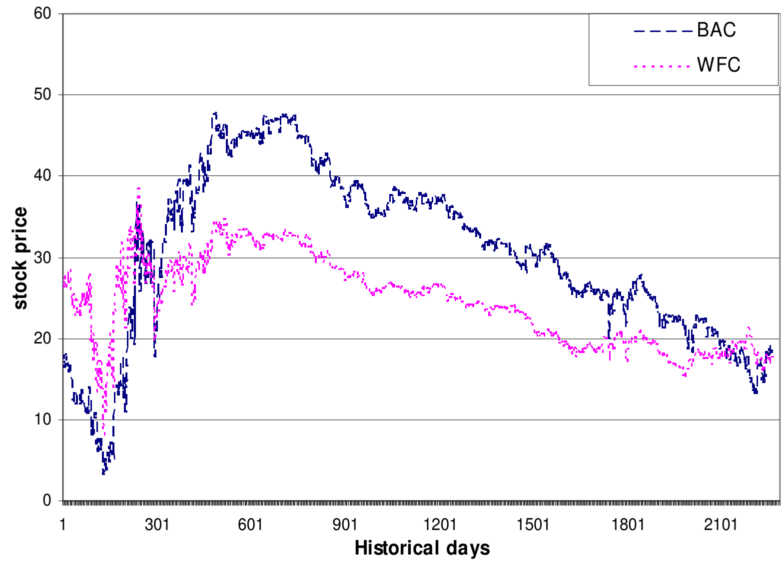

Figure 6 Historical stock price for BAC and WFC equities.

We carried the calibration of the copula parameters for different window days and noticed a significant difference in the estimated parameters.

Table 6.2 presents the relation between the estimated parameters with increasing day's history for each of the three copulas.

Days history	Gaussian	Clayton	Gumbel
300	0.850130	2.42844	2.81950
600	0.827381	2.38284	2.78176
900	0.799282	2.31442	2.62138
1200	0.782976	2.23496	2.52921
1500	0.765178	2.09087	2.38932
1800	0.776166	2.13293	2.45214
2100	0.760398	1.98788	2.32476
2260	**0.746846**	**1.88459**	**2.26684**

Table 6.2 Estimated parameters for various copulas using different days for BAC and WFC equity pair

We see that the dependence between the two stocks is a decreasing function of the number of trading days used in calibration.

The difference between the estimated parameters for different days will be useful to do analysis between the prices obtained for various products using different copulas in the next chapters.

6.4 Copula Calibration – Interest Rate Case

In this section we will calibrate the copula parameters using same maturity different tenor swap rates as the underlying. The data used are the daily log returns on each swap rate for a period between 03-Jan-05 and 31-Dec-07.

Table 6.3 shows the calibration results for the 1Y-2Y and 1Y-10Y swap pair using the CML method for 400 and 780 trading days. The shape parameters for Gaussian copula suggest that the two rates have a highly correlated.

Days history	Gaussian	Clayton	Gumbel
400	0.88625	2.99344	2.95116
780	0.86527	2.64661	2.78210

Table 6.3 Estimated parameters for various copulas using different days for 1Y-2Y and 1Y-10Y swap pair

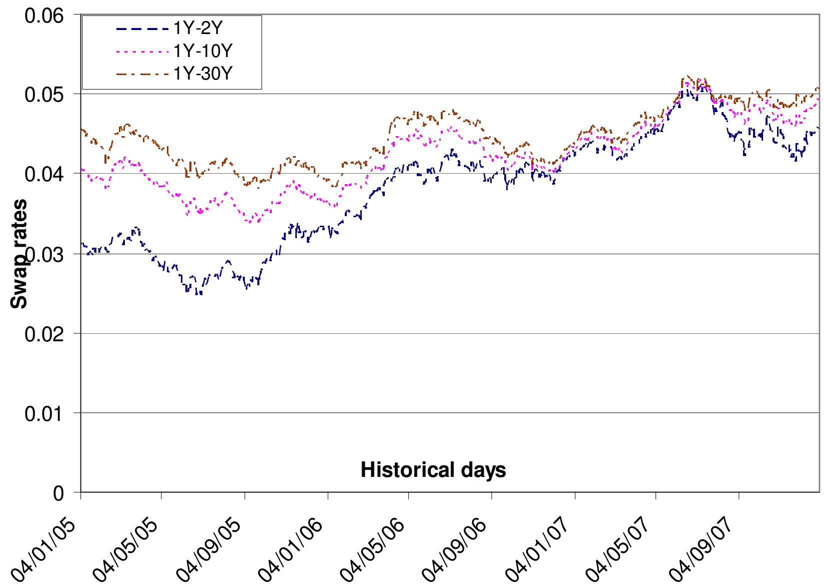

Figure 6.4 Different swap rates between 03-Jan-05 and 31-Dec-07

Table 6.5 shows the calibration results for the 1Y-2Y and 1Y-30Y swap pair using the CML method for the complete period i.e., 780 trading days.

Days history	Gaussian	Clayton	Gumbel
400	0.80462	2.03595	2.34602
780	0.76848	1.74320	2.15545

Table 6.4 Estimated parameters for various copulas for 1Y-2Y and 1Y-30Y swap pair

Table 6.3 shows the calibration results for the 1Y-2Y and 1Y-10Y swap pair using the CML method for the complete period i.e., 780 trading days, from 03-Jan-05 till 31-Dec-07.

Days history	Gaussian	Clayton	Gumbel
400	0.781013	1.89201	2.53623
780	0.782090	1.94852	2.57149

Table 6.5 Estimated parameters for various copulas using different days for 5Y-2Y and 5Y-10Y swap pair

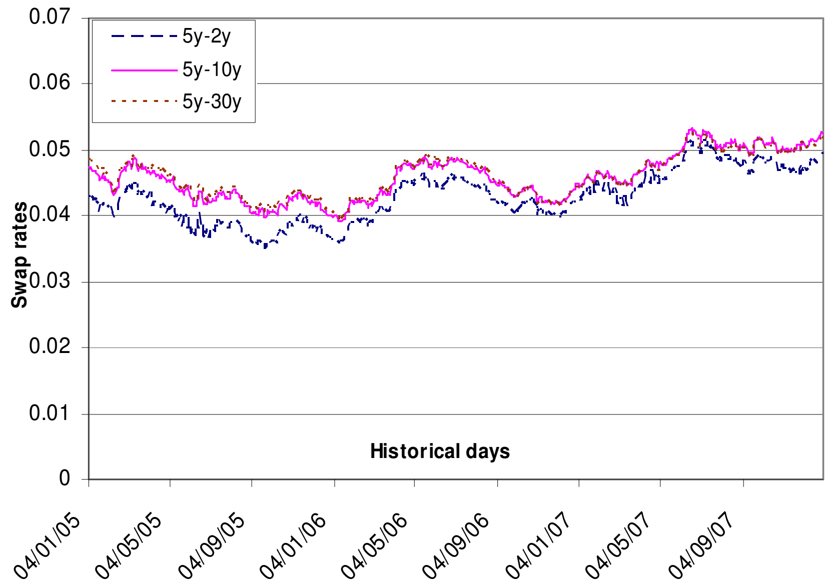

Figure 6.4 Different swap rates time series from 03-Jan-05 till 31-Dec-07

Table 6.5 shows the calibration results for the 5Y-2Y and 5Y-30Y swap pair using the CML method for the complete period i.e., 780 trading days.

Days history	Gaussian	Clayton	Gumbel
400	0.751766	1.82847	2.40185
780	0.694575	1.64086	2.28943

Table 6.6 Estimated parameters for various copulas for 5Y-2Y and 5Y-30Y swap pair

We notice from Table (6.4) and Table (6.5) that the 5Y-2Y and 5Y-10Y swap pair have more correlation than the 5Y-2Y and 5Y-30Y pair.

Also the correlation between short maturity swaps is much higher than the longer maturity swap with the same tenors.

Chapter 7
Pricing – Equity

In this chapter we will assess the implications of changing copulas on equity derivatives prices. We address this main question: how does changing from the Normal copula to one that accounts for tail dependence affect the prices of derivatives. The parameters estimated in the previous chapters for the equity case will be used to price some of the most commonly traded European style bivariate options.

In this report we start by broadly dividing the pricing process into four cases, presented in Figure 7.1. The various cases broadly differ on inclusion of two properties: smile of the underlying and tail dependence between them. **Case A -** "**GBM + Gaussian**" is the simplest way of pricing where Geometric Brownian Motion (GBM) is assumed for the marginals (no smile) and the joint distribution is assumed to be "Gaussian", which has zero tail dependence. In **Case B** - "**UVDD + Gaussian"** smiles are included by using the UVDD model but still no tail dependence [36]. **Case C** - "**GBM + non-Gaussian**" includes the tail dependence between the underlying, but skips the smile in their marginal distributions [35]. **Case D** - "**UVDD + non-Gaussian**" incorporates both smile through UVDD model and tail dependence by use of non-Gaussian copula, in our case Clayton and Gumbel. We will price mostly under the last case settings and wherever necessary will compare them with other cases.

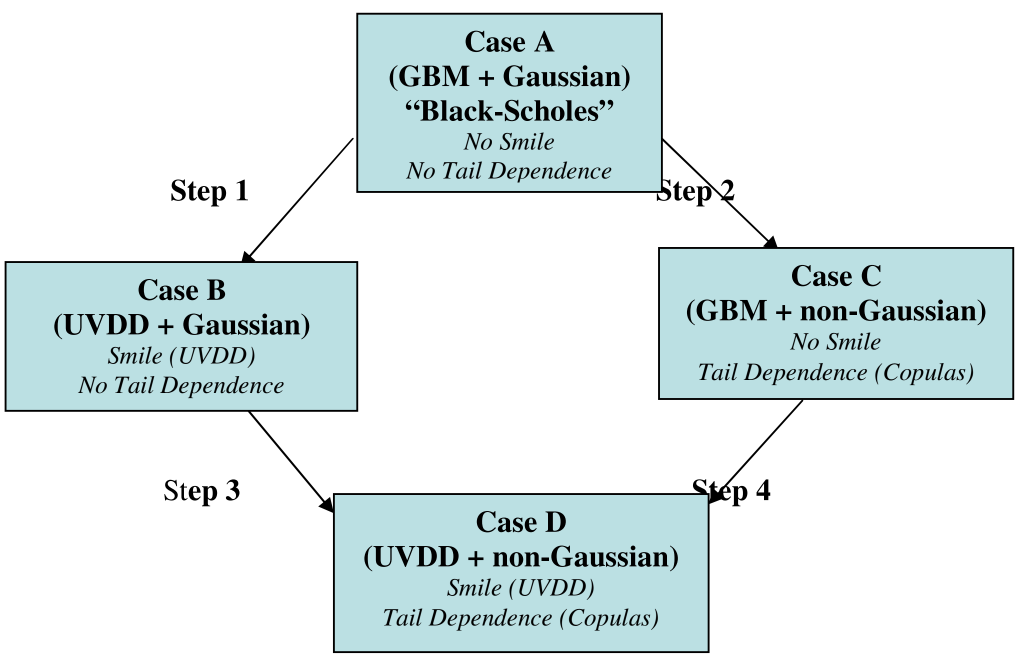

Figure 7.1 Four major cases in option pricing

7.1 Building a pricing model using Copulas

We start by first introducing the Black Scholes model which is the starting point of almost every pricing model and then move on to discuss our pricing methods and the calibration of our models together with the problems faced while calibrating the copula parameters for respective pricing methods.

The objective of this section is to develop a relationship between the Black Scholes model and Gaussian copula and later replace the Gaussian copula with a non-Gaussian copula while keeping the marginal distribution fixed.

7.1.1 Black Scholes model and Gaussian Copula

The famous Black Scholes model describing the process of two underlyings, S_1 and S_2, under the risk-neutral measure Q is given by [13]:

$$dS_1 = rS_1dt + \sigma_1 S_1 dW_1^{\Theta} \tag{7.1a}$$

$$dS_2 = rS_2dt + \sigma_2 S_2 dW_2^{\Theta} \tag{7.1b}$$

$$dW_1^{\Theta} dW_2^{\Theta} = \rho dt \tag{7.1c}$$

$$dB = rBdt$$

where,

- r is the risk-free constant interest rate,
- ρ is the linear correlation coefficient between the two assets,
- σ_1 and σ_2 are the volatility of the S_1 and S_2 respectively,
- W_1 and W_2 are two correlated Wiener processes.
- B is a deterministic process (bank account) with starting value $B(0) = 1$.

Under the Black-Scholes (BS) Model the marginal distribution of the assets has a lognormal distribution and the joint terminals as well as the joint transition distribution functions follow a bivariate normal distribution.

For the BS model we know that the marginal transition density function for $\ln S_1(t_{j+1}) - \ln S_1(t_j)$ between time step j to j+1, j = 0,1,2,.....,n-1 , where $t_n = T$ and $\Delta t = t_{j+1} - t_j$, is normally distributed, with mean $(r - \sigma^2/2)\Delta t$ and variance $\sigma^2 \Delta t$ and written as [34]:

$$\ln S_1(t_{j+1}) - \ln S_1(t_j) \sim \Phi\left[\left(r - \frac{\sigma^2}{2}\right)\Delta t, \sigma\sqrt{\Delta t}\right] \tag{7.2}$$

where, $S_1(t_{j+1})$ is the stock price for asset 1 at a future time t_{j+1}, $S_1(t_j)$ is the stock price at time t_j, and $\Phi(m, s)$ denotes a normal distribution with mean m and standard deviation s. Similarly the joint transition density of $ln\ S_1$ and $ln\ S_2$ follows a bivariate normal distribution.

7.1.2 Pricing methods

The following two pricing methods are widely used to price European style bivariate products under the BS model framework:

1. **Using the Joint terminal density function:**

   The joint terminal density approach described in this section is taken from Cherubini, Luciano, Vecchiato [11, pp 232].

   We obtain the option price by double integrating the product of the payoff and corresponding terminal joint density function (copula function) over the whole range of asset values (zero to infinite). The price of the European style bivariate contingent claim using the above method is given by the following integral:

   $$g(S_1(t), S_2(t), t) = P(t,T)\int_0^{\infty}\int_0^{\infty} G(S_1(T), S_1(T), T)\, q(S_1(T), S_1(T))\, dS_1(T)\, dS_1(T)$$

   where,

   - $g(S_1(t), S_2(t), t)$ is the price at time t of the option,
   - $P(t,T)$ is the price of zero coupon bond at time t expiring in time T-t with unit payoff,
   - $G(S_1(T), S_1(T), T)$ is the pay off function,
   - $q(S_1(T), S_1(T))$ is the copula density function[11, pp-81].

   The lognormal marginal dynamics used in the above integral can be derived using Equation (7.2) by putting t_{j+1} = T and t_j = 0, i.e.,

   $$\ln S_1(T) - \ln S_1(0) \sim \Phi\left[\left(r - \frac{\sigma^2}{2}\right)T, \sigma\sqrt{T}\right] \tag{7.3}$$

   The terminal joint density q is given by:

   $$\frac{d^2 Q(S_1, S_2)}{dS_1 dS_2} = q(S_1, S_2)$$

   where

   $$Q(S_1, S_2) = C(F(S_1), G(S_2))$$

   and *C* is any copula function and *F* and *G* are the univariate marginal distributions of the terminal sport prices $S_1(T)$ and $S_2(T)$.

   For our purpose we cannot use this method as for longer maturity options the calibration of the parameters using the available historical data set becomes difficult. The reason is explained in detail in Section 7.1.3.

2. **Using the Joint transition density function:**

   We can also use the joint transition densities and apply Euler's scheme for discretization of the asset equations and then using Monte Carlo Simulation over a number of time steps and number of simulation to calculate the price. This method is used to price a wide range of complex and exotic options which are hard to price analytically using joint Terminal density function.

The discretized asset dynamics using Equation (7.2) between any time step j to j+1 are given by:

$$\ln S_1(t_{j+1}) - \ln S_1(t_j) = \left(r - \frac{\sigma_1^2}{2}\right)\Delta t + \sigma_1 (W_1^Q(t_{j+1}) - W_1^Q(t_j)) \tag{7.4}$$

Furthermore we can generate the terminal density from Equation (7.4) by summing up the asset values $\ln S_1(t_{j+1}) - \ln S_1(t_j)$ over the complete set of time steps.

$$\ln S_1(T) - \ln S_1(0) = \sum_{j=0}^{n-1} (\ln S_1(t_{j+1}) - \ln S_1(t_j))$$

$$= \sum_{j=0}^{n-1}\left(\left(r - \frac{\sigma_1^2}{2}\right)\Delta t + \sigma_1 (W_1^Q(t_{j+1}) - W_1^Q(t_j))\right)$$

A drawback of this discretized pricing method is that the computational time increases with increasing number of time step n and with the number of simulations.

In Section 7.1.4 we will discuss how to switch between different copulas.

7.1.3 Calibration of Joint Density functions

Both the pricing methods discussed above can be used efficiently to price the common bivariate options but a problem arises when calibration of the copula parameter is done using historical returns. In our case calibration of the copula function parameter is a problem if the maturity of the option increases. This is due to the following two reasons:

1. To apply Monte Carlo methods we need sufficiently large number of i.i.d. data points. For a given data set the availability of data points decreases with increase in option maturity which affects the accuracy of the calibration methods.
2. When overlapping periods are considered, to increase the data points, there is problem of high autocorrelation between them, this is not acceptable since Maximum Likelihood methods assume i.i.d of the data used.

Hence we cannot efficiently calibrate terminal distribution functions and thus switch to the second pricing method and calibrate the copula parameters using historical daily log returns, which are shown to have low autocorrelation [35, pp-36], and in this way we obtain the daily transition densities which can be used in the Monte Carlo simulation of the prices.

7.1.4 Changing the Copula

In this section we start by showing that the bivariate normal distribution generated from the BS model can equivalently be expressed in terms of a Gaussian copula and show how it can be used in Monte Carlo simulation. Later we replace the Gaussian copula with non-Gaussian copulas to add the desired dependence structure. We will show how various copula functions can be used to add dependence between the discretized asset equation (7.2) for $i = 1, 2$.

To use equation (7.2) to perform the Monte Carlo simulation using bivariate normal distribution under the BS framework (with lognormal marginal) we perform the following steps:

1. Simulate independent uniform random variables, u_j^i, $i = 1, 2$ and $j = 1,..,n$ (*time steps*).
2. Transform the uniforms into standard normal random variables, $x_j^i = \Phi^{-1}(u_j^i)$, where $\Phi(\bullet)$ is the standard normal distribution function.
3. Obtain correlate normal random variables, $y_j^1 = x_j^1$ and $y_j^2 = \rho x_j^1 + \sqrt{1-\rho^2}\, x_j^2$.
4. Transform the standard normal random variables into uniform, $v_j^i = \Phi(y_j^i)$, $i = 1, 2$.
5. Transform the uniform r.v.s into standard normal random variables, $z_j^i = \Phi^{-1}(v_j^i)$.
6. Put $W_{i,j} = z_j^i \sqrt{\Delta t}$, for $i = 1, 2$ in equation (7.4) for all j.
7. Calculate the payoff at expiry,
8. Repeat steps 1-7, average payoffs and discount to price the option.

First observe that steps 4 and 5 are superfluous though they are included to illustrate how the Gaussian copula enters the simulation algorithm. The relationship between the Gaussian copula and BS Model can be recognized by observing steps 2, 3 and 4 and comparing them with the algorithm in section 4.5. The construction of v_j^i is equivalent to simulating a random pair from a Gaussian copula with shape parameter ρ.

To switch from Gaussian to non-Gaussian copula we replace steps 2, 3 and 4 by a single step:

2" Construct dependent uniforms, $v_j^i = F^i(u_j^1, u_j^2)$ as a function of the two relevant independent uniform r.v.s (from step 1),

This new step is equivalent to simulating a random pair from a given copula function, be it Gaussian or non-Gaussian.

After changing the Gaussian copula with non-Gaussian copulas to incorporate the desired tail dependence we will replace the lognormal asset dynamics from the BS model with the UVDD model discussed in Chapter 5 to include smile also.

We will also study the effect of change of number of time-steps (maturity) and the number of paths used in Monte Carlo simulation on pricing some bivariate options.

7.2 Accuracy of the Monte-Carlo Simulation

We will apply the model from section 7.1 to hypothetical market data to check for the accuracy of the Monte Carlo simulation method in the pricing of ATM Spread options, i.e., the payoff $([S_1(T) - S_2(T) - K]^+)$ at option maturity T. The analytic price of a spread option under the BS framework is the (discounted) double integral of the option payoffs over the risk-neutral joint distribution of the terminal prices of the two underlying assets. But analytic expressions for the values of spread puts and calls in a Black-Scholes framework are not known, and hence various numerical algorithms are used to price such products [32]. The most commonly cited approximated closed form formula is the Kirk's formula [33].

The hypothetical equity data used is: $S_1(0) = 90$; $S_2(0) = 80$; $K = 10$; $r = 10\%$; $\sigma_1 = 30\%$; $\sigma_2 = 20\%$; $T = 1$yr; *NumOfSim* = 2097150. The univariate marginals are assumed to be lognormal with constant volatility.

We will first compare the difference in prices observed due to change in copula functions with the error coming from the simulation method used. Later we will price ATM Spread option using Kirk method and Monte Carlo simulation method under Gaussian copula to check the implementation of our simulation method.

ρ	***Clayton***	***Gaussian***	***Rel %Difference***
0.1	12.3366	12.3498	-0.1069%
0.2	11.7354	11.7677	-0.2745%
0.3	11.1166	11.1525	-0.3219%
0.4	10.4814	10.4981	-0.1591%
0.5	9.82623	9.79626	0.3059%
0.6	9.14212	9.03539	1.1812%
0.7	8.41223	8.19804	2.6127%
0.8	7.60232	7.25587	4.7748%
0.9	6.62567	6.15690	7.6137%

Table 7.1 ATM Spread Call option price and relative %Diff using various copulas

We start by calculating at time t = 0 price of the spread option using the Gaussian and Clayton Copula separately for different values of correlation coefficient, presented in Table 7.1. The value of the Clayton shape parameter is derived by keeping the Kendall's tau constant across copulas.

We notice from Table 7.1 that the price of the spread option decreases and the relative percentage difference in prices between Clayton and Gaussian increases with increase in value of correlation coefficient. For low correlation values the difference is very small and hence it is hard to say if this difference is due to change in copula or error in the Monte Carlo simulation of prices. Figure 7.2 plots the results from table 7.1 for qualitative analysis.

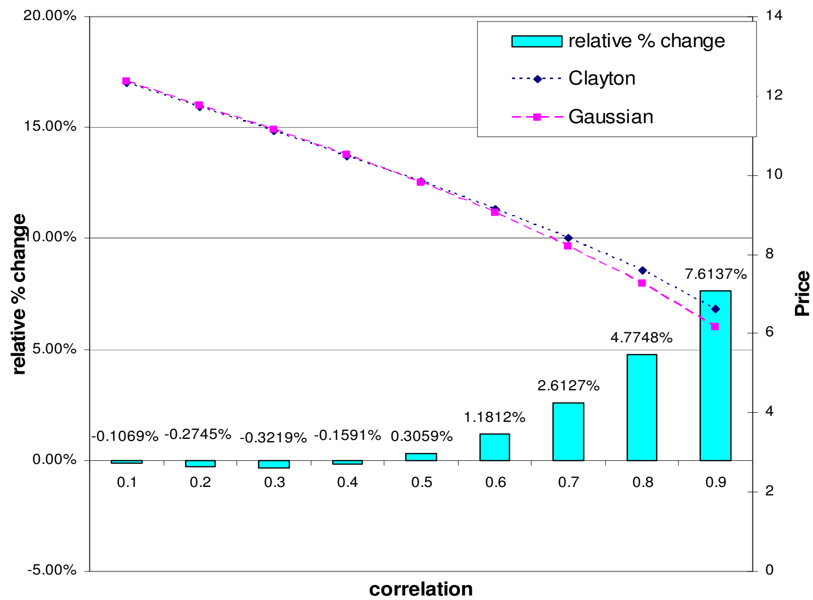

Figure 7.2 Spread Call option prices vs correlation coefficient for ATM strike

To study the effect of error due to Monte Carlo simulation we used a confidence interval of 95% for the prices and checked if the interval overlaps for the two copula functions. If they overlap (hence low percentage difference between prices) then we are not sure about the prices differences obtained in Table 7.1 and if it does not than we can say that the price difference is mainly due to change in copula functions and can be used for analysis. To carry out this test we plotted the Monte Carlo prices using Clayton and Gaussian copula for ATM spread call option with their respective bounds for correlation value of 0.5 and 0.8.

Figure 7.2 suggest that higher value of correlation coefficient rho ρ gives a clear difference in prices for a spread option whereas for lower values the confidence interval for both copulas are overlapping making it hard to compare the prices from different copulas as they could be the result of error from Monte Carlo simulation method used in pricing and not actually from the change in copula functions. Therefore for our analysis we plan to choose underlyings with a high correlation value (>0.7) between them and then studying the impact of different types of tail dependence on the pricing of some bivariate products which are sensitive to dependence structures between underlyings.

For correlation of 0.5 we notice from Figure 7.3 that the upper bound of Gaussian copula overlaps with the lower bound of the Clayton copula, whereas from Figure 7.4 we notice that the bounds are non-overlapping.

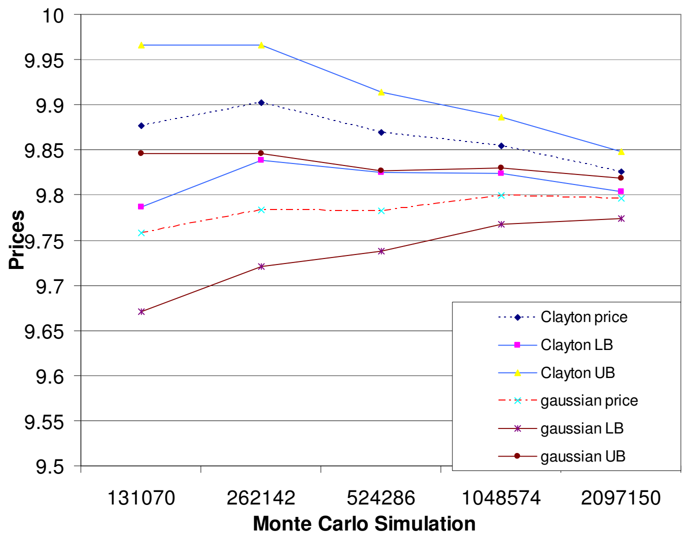

Figure 7.3 Spread option price for Gaussian and Clayton with 95% CI, rho = 0.5

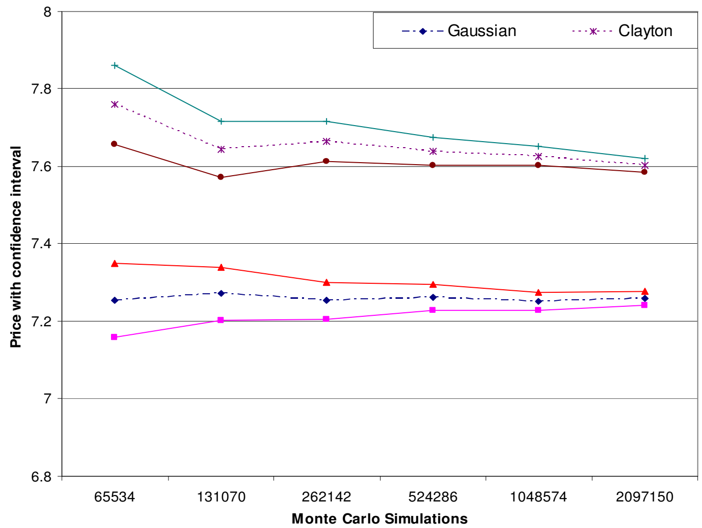

Figure 7.4 Spread option price for Gaussian and Clayton with 95% CI, rho = 0.8

The above analysis will be useful when comparing the prices from different copulas primarily for the spread option case. For other type of options we *assume* that if the price differences are very low then it could be due to error from pricing method and not from the copulas and hence will not be included into the analysis, as the main objective of this project is to study the effect in prices due to change in copula functions and not the error coming from the Monte Carlo pricing methods.

We now compare the prices coming from closed form analytic Kirk formula and Monte Carlo simulation using Gaussian copula with lognormal marginals. Figure 7.5 suggest that these two prices are almost equal (with an error or 0.1%) and hence we are convinced about our implementation of pricing method (algorithm) in C++ language.

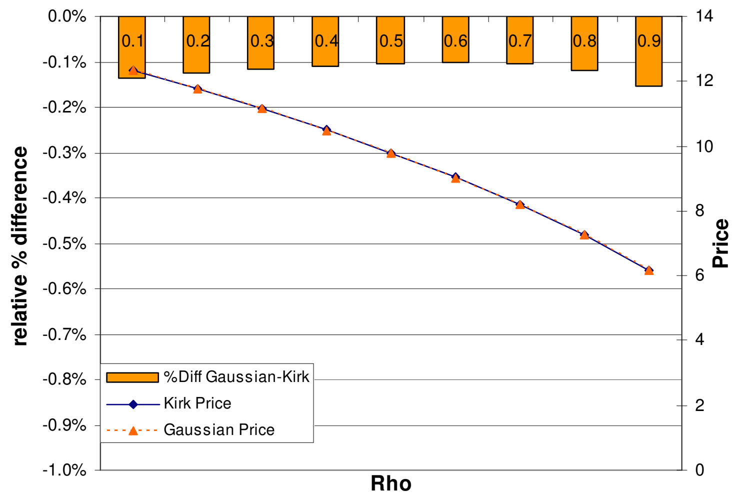

Figure 7.5 Spread option prices and Relative % Difference

K_{ATM} = 10, T = 1year, *NumOfSim* = 500,000

7.3 Test Strategy

We now provide the notation used throughout this chapter: $S_1(T)$ and $S_2(T)$ are the values of the WFC and BAC equities respectively at maturity time T, K_1 and K_2 are the respective strikes. The maturity used is 0.3589years, unless stated otherwise, and constant interest rate is given by 0.3346%. All the results are derived assuming the *2-Scenario UVDD model* developed in Chapter 5 for the equities, and the copula parameters is calibrated by using *2260* trading days, unless stated otherwise. Wherever log-normal marginals are assumed to provide no smile to the model it will be written explicitly and the constant volatility used in this case (Case A - Figure 7.1) is ATM volatility from the respective smiles. The number of Monte-Carlo simulations used for pricing is equal to 524,286.

We start by bivariate digital call options and price them under all the four cases and then compare the observed prices to study the effect of including smile and dependence individually and together.

7.4 Bivariate Digital Options

A very interesting product used in the market is the bivariate digital options. The payoff of such option at maturity T is given by:

$$DC = \begin{cases} 1.0 & if \quad S_1(T) \geq K_1 \ \& \ S_2(T) \geq K_2, \\ 0.0 & Otherwise. \end{cases}$$

We start our discussion by observing the percentage change in the prices of the options under the transitions "**Case A to Case B**" and "**Case A to Case C**" from Figure 7.1, for a range of strikes. The ATM volatilities are *53.74%* for WFC and *54.46%* for BAC and ATM strike are given by (K_1^{ATM} , K_2^{ATM}) = ($S_1(0)$, $S_2(0)$) where $S_1(0)$ = 26.91 and $S_2(0)$ = 17.09.

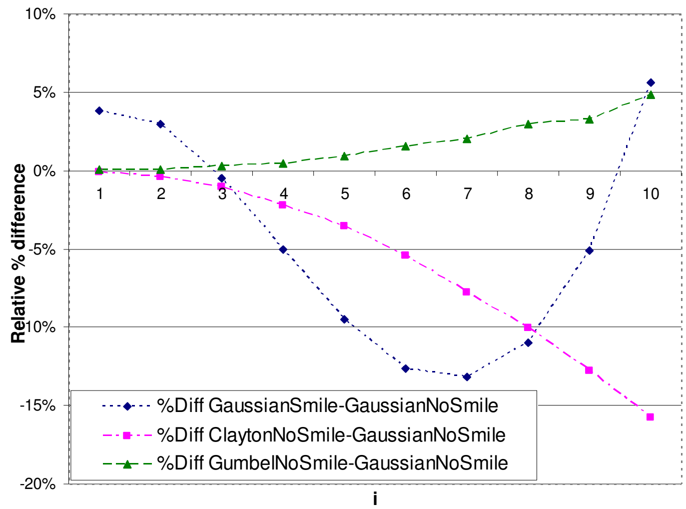

Figure 7.6 Relative % Difference in Prices for "Step 1" and "Step 2"

$K_1 = S_1(0)$ (0.5 + 0.1* i) ,$K_2 = S_1(0)$(0.5 + 0.1* i) ; ATM at i = 5.

Figure 7.6 suggest that for digital-call options the effect in prices due to inclusion of smile is more than due to inclusion of tail dependence. And the Clayton copula changes the prices more than the Gumbel copula. Figure 7.7 plots the digital call prices for different copulas. We observe that Clayton copula under-prices the option whereas Gumbel copula overprices it.

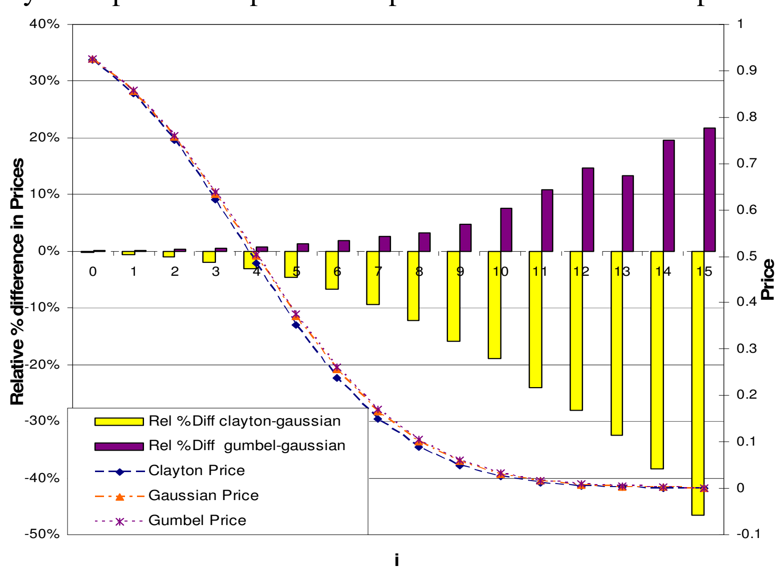

Figure 7.7 Digital Call prices and Relative % Difference between different Copulas

$K_1 = S_1(0)$ (0.5 + 0.1* i) , $K_2 = S_2(0)$(0.5 + 0.1* i) ; ATM for i = 5.

The results from Figure 7.7 can be explained by comparing the pdfs of each copula given in Chapter 4, section 4.2.1. Since Clayton copula has lower tail dependence, Figure 4.3, it will price a bivariate digital call option less than the Gaussian copula, Figure 4.1, which has zero lower and upper tail dependence (symmetrical distribution), whereas Gumbel copula, Figure 4.5, with upper tail dependence will give higher payoff for such an option. The joint distribution in this option can also be interpreted as a survival copula (section 2.6).

For zero strike we notice that this price difference is very small, this is because the whole distribution is used while integrating the payoff function along all strikes above zero and this will generate same payoff for all the three copula functions. We also notice that this percentage difference in prices increases with increase in strike. As the strike is increased we notice from Figure 4.3 that the probability mass in the area of the payoff for Clayton copula decreases rapidly when compared to the Gaussian copula in Figure 4.1, more mass concentrated in the lower strike region for Clayton copula, hence the percentage difference between the two copulas increases with strike. In the Gumbel case it is opposite of the Clayton copula and more probability mass is concentrated in the region of higher strikes, Figure 4.4, and when compared with Gaussian copula we see an increase in percentage difference in prices with increase in strike.

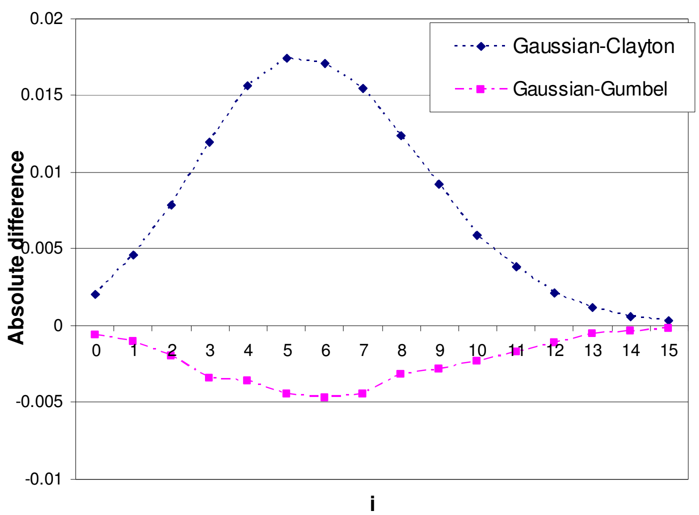

Figure 7.8 Absolute differences between different Copulas for digital call option

$K_1 = S_1(0)\ (0.5 + 0.1^*\ i)$ and $K_2 = S_2(0)(0.5 + 0.1^*\ i)$; ATM at $i = 5$.

Figure 7.8 plots the absolute differences in the prices for the digital call option for different values of strike K_1 and K_1 which are parameterized in terms of variable i. We extended our analysis by keeping K_2 fixed at 34.0 (OTM = Out of the Money), 17.09 (ATM = At the Money) and 10.0 (ITM = In the Money), and changing K_1 between 1 till 50.

The following three figures plot the prices for each of these three scenarios along with the relative percentage difference (Rel %Diff) of Clayton and Gumbel with respect to Gaussian Copula.

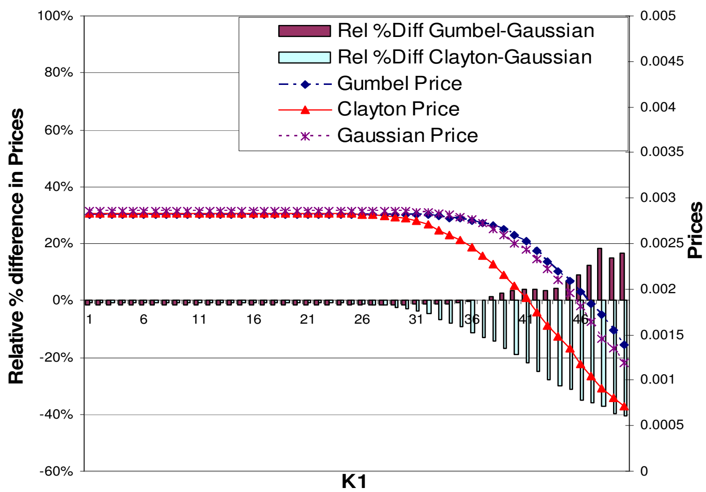

Figure 7.9 Prices and Relative % Difference for fixed K_2 = 34(OTM) and changing K_1

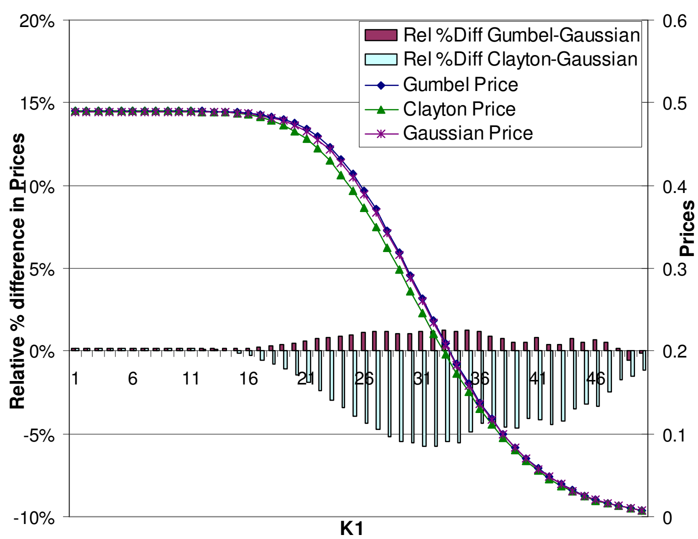

Figure 7.10 Prices and Relative % Difference for fixed K_2 = 17.09(ATM) and changing K_1

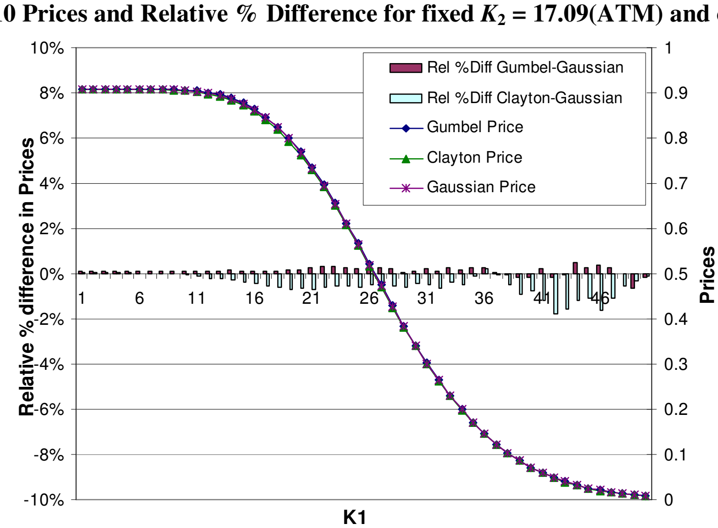

Figure 7.11 Prices and Relative % Difference for fixed K_2 = 10(ITM) and changing K_1

From Figures 7.9-7.11 we observe that the relative percentage difference in the prices between various copulas decreases as we shift from OTM to ITM (respect to strike K_2) options. For OTM case we notice that although K_2 is very high the price difference is relatively less for K_1 varying from zero to K_1^{ATM} (=26.91). This shows that as long as one of the strikes is ITM we can expect same prices under different dependence structures. A similar effect can also be noticed by comparing Figure 7.9 with Figure 7.11, as expected since K_2 is already ITM we notice very less difference in prices even for K_1 much higher than K_1^{ATM} .

One more thing to notice in Figure 7.9 is that for OTM K_2 and K_1 higher than K_1^{ATM} , the price differences are extremely high and increases with strike K_1. This suggests that the effect of tail dependence on pricing can become crucial when both strikes are OTM. As the value of K_2 is decreased to 17.09 in Figure 7.10 we notice that the magnitude of the relative price differences has decreased dramatically when compared to Figure 7.9 for strikes K_1 higher than K_1^{ATM} , with the maximum occurring around K_1^{ATM} .

Now as the value of K_2 is decreased to 10 in Figure 7.11, all the three copulas offer roughly the same payoff. Since K_2 is deep ITM we expect same payoff from each copula, as suggested by Figure 7.9 that if either of the strikes is ITM the prices differences are minimum.

The above analysis can help one to make decision over questions like: under what values of the strikes it is wise to add smile and tail dependence into the pricing model and when is it safe to exclude it to make the model simple.

7.5 Spread Options

In this section we will analyse spread call options whose payoff SC at maturity T (=0.3years) is given by:

$$SC = max \{S_1(T) - S_2(T) - K , 0.0\}$$

Again we will study the change in the prices for "Step 1 (Add Smile only)" and "Step 2 (Add Tail dependence only)", from Figure 7.1, and also the effect of change of copulas on pricing these products for various levels of strikes. The ATM is given by K^{ATM} which is equal to $S_1(0) - S_2(0)$, where $S_1(0) = 26.91$ and $S_2(0) = 17.09$.

From Figure 7.12 we notice that the percentage difference in prices due to shift to smile and tail dependence increases with increase in strikes, with smile showing relatively more differences for higher strikes, whereas for lower strikes the effect due to Clayton copula is much higher.

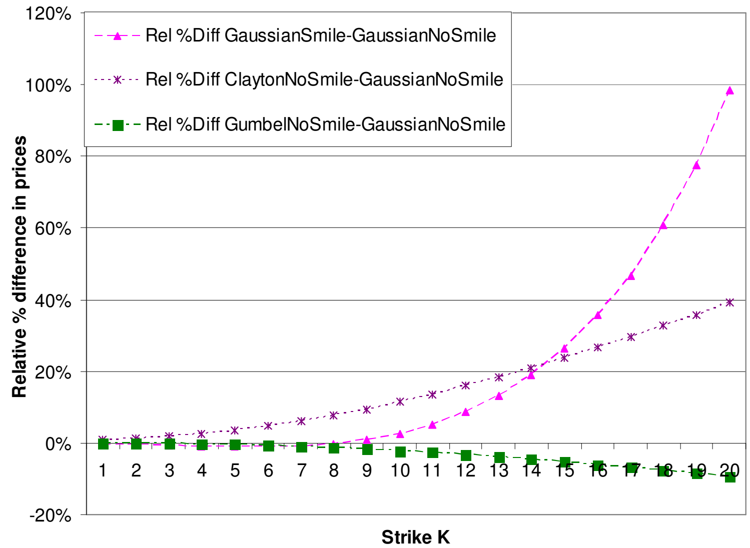

Figure 7.12 Relative % Difference in Spread option Prices from inclusion of smile and tail dependence; ATM Strike K^{ATM} = 9.82, T = 0.3 years

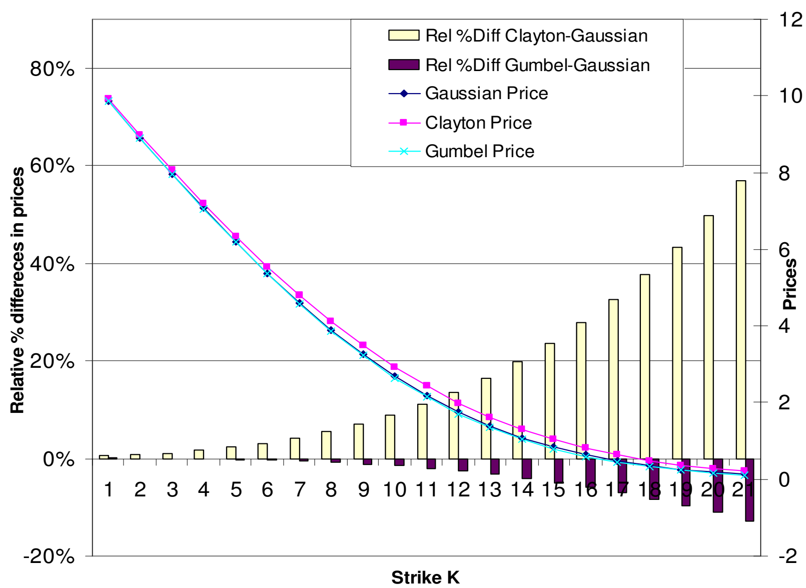

Figure 7.13 Spread Call price and Relative % Difference for different copulas, ATM Strike K^{ATM} = 9.82, T = 0.3 years

Figure 7.13 plots the price for spread call options for different copulas and also the relative percentage difference between Clayton-Gaussian and Gumbel-Gaussian. We notice that the difference due to the Clayton is much higher than due to the Gumbel copula.

To explain the above results we simulated values of $S_1(T)$ and $S_2(T)$ during the Monte Carlo pricing of this product for maturity of 7/365years, 0.3 years 3.3 years and 5.3 years. We then plotted the empirical pdf of the difference $S_1(T) - S_2(T)$ derived from the simulated data in Figure 7.14 – Figure 7.17.

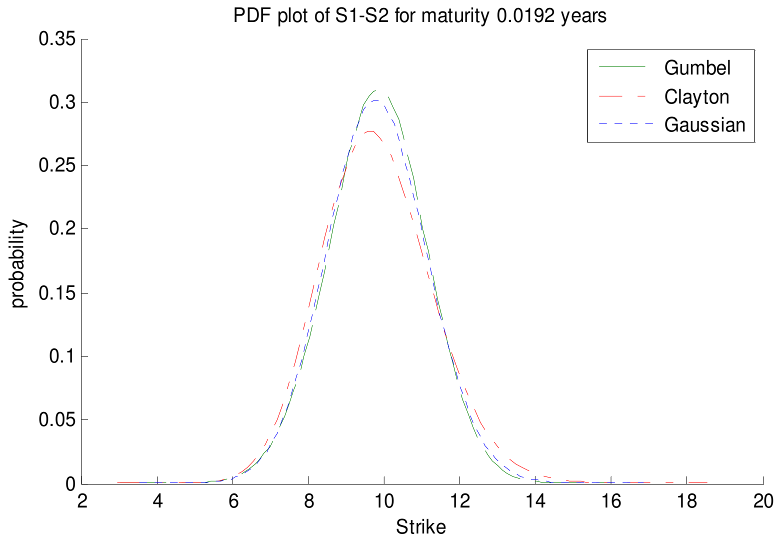

Figure 7.14 Empirical PDF plot for the variable $S_1(T) - S_2(T)$ with maturity 7/365years (7 days)

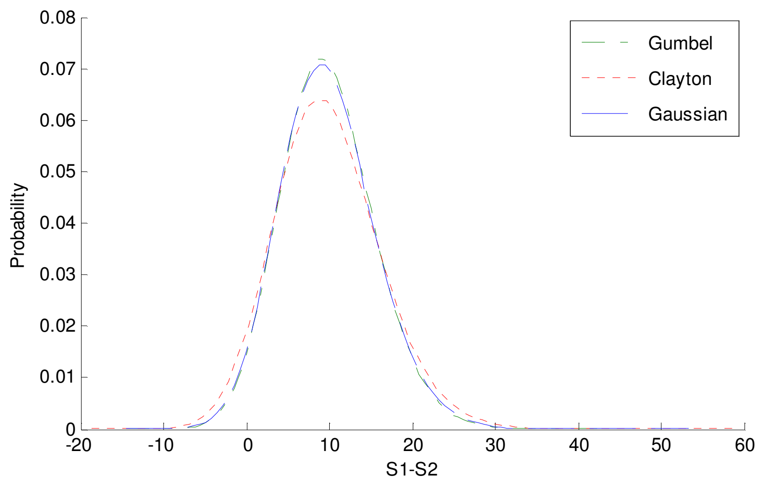

Figure 7.15 Empirical PDF plot for the variable $S_1(T) - S_2(T)$ with maturity 0.3years

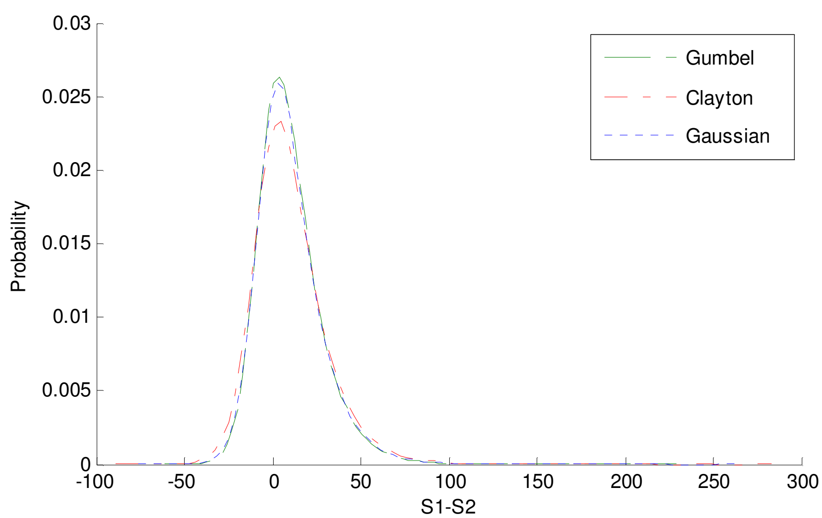

Figure 7.16 Empirical PDF plot for the variable $S_1(T) - S_2(T)$ with maturity 3.3years

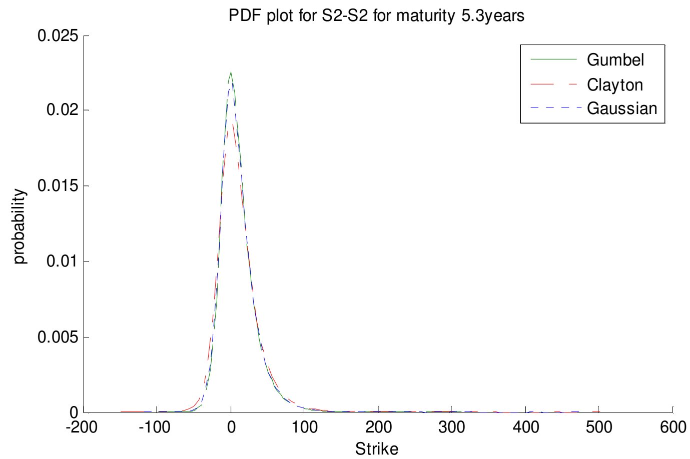

Figure 7.17 Empirical PDF plot for the spread $S_1(T) - S_2(T)$ with maturity of 5.3years

It is suggested by the Figure 7.15 that the empirical pdf for the Clayton copula has more probability mass than the Gaussian one for the strikes roughly higher than 12 and lower than 9, and it is vice-versa for pdf of Gumbel copula, which is just below the Gaussian pdf for the mentioned strikes. We also note that this difference is higher for Clayton-Gaussian case than the Gaussian-Gumbel case, for the above mentioned region of strikes, hence the relative percentage difference in prices will be more in the former case as also observed in Figure 7.13. From Figure 7.15 we also notice that the relative percentage difference in prices also increases with strike, the same trend observed in digital call option from Figure 7.7.

We observed in Chapter 6 Table 6.2 that we get different copula parameters for different data sets used. We will now study the price differences due to change in estimated Gaussian copula parameter using 300 and 900 days and whether this difference is more or less than the difference obtained due to shift in copula functions, calibrated using 300 days.

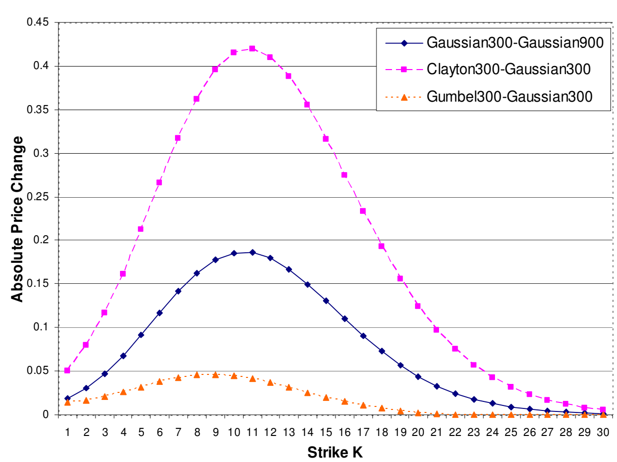

Figure 7.18 Absolute Change in prices due to difference in calibrated parameters and copulas

Figure 7.18 shows the absolute difference in the prices due to change in calibrated parameters for Gaussian copula and change in copula functions, all calibrated using 300 days.

In this case we observed that difference due to change of estimated parameters is higher than the difference due to change of copula functions from Gaussian. But the shift from Gaussian to Clayton is higher than the shift observed for the shift from Gaussian to Gumbel copula. The results are plotted in Figure 7.18.

Figure 7.19 plots the absolute differences to compare the differences in the prices of a spread option due to a +1% shift in Gaussian copula shape parameter ρ with the differences due to change in dependence structure – different copulas. The parameters used in the copulas are calibrated using 2260 trading days and the maturity of the option is 0.3years.

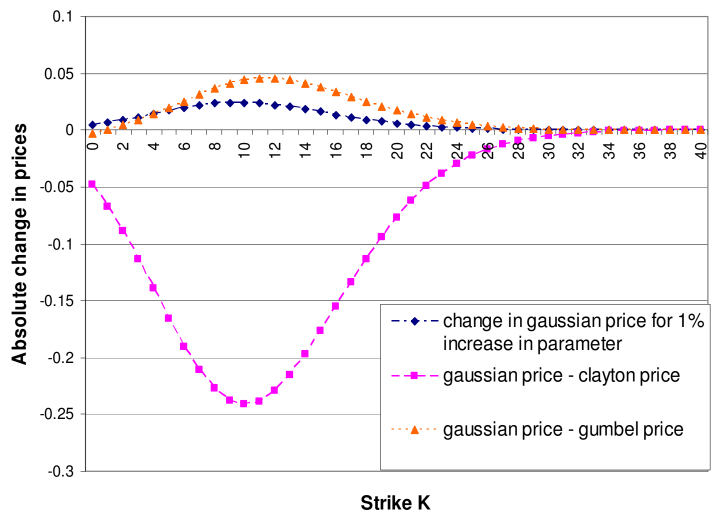

Figure 7.19 Absolute differences in prices: To study the effect of change in *SC* price of Gaussian copula for 1% increase in its parameter with change in prices due to change in copulas, K^{ATM} = 9.82, T=0.3years

We notice from Figure 7.19 that the effect in prices due to change of copulas from Gaussian to Clayton is much more than the change due to increasing the Gaussian copula parameter by 1%. This shows that the pricing model is very sensitive to change in dependence structure.

Figure 7.20 plots the relative percentage difference in prices for Clayton-Gaussian case for different maturities. We notice that this relative percentage difference in prices decreases with maturity. This indicates that the distribution of the spread ($S_1(T) - S_2(T)$) for every copulas becomes identical as the maturity of the options is increased. This can be explained by comparing Figure 7.15 and Figure 7.17, where in the latter plot the differences between the three distributions are much less profound than the differences in the short maturity spread. Mathematically, the smaller differences in prices for larger maturities are the result of application of Central Limit Theorem [37] because as the number of distributions/daily observations adding together is increased each distribution of spread coming from different copula assumptions converges to a standard normal distribution.

From Chapter 5 Section 5.1.1 we know that the the probability distribution p of $S_{a,b}$ under the 2-scenario UVDD model assumption is given by:

$$p(S) = \sum_{i=1}^{2} \lambda_i LN\left(S \ + \alpha^i ; m_i, v_i\right)$$

Where m_{i} and v_{i} are the mean and standard deviation of each of lognormal distributions. We start any simulation we picking, after time ε>0, scenario i with probability λ_{i}. After we have selected the scenario i we get a single lognormal distribution which will be discretized and used through all time steps until the end of the simulation. We now know from the BS model that this transition density function for $\ln S_1(t_{j+1}+\alpha_i) - \ln S_1(t_j+\alpha_i)$ between time step j to j+1, j = 0,1,2,.....,n-1 , where t_n= T and $\Delta t = t_{j+1} - t_j$, with mean $(r - \sigma_i^2/2)\Delta t$ and variance $\sigma_i^2 \Delta t$ and is written as:

$$\ln(S_1(t_{j+1})+\alpha_i) - \ln(S_1(t_j)+\alpha_i) \sim \Phi\left[\left(r - \frac{\sigma_i^2}{2}\right)\Delta t, \sigma_i\sqrt{\Delta t}\right]$$

Suppose for simulation number k, k = 1,2,....,N, the scenario chosen is i then under the above mentioned transition density approach we obtain the terminal distribution for asset $ln\ S_1$ by adding all the transition densities over n number of time steps given by:

$$\begin{aligned}\ln(S_1^k(T)+\alpha_i) - \ln(S_1^k(0)+\alpha_i)) &= \sum_{j=0}^{n-1}(\ln(S_1^k(t_{j+1})+\alpha_i) - \ln(S_1^k(t_j)+\alpha_i)) \\ &= \sum_{j=0}^{n-1}\left(\left(r - \frac{\sigma_i^2}{2}\right)\Delta t + \sigma_i(W_1^Q(t_{j+1}) - W_1^Q(t_j))\right)\end{aligned}$$

or equivalently we have,

$$S_1^k(T) + \alpha_{1i} = (S_1^k(0)+\alpha_{1i})Exp\left(\sum_{j=0}^{n-1}\left(\left(r - \frac{\sigma_{1i}^2}{2}\right)\Delta t + \sigma_{1i}(W_1^Q(t_{j+1}) - W_1^Q(t_j))\right)\right)$$

Simultaneously we can calculate the distribution for the asset S_2 for simulation number k with scenario h is given by:

$$S_2^k(T) + \alpha_{2h} = (S_2^k(0)+\alpha_{2h})Exp\left(\sum_{j=0}^{n-1}\left(\left(r - \frac{\sigma_{2h}^2}{2}\right)\Delta t + \sigma_{2h}(W_3^Q(t_{j+1}) - W_3^Q(t_j))\right)\right)$$

where, $W_3 = \rho W_1 + \sqrt{1-\rho^2}W_2$.

The distribution for the spread S_1-S_2 for the simulation number k and scenario i for asset S_1 and scenario h for asset S_2 can be written as following:

$$\begin{aligned}S_1^k(T) - S_2^k(T) = (S_1^k(0)+\alpha_{1i})Exp\left(\sum_{j=0}^{n-1}\left(\left(r - \frac{\sigma_{1i}^2}{2}\right)\Delta t + \sigma_{1i}(W_1^Q(t_{j+1}) - W_1^Q(t_j))\right)\right) \\ - (S_2^k(0)+\alpha_{2h})Exp\left(\sum_{j=0}^{n-1}\left(\left(r - \frac{\sigma_{2h}^2}{2}\right)\Delta t + \sigma_{2h}(W_3^Q(t_{j+1}) - W_3^Q(t_j))\right)\right)\end{aligned}$$

Now if we add the distribution for each simulation k we get:

$$\sum_{k=1}^{N}\left(S^k(T)-S^k(0)\right)=\sum_{i=1}^{2}\sum_{k=1}^{\lambda_{1i}N}(S_1^k(0)+\alpha_{1i})Exp\left(\sum_{j=0}^{n-1}\left(\left(r-\frac{\sigma_{1i}^2}{2}\right)\Delta t+\sigma_{1i}(W_1^Q(t_{j+1})-W_1^Q(t_j))\right)\right)$$

$$-\sum_{h=1}^{2}\sum_{k=1}^{\lambda_{2h}N}(S_2^k(0)+\alpha_{2h})Exp\left(\sum_{j=0}^{n-1}\left(\left(r-\frac{\sigma_{2h}^2}{2}\right)\Delta t+\sigma_{2h}(W_3^Q(t_{j+1})-W_3^Q(t_j))\right)\right)$$

And using Central Limit Theorem we conclude that this sum of distributions will converge to standard normal distribution for both N and n going to infinity (long maturity options).

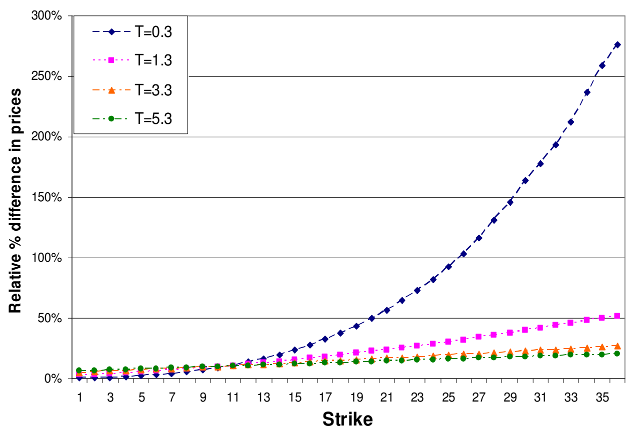

Figure 7.20 Relative % Difference between Clayton-Gaussian for different maturities T, K^{ATM} = 9.82

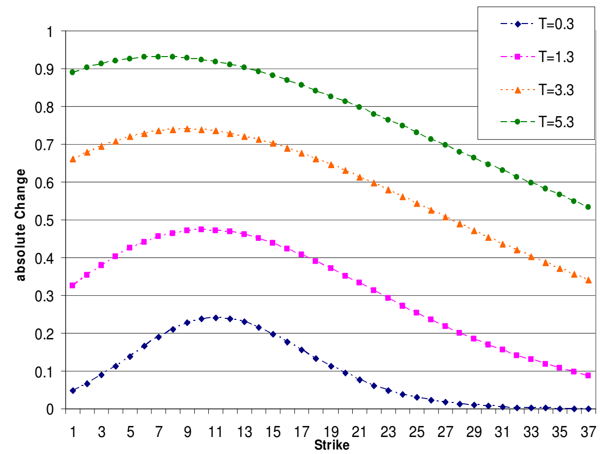

Figure 7.21 Absolute Change in prices between Clayton-Gaussian for different maturities T, K^{ATM} = 9.82

Figure 7.21 plots the absolute difference in the prices for Clayton-Gaussian case for different maturities T. We observe from Figure 7.21 that the absolute difference in prices increases with increase in maturity T. We also observe the maximum absolute difference close to ATM strike of 9.82 for every maturity.

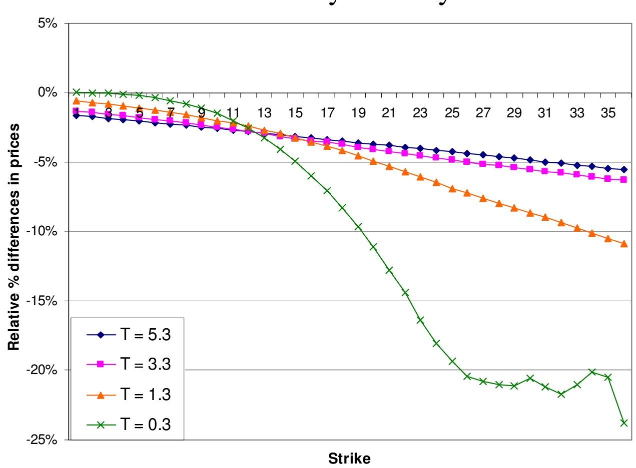

Figure 7.22 Relative % Difference in prices between Gumbel-Gaussian for different maturities T, K^{ATM} = 9.82

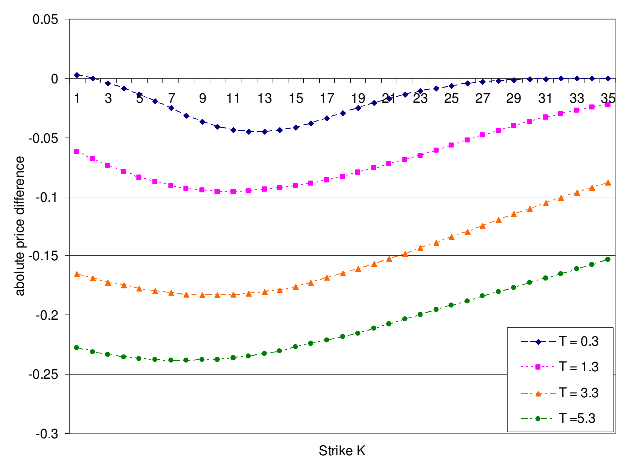

Figure 7.23 Absolute Change in prices between Gumbel-Gaussian for different maturities T, K^{ATM} = 9.82

Figure 7.22 plots the relative percentage difference in prices for Gumbel-Gaussian pair for different maturities. We observe that the relative percentage difference decreases with increase in maturity T, a similar trend observed in Clayton case. This supports our hypothesis that the two distributions become identical as the maturity of the options is increased.

Hence we can apply similar arguments used in the case of Clayton copula for decreasing price difference in options with increasing maturities to explain the results from Figure 7.22.

Figure 7.23 plots the absolute difference in the prices for Clayton-Gaussian case for different maturities T. The absolute differences increase with increase in maturity of the option. We can say that the maximum absolute difference happens approximately near the ATM strike of 9.82.

Figure 7.24 plots the prices for different copulas for Spread Put options whose payoff SP at maturity T is give by:

$$SP = max\ \{K - (S_1(T) - S_2(T))\ ,\ 0.0\}$$

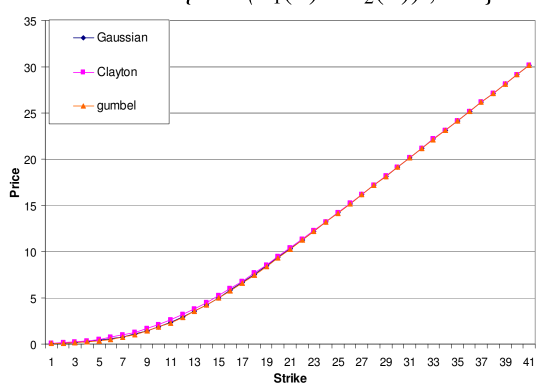

Figure 7.24 Spread Put options prices for different copulas, K_{ATM} = 9.82, T=0.3year

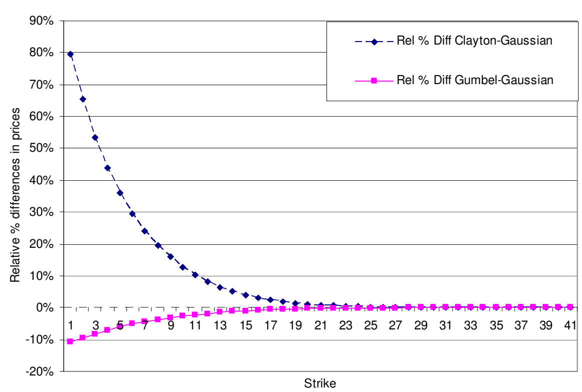

Figure 7.25 Relative % Difference in prices between different copulas, K_{ATM} = 9.82, T=0.3year

In Figure 7.25 we see that the relative percentage difference for Clayton-Gaussian case is much higher than due to the Gumbel-Gaussian case. This can be explained by looking at the empirical distributions of spread ($S_1(T) - S_2(T)$) in Figure 7.15 which shows a clear lower fat tail for the empirical Clayton case when compared to the Gaussian case, whereas empirical distribution using Gumbel copula has tails thinner than the Gaussian case, hence it underprices the option. The results in Figure 7.25 are hence consistent with the distribution obtained in Figure 7.15.

7.6 Worst of Call Option

In this section we will price the worst of call option whose payoff *WC* at maturity *T* is given by:

$$WC = max\ (min\ (S_1(T)/S_1(0),\ S_2(T)/S_2(0)) - K,\ 0.0)$$

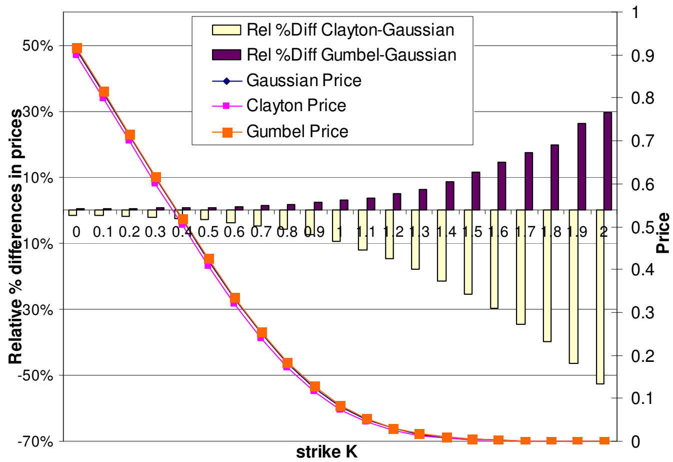

Figure 7.26 Price and Relative % Difference for worst of call option for different copulas, K^{ATM} = 1, T=0.3year

Figure 7.26 plots the prices for the three copulas and the relative percentage difference between Clayton-Gaussian and Gumbel-Gaussian. In this case Clayton under-prices the option whereas Gumbel over-prices it. The effect of different types of tail dependence on worst of call prices can be understood by studying the payoff in Figure 7.27.

In Figure 7.27 we plot the discrete payoff lines (dashed lines) for the worst of call option.

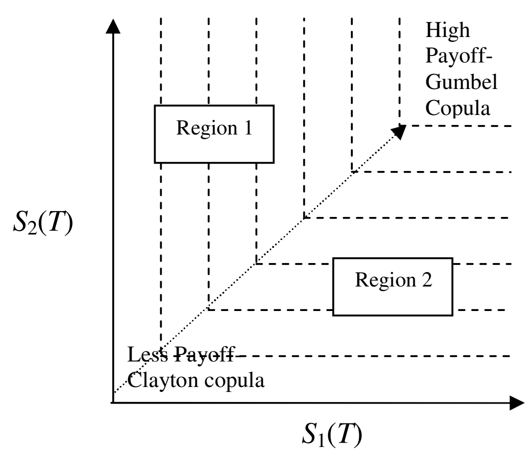

Figure 7.27 Discreet payoff lines (dash) for worst of call option for Clayton and Gumbel (Region 1-Payoff by S_1, Region 2-Payoff by S_2)

As we already know that transition Gumbel copula distribution after end of each simulation gives more probability weight to the upper right corner of the plot in Figure 7.27 and this will lead to higher chances of getting a payoff from function $max(min(S_1(T)/S_1(0), S_2(T)/S_2(0)) - K)$ when compared to Gaussian copula which has a symmetrical distribution. When looking at the bottom left corner of the Figure 7.27 we know that transition Clayton copula distribution gives more weight to this area and which means that we have lower chances of obtaining a payoff than the Gaussian copula.

Figure 7.28 plots the relative percentage difference between different copulas for different estimated parameters to compare the effect of change in estimated parameters to change in copula functions. The days used in calibration of the copula parameter are 300 and 900. In the figure we represent the prices with the copula name as prefix and number of days used in calibration as suffix, for e.g., Gaussian300 means that the copula used for pricing is the Gaussian copula and 300 is equal to the number of historical data points used for parameter estimation for Gaussian copula.

We notice from Figure 7.28 that the relative percentage difference in prices for change in estimated parameters is lower than the difference due to change in copula functions for both Clayton and Gumbel. This means that change in price due to incorporation of tail dependence is significant when compared to the change in prices due to different shape parameters for Gaussian copula estimated using 300 and 900 days.

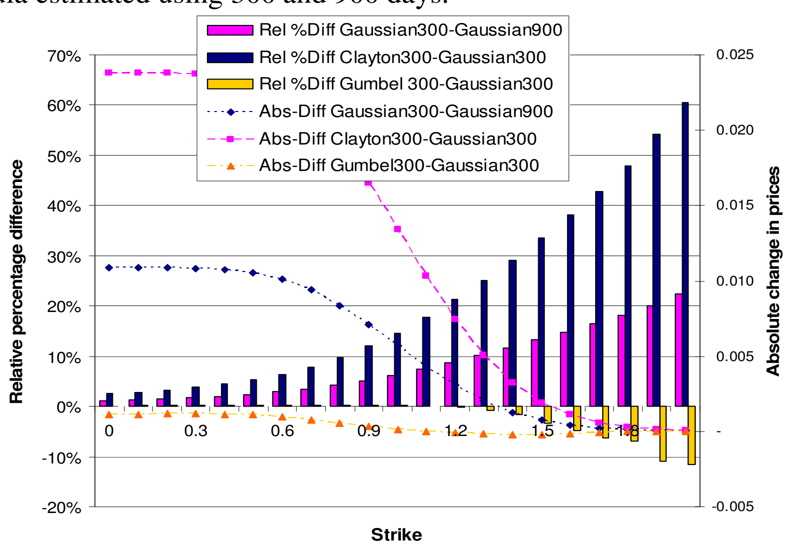

Figure 7.28 Absolute and Relative % Difference in prices to compare the effect of change in estimated parameters to change in copula functions, K^{ATM} = 1, T=0.3year

Figure 7.29 plots the absolute differences to compare the differences in the prices of a spread option due to a +1% shift in Gaussian copula shape parameter ρ with the differences due to change in dependence structure – different copulas. The parameters used in all the other copulas are calibrated using 2260 trading days and the maturity of the option is 0.3years.

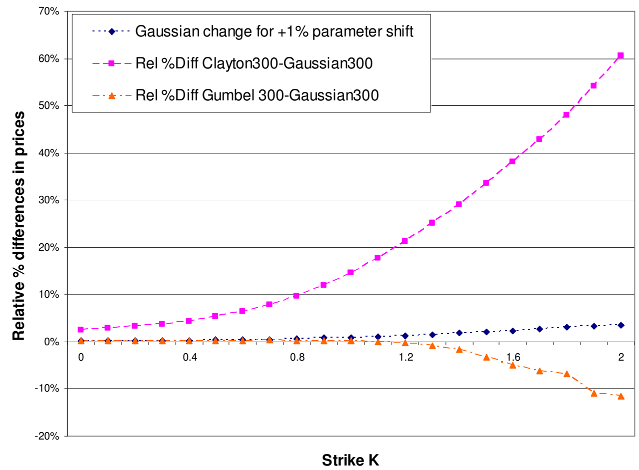

Figure 7.29 Relative% differences in prices: To study the effect of change in *WC* price of Gaussian copula for 1% increase in its parameter with change in prices due to change in copulas, K^{ATM} = 1, T=0.3 year

We notice from Figure 7.29 that the effect in prices due to change of copulas from Gaussian to Clayton is much more than the change due to increasing the Gaussian copula parameter by 1%. This shows that the pricing model is very sensitive to change in dependence structure, the same trend was observed for spread call options.

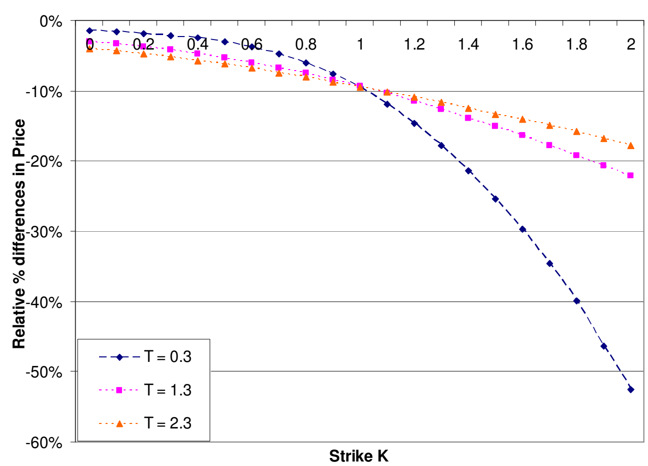

Figure 7.30 Relative % Difference for Clayton-Gaussian *WC* prices for different maturities

Figure 7.30 plots the relative percentage change between the Clayton and Gaussian copulas for different maturities. We notice that this difference decreases with increase in maturity *T*, identical to the trend observed for spread options, Figure 7.20. We apply similar arguments to this case also that both these distributions - Clayton and Gaussian, converge individually to standard normal distribution under the Central Limit Theorem assumption as the maturity of the option is increased.

7.7 Best of Call Option

In this section we will price the best of call option whose payoff BC at maturity T is given by:

$$BC = max\ (max\ (S_1(T)/S_1(0),\ S_2(T)/S_2(0)) - K,\ 0.0)$$

Figure 7.31 plots the prices for different copulas and also the relative price difference between them. The figure suggests that lower tail dependence assumption between the underlying can increase the price when compared to zero tail dependence between them. The price is also marginally decreased when upper tail dependence is assumed in pricing. This observation is opposite to the worst-of-call option covered in Section 7.6 where the Clayton copula assumption decreased the price whereas Gumbel copula assumption increased the price of the worst-of-call option.

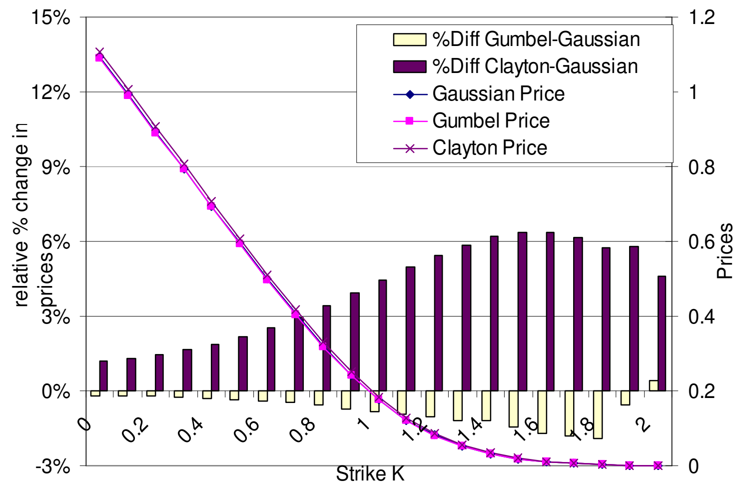

Figure 7.31 Best of Call price and Relative % Difference between different copulas, T = 0.3 year

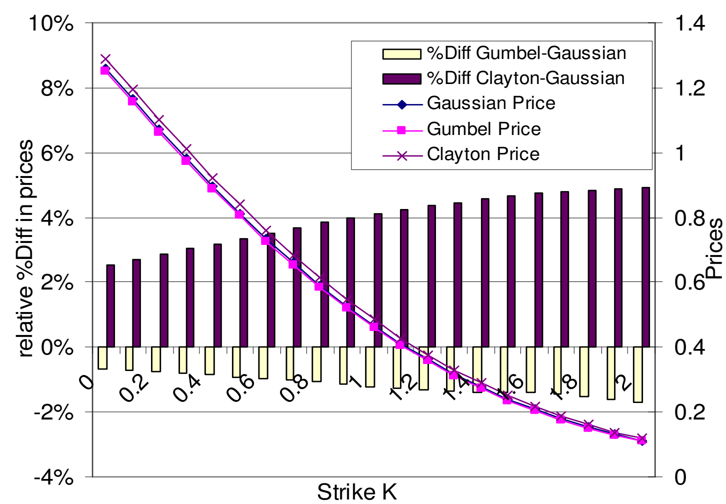

Figure 7.32 Best of Call price and Relative % Difference between different copulas, T = 5.3 year

We extended our analyses by increasing the maturity of the option and plotting the results in Figure 7.32. The figure suggests that the price difference between different copula functions has decreased with increase of option maturity. This result is similar to the one obtained in previous sections where the price differences between different copula functions decreased with increase in option maturity. We will again apply Central Limit Theorem to explain this result on the basis that as the maturity is increased more number of observations/random variables are added into the model and as a result it converges to a standard normal distribution.

Chapter 8
Pricing – CMS Spread products

After pricing some interesting bivariate products in the equity framework we now switch to interest rate framework where we will price some selected bivariate options using different maturity-tenor swaps as the underlying. We will analyse the products under four broad "**Cases**" defined in Figure 7.1 and study the effect of inclusion of smile and tail dependence, individually and together.

Here again the inclusion of smile is achieved by assuming a UVDD model for the underlying swap rate and the tail dependence is incorporated by using different copula functions. The parameters for these models have been derived in Chapter 5 and 6.

8.1 Extension of the pricing algorithm under swaps

The pricing method used in the equity case will also be applied in this chapter. The Monte Carlo simulation is done by using Equation (7.2) and keeping the drift term equal to zero.

In most interest rate products the observation and payment time are mostly different. For such options with a difference in observation and payment times a small adjustment is needed knows as the convexity correction, discussed in detail in Appendix A, to price consistently under a unique measure. This new measure in our case has the zero coupon bond maturing at the payment date as the numeraire.

The pricing algorithm used in section 7.1.4 can still be used but with an extra step between steps 6 and 7 to perform the simulation:

- Add to each simulated swap rate (simulated under their respective annuity measure) their respective convexity correction (A.4) term at the end of each simulation and then calculate the payoff with these modified rates.
- Discount the payoff using payment time and related interest rates.

8.2 Test Strategy

We now provide the notation used throughout this chapter: $S_{a,b}$(t) denoted the swap rate with maturity time T_a and tenor T_b. The rates are observed after 1 year and the payment is done after 3 months, unless stated otherwise. The valuation date for the option is 16-Mar-09. The interest rate from the valuation date for a period of 1year is given by 0.761434%, calculated from zero copoun bond price with maturity of 1 year using continous compounding. We also assume that fixed leg in swap makes payment semiannually.

All the results are derived assuming the *2-Scenario UVDD model* developed in Chapter 5 for the swaps, and the copula parameters are calibrated by using 2433 trading days (≈ 9 years), unless stated otherwise. Wherever log-normal marginals are assumed it will be written explicitly and the constant volatility used in this case (**Case A** - Figure 7.1) is ATM volatility. The number of Monte-Carlo simulations used for pricing is equal to 524,286.

8.3 Spread options

The product under study is a spread option whose payoff structure is given by:

$$SC(T_{\alpha+k}) = N\tau_h \max \{ S_{a,b_1}(T_\alpha) - S_{a,b_2}(T_\alpha) - K , 0.0\} \tag{8.1}$$

where S_{a,b_1} and S_{a,b_2} are the two swap rates with same maturity T_a and tenors T_{b1} and T_{b2}, K is the strike, N is the notional, T_α is the observation time, $T_{\alpha+k}$ is the payment time and τ_h is the year fraction for both swaps (assumed to be six months for each fixed leg of swap). The payment is done on a notional N which we keep equal to 10000 so that we can represent the prices in terms of *bp* (basis points).

Since the payment is done at time $T_{\alpha+k}$ we have to incorporate the convexity correction to price consistently, we achieve this by taking the zero coupon bond with maturity $T_{\alpha+k}$ as our new numeraire and calculate the convexity correction for each swap and use section (8.1) to perform the Monte Carlo simulation. As we already discussed, the current market standard for pricing such product is the Kirk formula which is exact for a zero strike under BS framework.

8.3.1 Kirk with no smile

The modified Kirk formula with the convexity adjustment without smile is given by [36]:

$$V(0)^{Kirk\_ATM} = N\tau_h P(0,T_{\alpha+k})(\tilde{S}_2 + K)Bl(\tilde{S},1,\sigma\sqrt{T_\alpha}) \tag{8.2}$$

$$\tilde{S}_i = S_i + CA(S_i) \quad \text{with } i = 1,2.$$

$$\tilde{S} = \frac{\tilde{S}_1}{\tilde{S}_2 + K}$$

$$\sigma = \sqrt{(\sigma_1)^2 + (\sigma_2)^2\left(\frac{\tilde{S}_2}{\tilde{S}_2 + K}\right)^2 - 2\rho_i\sigma_1\sigma_2\left(\frac{\tilde{S}_2}{\tilde{S}_2 + K}\right)}$$

In equation 8.1,

- the indices (a, b) associated to each swap rate were omitted for simplicity,
- σ_1 and σ_2 are the ATM volatilities for S_1 and S_2 respectively,
- ρ is the correlation coefficient between them.

The limitation of this formula is that it does not take into account the smile and the correlation skew [36].

8.3.2 Kirk with Smile

One way of adding the smile is to assume UVDD model for the underlying and use the Kirk formula to get a closed form solution for spread options given by [36]:

$$V(0)^{Kirk\_UVDD} = N\tau_h P(0,T)\sum_{i=1}^{m}\sum_{j=1}^{m'}\lambda_i\lambda_j\left(S*_2^j + K\right)Bl\left(S^{ij},1,\ \sigma^{ij}\right) \tag{8.3}$$

$$S*_k^j = S_k^j + CA(S_k^j) + \alpha_k^j \qquad k = 1,2$$

$$S^{ij} = \frac{S*_1^i}{S*_2^j + K*^{ij}} \qquad K*^{ij} = K + \alpha_1^i - \alpha_2^j$$

$$\sigma^{ij} = \sqrt{\left(\sigma_1^i\right)^2 + \left(\sigma_2^j\right)^2\left(\frac{S*_2^j}{S*_2^j + K*^{ij}}\right)^2 - 2\rho_{ij}\sigma_1^i\sigma_2^j\left(\frac{S*_2^j}{S*_2^j + K*^{ij}}\right)}$$

where ρ_{ij} is the correlation between swap rate 1 in scenario *i* and the swap rate 2 in scenario *j*. In all tests performed we assumed the same correlation parameter for all scenarios.

8.3.3 Spread call option with $S_{1,2}$ and $S_{1,10}$ pair

We start our analysis by comparing the prices obtained from Kirk formula with smile (Equation 8.3) and the Monte Carlo simulation with Gaussian copula and UVDD model for the swap rates $S_{1,2}$ and $S_{1,10}$, the copula parameters are estimated by using 780 days (Chapter 6, Table 6.3).

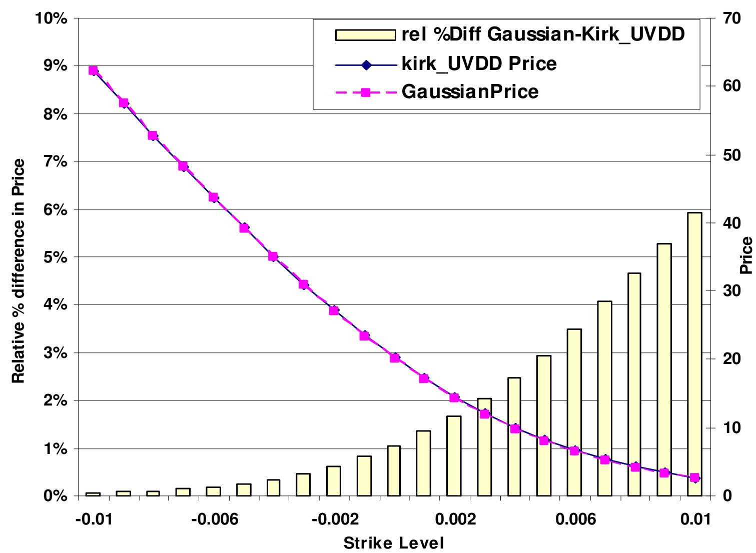

Figure 8.1 Spread option prices/ Relative % Difference for different strike level

$S_{1,2}$ and $S_{1,10}$ pair, T = 1 year

The spread option prices are plotted for varying strike levels (= $K - K_{ATM}$) between -100bp and +100bp, the zero value of the strike level means $K = K_{ATM}$, where K_{ATM} is equal to $S_{1,10}(0)$ - $S_{1,2}(0)$ (=1.0237%) and N is equal to 10000. ($S_{1,10}(0)$ = 3.79411% and $S_{1,2}(0)$ = 2.6575%)

Figure 8.1 suggest that the relative percentage difference between the two pricing methods increases with increase in strike level. We also note that the option is always over-priced by the Kirk formula for the given correlation coefficient for Gaussian copula.

The effect of inclusion of tail dependence "**Case B-Case D"** from Figure 7.1 can be seen in Figure 8.2, the swap rates used in this case are again $S_{1,2}$ and $S_{1,10}$ with smile.

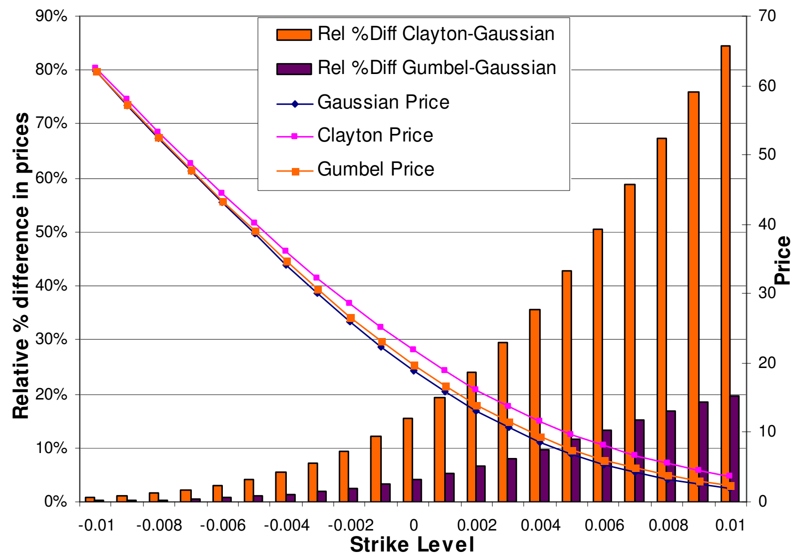

Figure 8.2 Spread option prices and Relative % Difference for different copulas, for $S_{1,2}$ and $S_{1,10}$ pair, T = 1 year

Figure 8.2 suggest that the change in prices due to inclusion of lower tail dependence by Clayton copula is much higher than due to inclusion of upper tail dependence by Gumbel copula. Hence for these products the inclusion of correct tail dependence is very necessary, for rates showing lower tail dependence in their historical data series the option has higher price than for the rates showing upper or zero tail dependence. Also this difference in prices increases when we shift from ITM strikes to OTM strikes options, hence extra care is needed while pricing options with higher strikes.

The difference in prices due to various copulas can be understood by looking at Figure 8.3 which plots the empirical pdf for the spread $S_{1,2}(T) - S_{1,10}(T)$ under different copula functions. It is suggested by the Figure 8.3 that the empirical pdf for spread under the Clayton copula assumption has more probability mass than under the Gaussian copula assumption one for the strikes roughly higher than 0.02 and lower than 0.01, and this difference is consistent with the huge prices difference observed for the spread option in Figure 8.2. Under the Gumbel copula assumption the empirical pdf is just above the Gaussian pdf for the above mentioned strikes and this is consistent with the slight increase in prices due to Gumbel copula. We also note that the difference in the probability mass is higher for Clayton-Gaussian case than the

Gaussian-Gumbel case, for the above mentioned region of strikes, hence the relative percentage difference in prices will be more in the former case as also observed in Figure 8.2. From Figure 8.3 we also notice that the relative percentage difference in prices also increases with strike as also observed in the prices in Figure 8.2

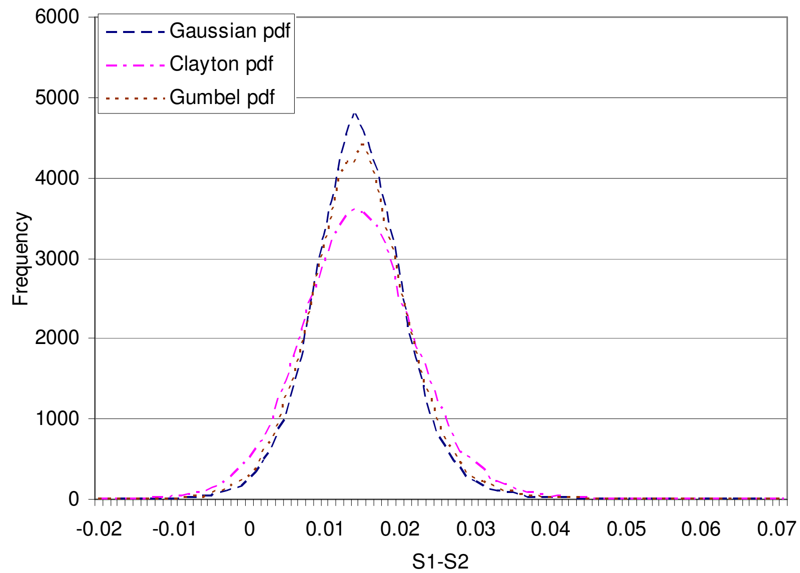

Figure 8.3 Empirical PDF plot for the variable $S_{1,10}(T) - S_{1,2}(T)$ with maturity 1 year

We now look at "**Case A-Case C**" and "**Case A-Case B**" from Figure 7.1 to study the effect of inclusion of smile and tail dependence separately to see which one has a higher impact on the prices of the spread option.

Figure 8.4 plots the price differences for Gaussian Copula with smile and no smile and difference for Clayton and Gumbel copula with Gaussian copula under lognormal marginals' assumption (No smile), the swap rates used are $S_{1,2}$ and $S_{1,10}$.

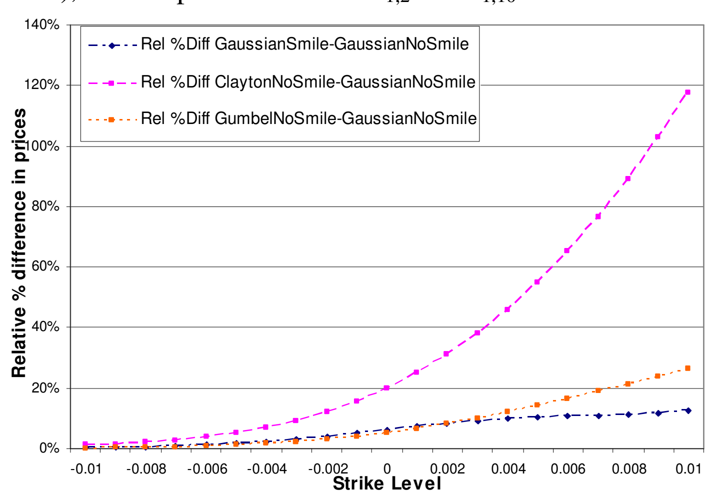

Figure 8.4 Relative % Difference in prices to study impact of smile and tail dependence, for $S_{1,2}$ and $S_{1,10}$ pair, T = 1 year

Figure 8.4 suggest that the effect of inclusion of tail dependence has a higher impact on the price of the option especially when the rates show lower tail dependence. For rates showing upper tail dependence the inclusion of smile is more important than the dependence itself.

Figure 8.5 shows the relative percentage difference in the prices due to change in calibrated parameters for Gaussian copula using 400 and 780 days and change in copula functions calibrated to 400 days. This study is done to see how much the prices change due to error in estimated Gaussian copula parameter and is this difference more or less than the difference obtained due to shift in copula functions.

The parameters used for the Gaussian copula is calibrated using 400 and 780 trading days, the estimated parameter values for these days is given in Chapter 6 Table 6.3. In this case we observed that price difference due to change in estimated parameters for Gaussian copula is higher than the difference due to change of copula functions from Gaussian to Gumbel.

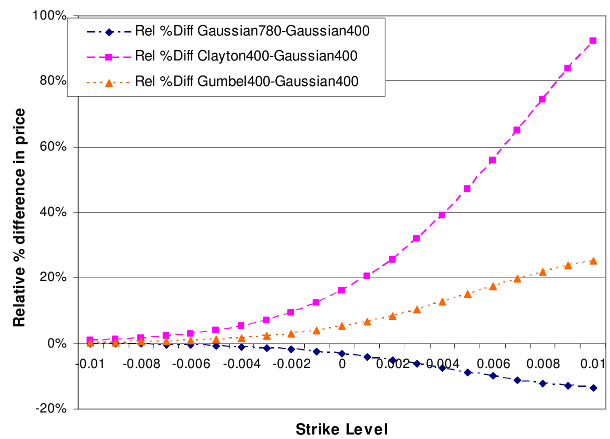

Figure 8.5 Relative % Difference in prices due to change in calibrated parameters for Gaussian copula with change in copulas functions, for $S_{1,2}$ and $S_{1,10}$ pair, T = 1year

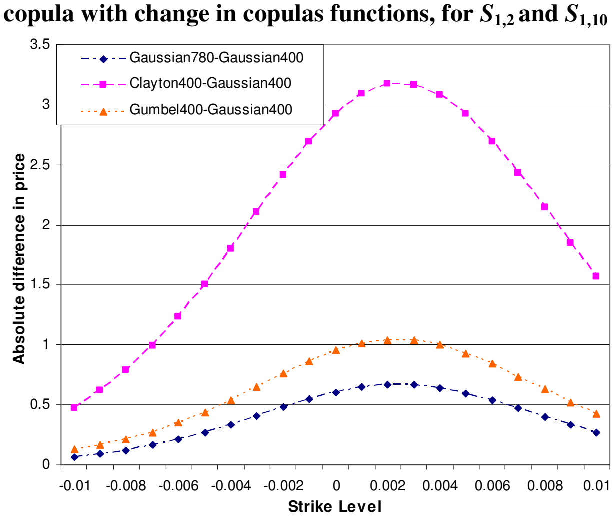

Figure 8.6 Absolute differences in prices due to change in calibrated parameters for Gaussian copula with change in copulas functions, for $S_{1,2}$ and $S_{1,10}$ pair, T = 1year

In Figure 8.6 we plotted the absolute differences in prices for the three cases obtained from the plots in Figure 8.5.

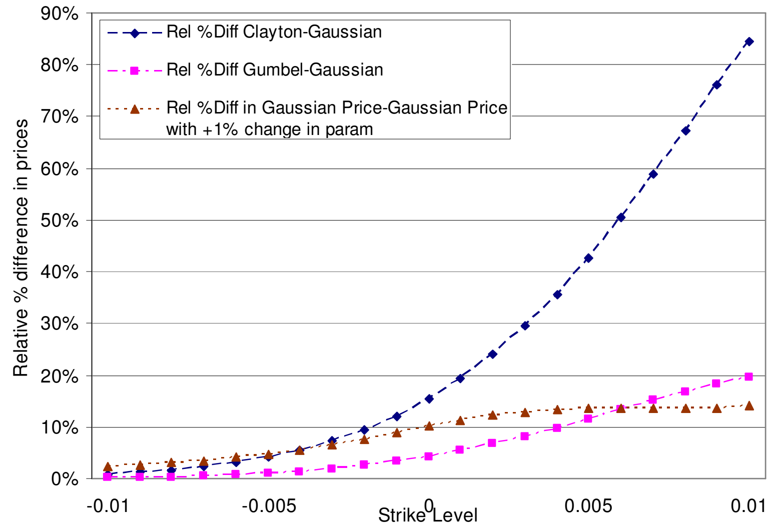

Figure 8.7 Relative % Difference in prices: To study the effect of change in price under shift of +1% in Gaussian parameter with change in copula functions

Figure 8.7 plots the absolute differences to compare the differences in the prices of a spread option due to a +1% shift in Gaussian copula shape parameter ρ with the differences due to change in dependence structure – different copulas. The parameters used in the copulas are calibrated using 780 trading days and the maturity of the option is 1 year.

We notice from Figure 8.7 that the effect in prices due to change of copulas from Gaussian to Clayton is much more than the change due to increasing the Gaussian copula parameter by 1%. This shows that the pricing model is very sensitive to change in dependence structure.

8.3.4 Spread call option with $S_{5,2}$ and $S_{5,10}$ pair

In this section we will analyse the prices of the spread call option (Equation 8.1) with swap rates $S_{5,2}$ and $S_{5,10}$ as the new underlying, the estimated parameter values is given in Chapter 6 Table 6.5. This pair is of interest mainly because we want to study the impact of tail dependence on prices of options with longer maturity. We did a similar study in the Equity case and observed that the difference in prices due to different copula functions decreases with increase in option maturity. Since the underlying in the section (8.3.3) and section (8.3.4) are different we will not compare the two cases together but will study them individually.

We start our analysis by comparing the prices using Gaussian copula and Kirk with smile formula (Section 8.3.2) with marginals following the UVDD model with parameters given in Chapter 5 Table 5.6 and Table 5.7. Figure 8.8 suggest that the relative price difference for longer maturity option is much lower than the differences observed for shorter maturity option (Figure 8.1).

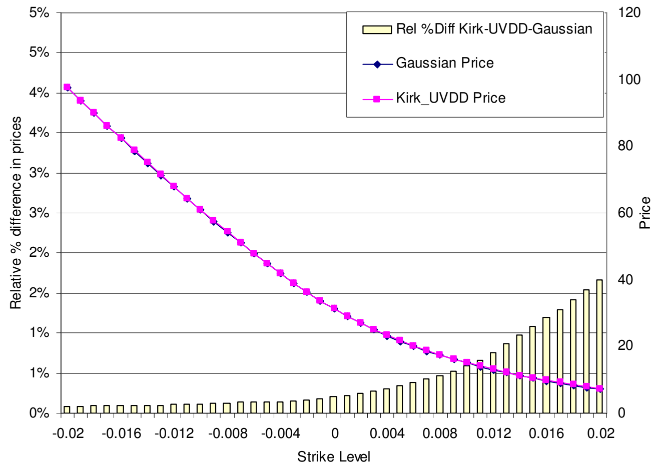

Figure 8.8 Spread option prices using Gaussian and Kirk with smile

From Figure 8.9 we notice that the option is overpriced by Clayton copula and under priced by Gumbel copula when compared to Gaussian copula. We observed similar impact on prices in the Equity case in Chapter 7.

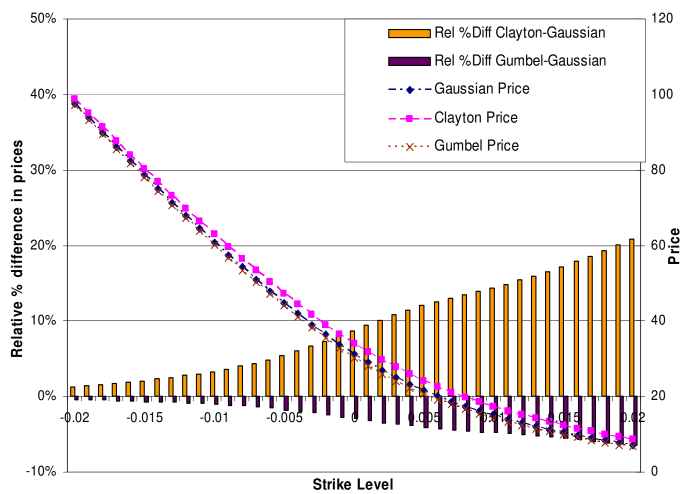

Figure 8.9 Spread option prices and Relative % Difference for different copulas, for $S_{5,2}$ and $S_{5,10}$ pair, T = 1 year

This difference in prices can be explained by looking at Figure 8.10 which plots the empirical probability distribution functions for the spread ($S_{5,2} - S_{5,10}$) under each copula function.

Figure 8.10 suggests that the empirical pdf for spread under the Clayton copula assumption has slightly more probability mass than the Gaussian one for the strikes roughly higher than 0.025 and lower than -0.025, and it is vice-versa for pdf of Gumbel copula, which is just below the Gaussian pdf for the above mentioned strikes. We also note that this difference in probability mass is higher for Clayton-Gaussian case than the Gaussian-Gumbel case, for the above mentioned region of strikes, hence the relative percentage difference in prices will be more in the former case as also observed in Figure 8.9. From Figure 8.10 we also notice that the relative percentage difference in prices also increases with strike.

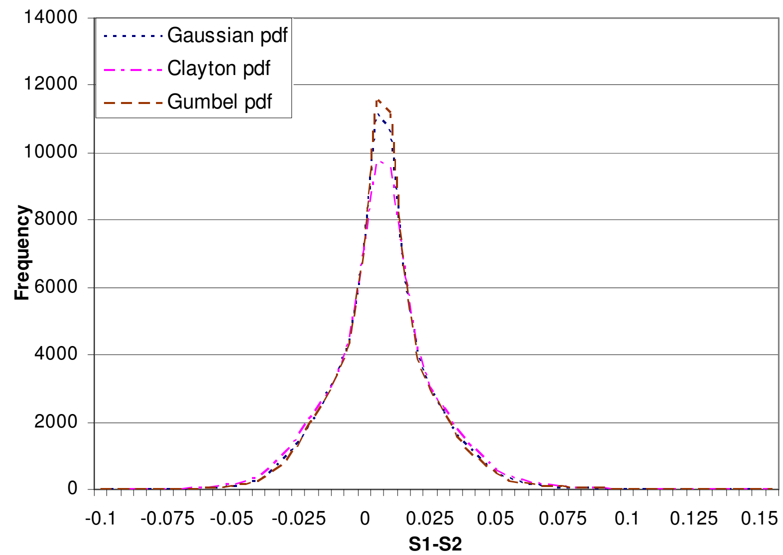

Figure 8.10 Empirical PDF plot for the variable $S_{5,10}(T) - S_{5,2}(T)$, T = 5 year

We now look at "**Case A-Case C**" and "**Case A-Case B**" from Figure 7.1 to study the effect of inclusion of smile and tail dependence separately to see which one has a higher impact on the prices of the spread option.

Figure 8.11 plots the price differences for Gaussian Copula with smile and no smile and difference for Clayton and Gumbel copula with Gaussian copula under lognormal marginals' assumption (No smile), the swap rates used are $S_{5,2}$ and $S_{5,10}$.

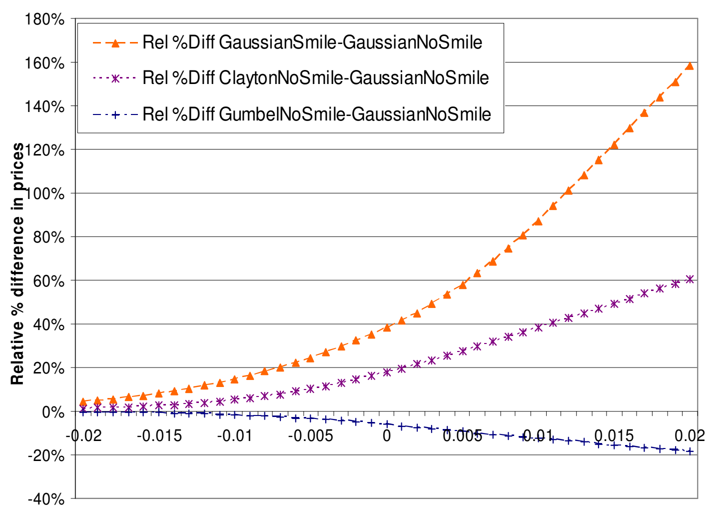

Figure 8.11 Relative % Difference in prices to study impact of smile and tail dependence, for $S_{5,2}$ and $S_{5,10}$ pair, T = 5 year

Figure 8.11 suggest that the effect of inclusion of smile has a much higher impact on the prices than the tail dependence especially and increases with increase in strikes. This shows that the inclusion of the smile for each underlying is more important than the inclusion of the right tail dependence between the two. And among the two types of tail dependence lower tail dependence has a much higher impact on prices than upper tail dependence.

We no study how much the prices change due to difference in estimated Gaussian copula parameters using different days for calibration and comparing it with the difference in prices obtained due to shift in copula functions. Figure 8.12 shows the relative percentage difference in the prices due to change in calibrated parameters for Gaussian copula using 400 and 780 days and change in copula functions calibrated to 780 days.

The parameters used for the Gaussian copula is calibrated using 400 and 780 trading days, the estimated parameter values for these days is given in Chapter 6 Table 6.5. In this case we observed that price difference due to change in estimated parameters for Gaussian copula is almost zero when compared to the difference due to change of copula functions from Gaussian to Gumbel or Gaussian to Clayton.

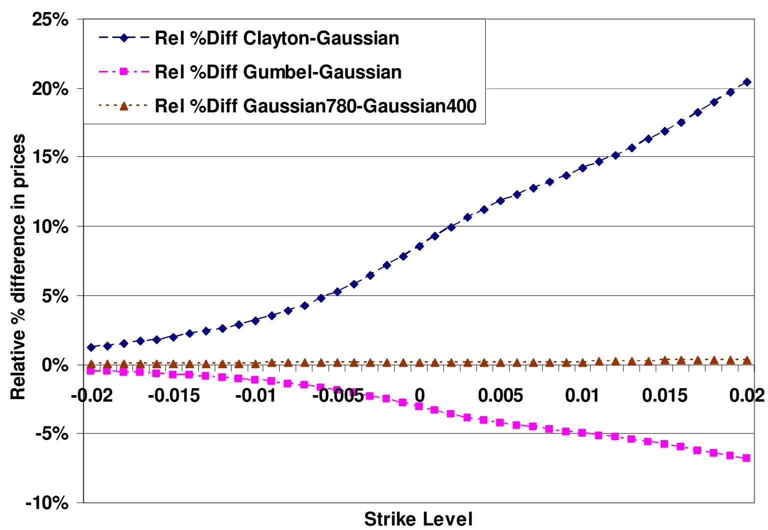

Figure 8.12 Relative % Difference in prices due to change in calibrated parameters for Gaussian copula with change in copulas functions, for $S_{5,2}$ and $S_{5,10}$ pair, T = 5 year

8.4 Spread Digital options

The option analyzed in this section is the spread digital call option whose payoff *SD* at maturity is given by:

$$SD = \begin{cases} c & if \quad S_{a,b1}(T_\alpha) - S_{a,b2}(T_\alpha) \geq K, \\ 0.0 & Otherwise. \end{cases}$$

where K is the strike with $K_{ATM} = S_{a,b1}(0) - S_{a,b2}(0)$, the rates are observed at time T_α and paid at $T_{\alpha+k}$, similar to spread call option from previous section, and the coupon of c on a notional of 100 is paid The valuation date for the option is 16-Mar-09.

We will price this option using Monte Carlo simulation with the pricing algorithm discussed in section 8.1.

Some practical applications of using univariate digital options are –

- A speculator betting on rising and falling prices can use digital options as cheaper alternatives to regular vanilla options,
- A hedger uses this cost-effective instrument to effectively draw upon a rebate arrangement that will offer a fixed compensation (that is, payout) if the market turned the other direction.

8.4.1 Spread digital option with $S_{1,2}$ and $S_{1,10}$ pair

In Figure 8.13 we study "**Case B – Case D**" from Figure 7.1 to understand the impact of tail dependence on the pricing of these digital spread options, the swap rates used are $S_{1,2}$ and $S_{1,10}$. The model parameters for UVDD model and copula function are calibrated using 780 days. The figure plots the prices and the relative percentage difference for the Clayton-Gaussian and Gumbel-Gaussian. $S_{1,2}(0)$ = 2.6575%, $S_{1,10}(0)$ = 3.79411%, K^{ATM} (%) = 1.1366%

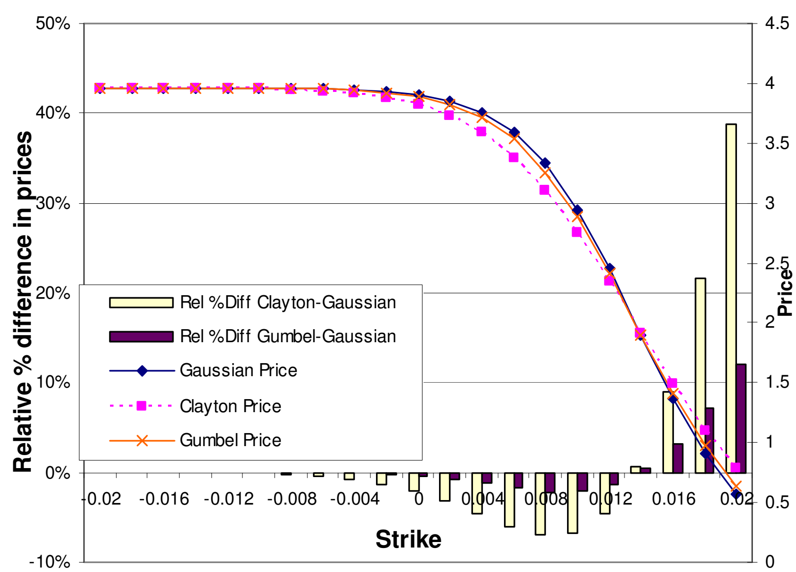

Figure 8.13 Spread digital price and Relative % Difference between various copulas for $S_{1,2}$ and $S_{1,10}$ pair, T = 1year, c = 4%, K^{ATM} = 0.011366

We notice from Figure 8.13 that the Clayton copula prices the option significantly higher whereas the Gumbel overprices it only slightly for strikes higher than 0.014 when compared to prices using Gaussian copula. For lower strike values the product is slightly under priced by both Clayton and Gumbel with Clayton under pricing the option relatively more than the Gumbel copula.

We now look at "**Case A-Case C**" and "**Case A-Case B**" from Figure 7.1 to study the effect of inclusion of smile and tail dependence separately and see which one has a higher impact on the prices of the spread option.

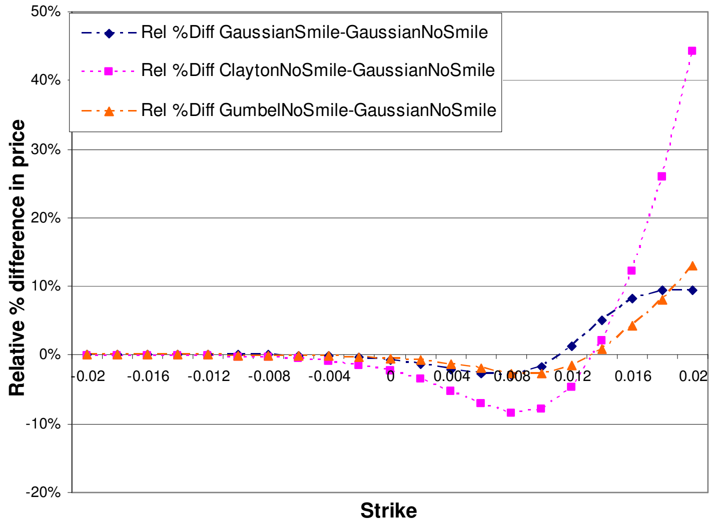

Figure 8.14 Relative % Difference in spread digital prices due to smile and tail dependence, for $S_{1,2}$ and $S_{1,10}$ pair, T = 1year, c = 4%, K^{ATM} = 0.011366

Figure 8.14 plots the price differences for Gaussian Copula with smile and no smile and difference for Clayton and Gumbel copula relative to Gaussian copula under lognormal marginal assumption (i.e., No smile), the swap rates used are $S_{1,2}$ and $S_{1,10}$. We conclude from the plot that neglecting tail dependence can result in huge errors in pricing especially for higher strikes and for underlyings showing high lower tail dependence values.

Figure 8.14 also suggest that the impact on prices due to inclusion of tail dependence is significantly higher for higher strikes (>0), especially for Clayton copula. For lower strike values (<0) the differences are almost negligible than the differences for higher strikes.

The next step is to study how much the price change due to error in estimated Gaussian copula parameter, coming from using different days in parameters calibration, and is this difference more or less than the difference obtained due to shift in copula functions. These parameters are given in details in Chapter 6 Table 6.3.

Figure 8.15 shows the relative percentage difference in the prices due to difference in values of the calibrated parameters for Gaussian copula by using 400 and 780 days for calibration, and change in copula functions calibrated to 400 days.

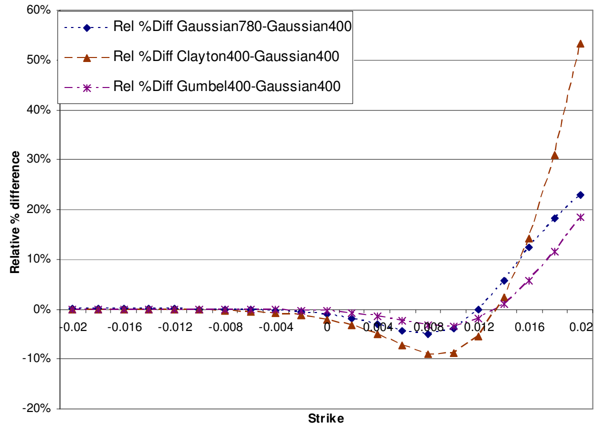

Figure 8.15 Relative % Difference in spread digital prices due to change in calibrated parameters for Gaussian copula and change in copulas functions, $S_{1,2}$ and $S_{1,10}$ pair, T = 1year, c = 4%

Figure 8.15 suggest that difference in prices due to change in copula functions from Gaussian to Clayton is always more than the difference in prices due to change in parameter for the Gaussian copula using different days. For change from Gaussian to Gumbel copula this change in prices is lower than the difference due to change in parameter value used for Gaussian copula. This difference in prices increases with increase in strike. We conclude that the impact on prices due to change in copula functions is much higher than due to change in parameter values for Gaussian copula calibrated using 400 and 780 days respectively.

8.4.2 Spread digital option with $S_{5,2}$ and $S_{5,10}$ pair

We now study the impact of maturity on the pricing of the spread digital options by taking $S_{5,2}$ and $S_{5,10}$ as the new underlyings. We noticed in previous products that the difference between various copulas decreases with increase in maturity of the option. $S_{5,10}(0) = 4.4683\%$, $S_{5,2}(0) = 4.12\%$, $K^{ATM} = 0.3483\%$

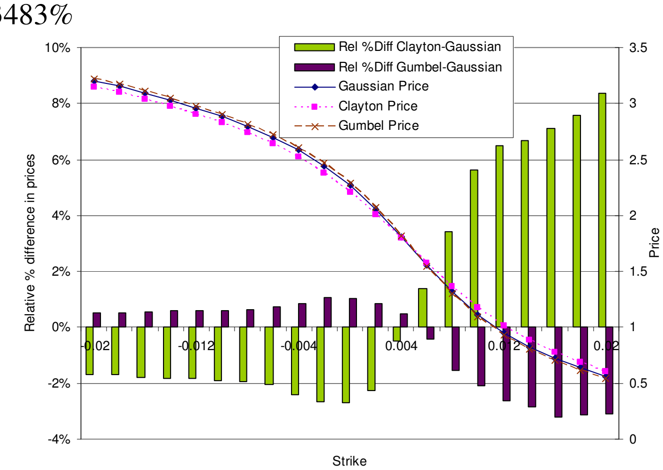

Figure 8.16 Spread Digital prices and Relative % difference between various copulas for 5Y-2Y and 5Y-10Y swap pair, c = 4%, K^{ATM} = 0.003483

The parameters for the UVDD model for the swap rates $S_{5,2}$ and $S_{5,10}$ is given in Chapter 5 Table 5.7 and Table 5.7 respectively. The copula parameter is given in Chapter 6 Table 6.5. The maturity of the option is 5 years and the payment is done after 3 months of the observation time.

Figure 8.16 suggest that the price difference due to various copula assumptions is relatively less than observed for the 1 year maturity option in section 8.4.1.

In Figure 8.17 we compare the impact of smile and tail dependence, when added individually, on the prices of a spread digital option under various copulas.

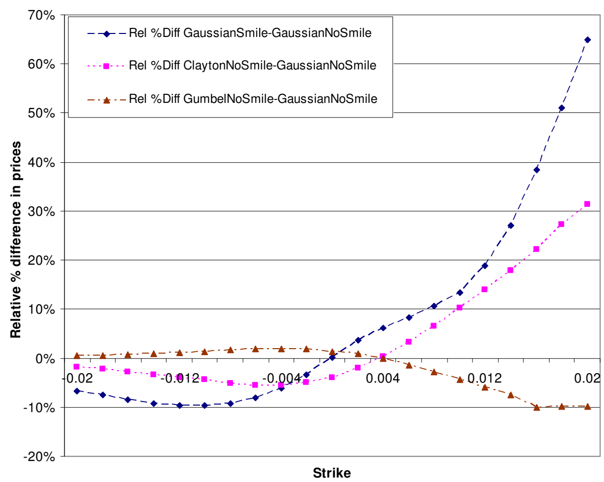

Figure 8.17 Spread Digital prices and Relative % difference to compare effect of smile and tail dependence for 5Y-2Y and 5Y-10Y swap pair, c = 4%, K^{ATM} = 0.003483

Figure 8.17 suggest that the inclusion of smile has a larger effect than the inclusion of right tail dependence. *Hence for products with longer maturity smile plays an important role than the tail dependence.*

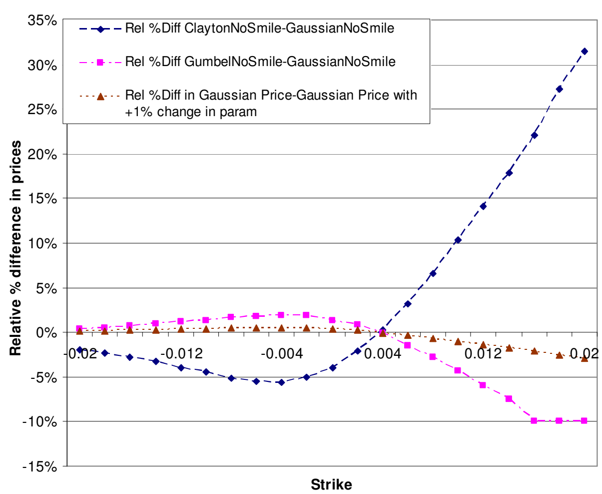

Figure 8.18 Relative % Difference in prices: To study the effect of change in price for +1% in Gaussian parameter and change in copula functions, K^{ATM} = 0.003483

Chapter 9
Conclusion

This thesis is an attempt to understand the impact of tail dependence and volatility smile on the prices of interest rate and equity derivatives. This project finds its base on the evidence of smile and empirical tail dependence present in the daily returns of various financial assets/rates presented in Section 1.3.

Since the Gaussian copula underestimates the probability of the extreme events there is a need to replace the Gaussian copula with a non-Gaussian copula to incorporate the right tail dependence to price options whose payoff depends largely on the tails of the terminal as well as transition distributions. These include Spread options, Spread Digital, Double-Digital options, Worst-of and Best-of options. This way we can price the options more realistically, efficiently and consistently.

The methodology used in my thesis can be broadly summarized as follows:

- The asset pairs were selected based on how large empirical lower or upper tail dependence is present in their historical returns. It was observed that pairs with high correlation value have high probability of having at-least one type of tail dependence.
- To incorporate volatility smile we used 2-scenario Uncertain Volatility with Displaced Diffusion (Chapter 5) model to model the dynamics of the underlying. The model parameters were calibrated using the historical log returns.
- With the use of copula functions we added the desired tail dependence without changing the marginal distributions and therefore the model is still consistent for the single-asset derivatives. In the analysis we used the following copulas into the pricing model:
    1. Gaussian to add zero tail dependence,
    2. Clayton to add lower tail dependence,
    3. and Gumbel to add upper tail dependence.
- The connection between the Gaussian copula and Black-Scholes model was explained and later this relationship was extended to replace the Gaussian copula with the non-Gaussian copula, while keeping the marginals intact. The algorithm to price the options under any bivariate copula function assumption using Monte-Carlo Simulation method was also presented.

- The copula parameters were calibrated (Chapter 6) using the Canonical Maximum Likelihood method over the historical returns. The calibration was done on non-overlapping daily returns to minimize autocorrelation.
- A confidence interval of 95% was used for the prices obtained from Monte Carlo simulation to distinguish between the error in prices due to simulation method and the chosen copula function.

As for the impact on pricing, we studied in detail the following three scenarios: the first is the change of copula functions, second is the change of the marginal distribution from lognormal (no smile) to UVDD model (smile consistent) and the third is change of option maturity.

Apart from this we also studied the change in prices due to choosing a different window size to estimate the Gaussian copula parameter and choosing a non-Gaussian copula calibrated using a fixed window size.

The main results can be summarized as below:

Equity options: Study of equity digital options confirmed the implementation of our algorithms and pricing methods. ITM options had no/negligible impact of tail dependence whereas OTM options showed high relative differences in prices.

For the spread options in the equity case we observed for hypothetical assets that price differences due to different copulas are only present for correlation higher than 0.7, below this value it was hard to say if the difference in prices is due to copula or error in the simulation method.

The need to add both smile and tail dependence was outlined for spread options. The empirical plots of the spread $S_1(T) - S_2(T)$ helped us to understand the price differences due change in copulas. *It showed that payoff of a spread option increase with presence of lower tail dependence and decreases with presence of upper tail dependence*. This relative difference in prices due to different copulas decreased with increase in option maturity due to application of Central Limit Theorem. *This shows that longer maturity options are less sensitive to tail dependence than the shorter maturity ones.*

Worst-of options showed that for higher strikes the relative difference in prices due to various copulas was an increasing function. This option also showed the decrease in relative price difference due to various copulas for long maturity. Results for Best-of option confirmed our implementation of pricing algorithm and methods.

Interest Rate options: For pricing CMS spread products using Monte Carlo Simulation we added to the pricing algorithm (Section 8.1) an extra step to incorporate convexity correction due to difference in observation and payment time. The Gaussian copula prices were compared to the Kirk formula which is the market standard to price spread options. For our chosen asset pairs and parameters we observed that Kirk formula over prices the options slightly for all strikes. For short maturity option the relative difference in spread option prices was relatively much higher than the difference for longer maturity. This result is supported by the empirical probability density plots of the spread $S_1(T) - S_2(T)$ for maturity 1 year and 5 year. In the equity case also we obtained the similar results.

Spread Options with short maturity showed more sensitivity towards addition of tail dependence than to smile whereas for longer maturity options it was a reverse trend, and this sensitivity increases with increase in strikes.

For spread digital options we again observed that shorter maturity options show higher differences in prices due to inclusion of tail dependence then for the longer maturity options. But for both short and long maturity options, ITM options have no or very little affect of tail dependence whereas OTM options showed relatively high difference in prices. We found similar trend in the equity case also.

The effect of smile on spread digital options is more for longer maturity options than for short maturity. ITM options with short maturity shows negligible changes in prices due to addition of smile or tail dependence but suddenly become sensitive to these variables for OTM options. The same applied to longer maturity options which are less sensitive to smile and tail dependence for ITM options and very sensitive for OTM options.

This research gives us full insight on the sensitive to smile and tail dependence for equity and interest rate options.

Further research may be carried out to perform hedge test using these instruments. It will also be very interesting and challenging to study the impact of tail dependence on the prices of path dependent and/or American style options.

Appendix A

A.1 Vanilla Swaps

It is a contract in which two parties agree to exchange periodic interest payments. In the most common type of swap arrangement, one party agrees to pay fixed interest payments(payers swap) on designated dates to a counterparty who, in turn, agrees to make return interest payments that float with some reference rate such as the rate on Treasury bills or the prime rate. The forward swap rate $S_{a,b}(t, T_a, T_b)$ at time t is defined as [27, pp. 92-93],

$$S_{a,b}(t,T_a,T_b) = \frac{P(t,T_a) - P(t,T_b)}{\sum_{j=a+1}^{b} \tau_j P(t,T_j)} = \frac{P(t,T_a) - P(t,T_b)}{A_{a,b}(t)} \tag{A.1}$$

where $P(t, T)$ is the discount factor at time t for maturity T, $T=\{T_{a+1},\ldots..,T_b\}$ are the payment times and τ_j the corresponding year fractions($T_{j+1} - T_j$), and $A_{a,b}(t)$ is the annuity. The swap starts at time T_a and ends at time T_b, where T_b - T_a is called the swap tenor.

A.2 Black's Formula for Swaptions

The Black-76 formula for, a maturity T_a and tenor (T_b - T_a), payer swaption with strike K is defined as [27, pp. 93]:

$$Bl(K; S_{a,b}(t); \sigma_{a,b}) = A_{a,b}(t)\{S_{a,b}(t)N[d_1] - KN[d_2]\}, \tag{A.2}$$

$$d_1 = \frac{1}{\sigma_{a,b}\sqrt{T_b - t}}\left[\ln\left(\frac{S_{a,b}(t)}{K}\right) + \frac{1}{2}\sigma_{a,b}^2(T_b - t)\right]$$

$$d_2 = d_1 - \sigma_{a,b}\sqrt{T_b - t}$$

The constant $\sigma_{a,b}$ is known as the *Black volatility*. Given a market price for the swaption, the Black volatility implied by the Black formula is referred to as the *implied Black volatility*. The Black swaption formula has been used by the market for a long time, without any explicit coherent underlying model.

A.3 CMS swaps

Constant Maturity Swaps (CMS) can be regarded as generalizations of vanilla interest rate swaps [27, pp. 149]. In a CMS swaps one of the legs pays (respectively receives) a swap rate of a fixed maturity, while the other leg receives (respectively pays) fixed (most common) or floating.

In our case each floating leg is a spot swap rate that will be determined in the future, like $S_{a,b}(t, T_a, T_b)$ with different set date t for each floating leg and swap tenor of length T_b - T_a.

To price the CMS swap we need forward swap rates which are unbiased forecast of the corresponding (future) swap rate under the *proper* forward swap measure A (using the annuity $A_{a,b}(t)$ as the numeraire):

$$S_{a,b}(0, T_a, T_b) = E_0^A [\, S_{a,b}(T_a, T_a, T_b)].$$

However, the above statement *does not* apply to CMS swap where the fixed leg (CMS swap) is not a simple combination of the expectations of each floating leg (vanilla swaps), since these expectations are based on different measures (due to different/longer maturity of vanilla swaps used).

With the use of convexity adjustment, described in next section, we can obtain expected "future" forward swap rates by applying change in numeraire.

A.4 Convexity Adjustment

The amount by which the *expected* interest rate exceeds the *forward* interest rate is known as a *convexity adjustment,* it is an adjustment necessary when a payment measure (or currency) is different from the martingale measure of the underlying rate (currency) as in the case of CMS swaps.

The time T_a value of the CMS floating leg single payment contract would be given by:

$$V^{floatingleg}(T_a) = S_{a,b}(T_a, T_a, T_b)P(T_a, T_{a+1})$$

Since payment is made at time T_{a+1}.

Using bond $P(0, T_{a+1})$ as the numeraire we can express the value of the above contract at time *0* as

$$V^{floatingleg}(0) = P(0, T_{a+1})\ E_0^{T_{a+1}} [S_{a,b}(T_a, T_a, T_b)]$$

However, using $P(0, T_{a+1})$ bond as the measure the process $S_{a,b}(T_a, T_a, T_b)$ is in general not a martingale.

But we can apply the change in numeraire on the expectation on the LHS to calculate the expected values, since under *annuity* measure A we have:

$$E_0^A [\, S_{a,b}(T_a, T_a, T_b)] = S_{a,b}(0, T_a, T_b),$$

And

$$E_0^A\left[\frac{P(T_a, T_{a+1})}{A_{a,b}(T_a)}\right] = \frac{P(0, T_{a+1})}{A_{a,b}(0)}$$

Hence using $A_{a,b}(0)$ as numeraire and applying change of numeraire theory [27, pp. 11], we rewrite $E_0^{T_{a+1}} [S_{a,b}(T_a, T_a, T_b)]$ as

$$E_0^{T_{a+1}} [S_{a,b}(T_a, T_a, T_b)] = A_{a,b}(0) E_0^A\left[\frac{S_{a,b}(T_a, T_a, T_b)P(T_a, T_{a+1})}{A_{a,b}(T_a)}\right] \tag{A.3}$$

We derive the convexity correction for single payment of the CMS swap.

The problem in first section is solved by first obtaining the corresponding forward swap rate $S_{a,b}(T_a, T_a, T_b)$ to each floating CMS leg and then *adjusting each* forward swap rate using the proper convexity adjustment [27, Ch. 11].

Expectation on RHS of (Equation A.3) can be expressed as:

$$E_0^{T_{a+1}}[S_{a,b}(T_a, T_a, T_b)] = E_0^A[S_{a,b}(T_a, T_a, T_b)] + CA(S_{a,b};\delta_a) \tag{A.4}$$

where the correction term $CA(S_{a,b};\delta_a)$ is the convexity correction which will depend on the corresponding volatility σ_{Ta} of the forward swaps, time 0, and the set date T_a.

After carrying out the calculations given in details in [29] we get the following result for CMS swap:

$$E_0^{T_{a+1}}[S_{a,b}(T_a, T_a, T_b)] = S_{a,b}(0, T_a, T_b) + \theta(\delta)\exp(\sigma_{a,b}^2 T_a - 1), \tag{A.5}$$

where, δ is the accrual period of the swap rate(i.e., we are assuming that in the CMS swap the swap rate is fixed at T_a and paid at $T_{a+\delta}$) and $\sigma_{a,b}^2$ is the average variance of the forward swap rate and is given by:

$$\sigma_{a,b}^2 = \int_0^{T_a} \sigma(\tau)_a^2 \, d\tau = E_0^Q\left[\frac{(S_{a,b}(T_a, T_a, T_b) - S_{a,b}(0, T_a, T_b))^2}{S_{a,b}^2(0, T_a, T_b)}\right].$$

And after comparing with (Equation A.5) we get the convexity adjustment $CA(S_{a,b};\delta)$ given by:

$$CA(S_{a,b};\delta) = \theta(\delta)\exp(\sigma_{a,b}^2 T_a - 1), \tag{A.6}$$

where after assuming $\tau_j = \tau$ and writing $S_{a,b}(0, T_a, T_b) = S_{a,b}(0)$ we have $\theta(\delta)$ given by :

$$\theta(\delta) = 1 - \frac{\tau S_{a,b}(0)}{1 + \tau S_{a,b}(0)}\left[\frac{\delta}{\tau} + \frac{b-a}{(1 + \tau S_{a,b}(0))^{b-a} - 1}\right]$$

Extending the above results to a multi-payment CMS swap, a sequence of CMS rates $X_{a,b}$ is paid against a sequence of Libor rate plus a spread. The receiving and paying legs have the same frequency. The market quotes the spread that makes the CMS swap a fair contract.

For a CMS swap starting at $T_0' = 0$ and paying at T_i the T_b-year swap rate $S_{i-1,b}$ set at T'_{i-1} ($=1,\ldots n$), the spread on top of the Libor rate that makes the swap a fair contract (i.e. the market quote) can be expressed in terms of the convexity adjustment (Equation A.6) and it value is given by:

$$\begin{aligned} V^{CMS\,swap}(0) &= \sum_{i=1}^{n} P(t, T'_i)\delta_i E^{T'_i}[S_{i-1,b}(T'_{i-1})] - \sum_{i=1}^{n} P(t, T'_i)\delta_i E^{T'_i}[L(T'_{i-1}, T'_i) + X_{n,b}] \\ &= \sum_{i=1}^{n} P(t, T'_i)\delta_i E^{T'_i}[S_{i-1,b}(T'_{i-1})] - [1 - P(0, T'_n)] - X_{n,b}\sum_{i=1}^{n} P(t, T'_i)\delta_i \end{aligned}$$

where $L(T'_{i-1}, T'_i)$ is the Libor rate set at T'_{i-1} and paid at T'_i, δ_i is the corresponding accrual period. In (Equation A.5), the accrual periods are assumed to be the same for both paying and receiving legs.

For the contract to be fair we put $V^{CMS\,swap}(0) = 0$ and obtain the CMS swap rate as:

$$X_{n,b} = \frac{\sum_{i=1}^{n}\left[S_{i-1,b}(0) + CA(S_{i-1,b};\delta_i)\right]\delta_i P(0,T'_i)}{\sum_{i=1}^{n}\delta_i P(0,T'_i)} - \frac{1-P(0,T'_n)}{\sum_{i=1}^{n}\delta_i P(0,T'_i)} \tag{A.7}$$

The next section covers the introduction to the Black's formula for swaption pricing.

A.4 Swaption pricing with UVDD Model

Swaption prices under the UVDD assumption for the swap rates are simply a mixture of adjusted Black's swaption prices. More precisely, the price of a (European payer) swaption with unit notional, maturity T_a, swap payments on times T_{a+1}, T_{a+2},….. T_b and strike K is given by [30, pp. 522-524]:

$$Swaption^{UVDD}(0;a,b;K) = \sum_{h=a+1}^{b}\tau_h P(0,T_h)\sum_{i=1}^{m}\lambda_i^{a,b} Bl\left(K + \alpha_{a,b}^{i}; S_{a,b}(0) + \alpha_{a,b}^{i}; \sigma_{a,b}^{i}\sqrt{T_a}\right) \tag{A.8}$$

A.5 Convexity Correction with UVDD Model

The extension of the convexity adjustment formula to the CMS swap UVDD model leads to the following correction term:

$$CA(S_{a,b};\delta) = S_{a,b}(0)\theta(\delta)\sum_{i=1}^{m}\lambda_i^{a,b}\left[\left(\frac{S_{a,b}(0)+\alpha_{a,b}^{i}}{S_{a,b}(0)}\right)^2\left(e^{(\sigma_{a,b}^{i})^2 T_a} - 1\right)\right] \tag{A.9}$$

where δ and $\theta(\delta)$ has the usual meaning as given in section A.4.

References

[1] Black, Fischer and Myron, Scholes – "*The Pricing of Options and Corporate Liabilities*", Journal of Political Economy 81 (3): 637–654; 1973.

[2] Clewlow, L., and C. Strickland – “*Exotic options: The State of the Art*”, Thomson Business Press, London; 1997.

[3] Rubinstein, M. – “*Nonparametric tests of alternative option pricing models using all reported trades and quotes on the 30 most active CBOE options classes from august 23, 1976 through august 31, 1978*”, Journal of Finance 40: 455-80;1985.

[4] Duffie, D. and J. Pan – “*An overview of value at risk*”, Journal of Derivatives, Vol. 4 (No.3): 7-49; 1997.

[5] Derman, E. and Kani, I. – “*The Volatility Smile And Its Implied Tree*”, Goldman Sachs Quantitative Strategies Research Notes; (January) 1994a.

[6] Dupire, B. – “*Pricing With A Smile*”, Risk **7**: 18-20; 1994b.

[7] Rubinstein, M. – “*Implied Binomial Trees*”, the Journal of Finance 49: 771-818; 1994.

[8] David X. Li – “*On Default Correlation: A Copula Function Approach*”, Journal of Fixed Income 9: 43-54; 2000.

[9] Harry, Joe. – “*Multivariate Models and Dependence Concepts*”, Monographs on Statistics and Applied Probability 73**,** Chapman & Hall; 1997.

[10] Nelsen, R.B. – “*An Introduction to Copulas*”, Lecture Notes in Statistics No. 139. Springer, New York; 1999.

[11] Cherubini, U., E. Luciano and W.Vecchiato – “*Copula methods in Finance*”, John Wiley Finance Series; 2004.

[12] Sklar, A. – "*Fonctions de répartition à n dimensions et leurs marges*", Publications de l'Institut de Statistique de L'Université de Paris 8: 229–231; 1959.

[13] Hull J.C. – “*Options, Futures, and Other Derivates*”, 4th edition, Prentice Hall; 2000.

[14] Scarsini, M. – “*On measures of concordance*”, Stochastica 8: 201–218; 1984.

[15] Blyth, S. – “*Out of line*," RISK, 9(10): 82-84; 1996.

[16] Embrechts, P., McNeil, A. & Straumann, D. – “*Correlation*: *Pitfalls and Alternatives*”, Departement Mathematik, ETH Zentrum, Zurich: 1999.

[17] Embrechts, P., McNeil, A. & Straumann, D. “*Correlation and dependency in risk management: properties and pitfalls*”, RiskLab, ETHZ: 16-17; 1999.

[18] http://en.wikipedia.org/wiki/Euler%27s_totient_function

[19] Schmidt, R. – "*Tail Dependence for elliptically contoured distributions*". Math, Methods of Operations Research 55: 301-327; 2002.

[20] Genest, C. & Mackay, J. – "*The joy of copulas: Bivariate distributions with uniform marginals*". The American Statistician 40: 280-283; 1986.

[21] Joe, H. – "*Multiple Models and Dependence Concepts*". Chapman & Hall, 1997.

[22] Durrleman,V., Nikaghlabi, A. & Roncalli, T. – "*Which copula is the right one*". Working paper, Reserche operarionelle, Credit Lyonnais, 2000.

[23] Shao, J. – "*Mathematical Statistics*". Springer, New York: 248-254; 1999.

[24] Joe, H. & Xu, J.J. – "*The estimation method of inference functions for margins for multivariate models*". Technical report 166, Dept. of Statistics University of British Columbia, 1996.

[25] Mashal, R. & Zeevi, A. – "*Beyond Correlation: Extreme Co-movements Between Financial Assets*", Manuscript, Columbia University; 2002.

[26] Marshall, A.W. & Olkin, I. – "*Families of multivariate distributions*", Journal of American statistics Association 83: 834-841; 1988.

[27] Pessler, Antoon. – "*Efficient Methods for Valuing Interest Rate Derivatives*", Springer Finance; 2000.

[28] Brigo, D. – "*The general mixture-diffusion SDE and its relationship with an uncertain volatility option model with volatility-asset decorrelation*", Fitch Solutions, Imperial College - Department of Mathematics; 2002.

[29] Selic, N. – "*An Examination of the convexity adjustment technique in the pricing of constant maturity swaps*", Advanced Mathematics of Finance Honours Project; 2003.

[30] Brigo, D. & Mercurio, F. – "*Interest Rate Models –Theory and Practice With Smile, Inflation and Credit*", Springer; 2007.

[31] Kirk, E. – "*Correlation in the Energy Markets, in Managing Energy Price Risk*", Risk Publications and Enron, London; 1995.

[32] Carmona, R. & Durrleman, V. – "*Pricing and Hedging Spread Options*", Society for Industrial and Applied Mathematics 45, No. 4: 627–685; 2003.

[33] Bjerksund, P. and Stensland, G. – "*Closed form spread option*", Stensland Department of Finance, NHH, Norway; 2006.

[34] http://faculty.maxwell.syr.edu/cdkao/teaching/ecn505/2002/lec18.htm

[35] J. P. de Kort – "*Pricing multi-asset financial products with tail dependence using copulas*", Delft University of Technology, ABN AMRO Bank, The Netherlands, 2007.

[36] Malafai. V. – "CMS spread option pricing with smile using UVDD Model", ING,2009.

[37] http://mathworld.wolfram.com/CentralLimitTheorem.html